Regulation of neural precursor self-renewal via E2F3-dependent transcriptional control of EZH2

Submitted by: Catherine Pakenham

This thesis is submitted as a partial fulfilment of the M.Sc. program in Neuroscience

February 17th, 2013

Neuroscience Program
Faculty of Medicine
University of Ottawa

Table of Contents

Acknowledgements

To begin, I would like to thank my supervisor, Dr. Ruth Slack, for giving me the opportunity to work in her lab as an Honours student what seems like a lifetime ago. Ruth has gone above and beyond the basic requirements of a thesis supervisor and has provided me with many opportunities that I would not otherwise have been able to experience. Beyond opportunities to attend and present at numerous conferences, Ruth provided me with a great balance of guidance and autonomy which has afforded me not only the ability to be a self-directed learner, but also to take responsibility for my own choices and directions.

I cannot begin to express my gratitude to my fellow lab members. I can sincerely say that despite any amount of hours hunched over a microscope plucking neurospheres, or seemingly endless days of ChIP washes, I always looked forward to coming to the lab. Despite any degree of stress or confusing results, there was always a line of people ready to offer their assistance, advice, and, possibly most importantly, ensure that you did not miss lunch.

I must start by thanking Ph.D. candidate, Lisa Julian. Over the last few years, she has been my mentor and my very good friend. Lisa constantly challenged me, from learning the literature, to understanding ChIP, to running a 10km race (never again). More than that, she has been more supportive than I ever could have asked. There have been infinite times when she has calmed me down, cheered me up, put me back on track, or has merely had an empathetic ear. Lisa has always put forth an astounding effort to help me whenever needed, while trusting me to guide my own way when appropriate. If my acknowledgements seem disjointed or have grammatical errors, it is because this is the only section of my thesis which Lisa has not generously donated her time to correct three times over. She has been a fantastic mentor and I know she will make a great principal investigator in the not so distant future.

Next, thank you to our lab technician, Angela Nguyen. Angela is the person who, despite the hundreds of PCR tubes arranged on her bench, will selflessly drop everything to help someone else without a second thought. She has helped me brave long allergy-ridden sessions in animal care, and most importantly, encouraged us all to partake in lunchtime. It seems trivial, but that one act has instilled a great sense of community in the lab and I think we've all stayed a little saner because of it.

To Jason MacLaurin, our lab technician and manager, thank you for always smiling when I give you bad news. Ninety-nine percent of my conversations with Jason begin with me telling him about broken or missing equipment, shipping problems, or tissue culture mishaps. Jason would simply smile, and proceed to drop what he was doing to fix the problem. Thank you for all of your help creating the LVX-EZH2A virus. Without your help, I would still be staring blankly at plasmid maps.

To the rest of Life Side, thank you for being the comedic relief in even my most stress-filled days. Dr. Renaud Vandenbausch, post-doctoral fellow and my human PubMed, thank you for always ensuring that I am the most up to date on all things Rb. You have always been more than helpful with my project and my questions, and of course, you've made laugh to me. Ph.D. candidate Matt Andrusiak, thank you for being a thoughtful sounding board, for enthusiastically finding answers to all of my molecular biology questions, and most importantly, thank you for convincing me to stop at quaternary spheres. Ph.D. candidate Delphie Dugal-Tessier, thank you for sticking it out. Many people in your shoes would have given up, but you just worked harder. Whether you realize it or not, your drive has been motivation for the rest of us. You have come such a long way and you have kept us all laughing inappropriately along the way. M.Sc. candidate Alysen Clark, my fellow soon to be Master of Science, no matter what anyone says, you are more than just the person who can get things off high shelves. Thank you for being the brilliant hilarious person that you are, and above all else, providing me with some much needed motivation to get this thing done.

Death Side, despite not necessarily understanding ChIP or the cell cycle, you have all been overly helpful in directing my project. I have greatly appreciated having a group of objective people who are so passionate about science and research. You are able to delve into a project completely outside of your field, and, not only identify problem areas, but come up with brilliant solutions as well.

I would also like to thank my thesis advisory committee members Dr. Diane Lagace and Dr. David Lohnes for their thoughtful input and discussion. I sincerely wish we could have had more meetings because I feel I gained so much insight from them. Thank you also to Dr. Alexandre Blais for use of many pieces of his equipment as well as for helpful discussion regarding ChIP. I also must thank Dr. Gustavo Leone for providing our lab with the E2F3 mouse colony. Without this contribution, my project would not have been possible.

Thank you to my family for instilling a sense of curiosity for the medical sciences from a young age. More importantly, thank you for taking an interest in what I was studying simply because it was how I spent my days. What I appreciated the most was having your support and your ability to ground me. When it seemed like having a single experiment not work was the end of the world as I knew it, you were able to help me put things in perspective and see the big picture.

Finally, to Patrick, my husband, thank you for always being my rock. For understanding weekends spent at the lab, for warm meals ready when I got home, for listening to my rants, for pep talks when I wanted to give up, and for picking up and leaving everything to start a new adventure with me, it has all meant the world to me. It has been a long road but we're almost there and I don't think I could have done it without you.

Abstract

Our lab has recently found that E2F3, an essential cell cycle regulator, regulates the self-renewal capacity of neural precursor cells (NPCs) in the developing mouse brain. Chromatin immunoprecipitation (ChIP) and immunoblotting techniques revealed several E2F3 target genes, including the polycomb group (PcG) protein, EZH2. Further ChIP and immunoblotting techniques identified the neural stem cell self-renewal regulators *p16*^{INK4a} and *Sox2* as shared gene targets of E2F3 and PcG proteins, indicating that E2F3 and PcG proteins may co-regulate these target genes. *E2f3*$^{-/-}$ NPCs demonstrated dysregulated expression of EZH2, p16^{INK4a}, and SOX2 and decreased enrichment of PcG proteins at target genes. Restoring EZH2 expression to *E2f3*$^{+/+}$ levels restores p16^{INK4a} and SOX2 expression levels to near *E2f3*$^{+/+}$ levels, and also partially rescues NPC self-renewal capacity toward *E2f3*$^{+/+}$ levels. Taken together, these results suggest that E2F3 controls NPC self-renewal by modulating expression of p16^{INK4a} and SOX2 via regulation of PcG expression, and potentially PcG recruitment.

List of Abbreviations

1°	Primary
2°	Secondary
Ac	Acetylation
Amp	Ampicillin
ATP	Adenosine triphosphate
bFGF	Basic fibroblast growth factor
bp	Base pair
BrdU	Bromodeoxyuridine
CBX	Chromobox homologue
CDK	Cyclin dependent kinase
CDKI	Cyclin dependent kinase inhibitor
cDNA	Complementary DNA
CDS	Coding DNA sequence
ChIP	Chromatin immunoprecipitation
ChIP-Seq	Chromatin immunoprecipitation sequencing
CO_2	Carbon dioxide

D. melanogaster	*Drosophila melanogaster*
dATP	deoxyadenosine triphosphate
DBD	DNA binding domain
DMEM	Dulbecco's modified eagle medium
DNA	Deoxyribonucleotide acid
DP	Dimerization protein
E14.5	Embryonic day 14.5
EDTA	Ethylenediaminetetraacetic acid
EED	Embryonic ectoderm development
EMSA	Electrophoretic mobility shift assay
EZH2	Enhancer of zeste homologue 2
FBS	Fetal bovine serum
G_0	Gap 0
G_1	Gap 1
GAPDH	Glyceraldehyde 3-phosphate dehydrogenase
GE	Ganglionic eminence
H1K26	Lysine 26 of histone H1

H2AK119	Lysine 119 of histone H2A
H_2O	Water
H3K27	Lysine 27 of histone H3
H3K36	Lysine 36 of histone H3
H3K4	Lysine 4 of histone H3
HAT	Histone acetyltransferase
HDAC	Histone deacetylase
HMTase	Histone methyltransferase
HSP	Heat shock protein
IgG	Immunoglobulin G
IP	Immunoprecipitate
IVP	Infection viral particles
kb	Kilobase
kDa	KiloDalton
LB	Lysogeny broth
LVX-EZH2	EZH2-expressing lentivirus
LVX-ZsGreen	Control lentivirus

LZ	Leucine zipper
MB	Marked-box
me2	dimethylation
me3	trimethylation
MEF	Mouse embryonic fibroblast
mg	Milligram
mL	Milliliter
mM	Millimolar
n	Sample size
NaCl	Sodium chloride
NPC	Neural precursor cell
PBS	Phosphate buffered saline
PcG	Polycomb group
PCR	Polymerase chain reaction
PEI	Polyethylene imine
PHC	Polyhomeotic homologue
pRB	Retinoblastoma protein

PRC1	Polycomb repressive complex 1
PRC2	Polycomb repressive complex 2
PRE	Polycomb response element
Rb	Retinoblastoma
RBBP	Retinoblastoma-binding protein
RING1	Ring finger protein 1
RNA	Ribonucleic acid
RNAP	RNA polymerase II
RNF2	Ring finger protein 2
RPM	Rotation per minute
s	Second
S phase	DNA synthesis phase
SDS	Sodium dodecyl sulfate
SDS-PAGE	Sodium dodecyl sulfate polyacrylamide gel electrophoresis
SEM	Standard error of the mean
SUZ12	Suppressor of zeste homologue 12
SVZ	Subventricular zone

TrxG	Trithorax group
Ub	Mono-ubiquitylation
WT	Wild-type
µg	Microgram
µL	Microlitre
µm	Micrometer

List of Tables

List of Figures

Chapter 1 - Introduction

1.1 Neural precursor cells in neurogenesis

1.1.1 Neural stem cells

Neural precursor cell populations consist of neural stem cells and lineage-restricted progenitor cells (Svendsen et al., 1999). In order for a cell to be considered a stem cell, in culture, it must be capable of: 1) proliferation 2) self-renewing divisions, and 3) multipotency, i.e., giving rise to multiple types of more specified cell types (Potten and Loeffler, 1990). Neural stem cells are limited to a neural fate and are thus multipotent, capable of giving rise to neural tissue: neurons and glial cells (oligodendrocytes and astrocytes).

Neural stem cells are derived from pluripotent embryonic stem cells and are found in high concentrations in the subventricular zone (SVZ) found within the ganglionic eminences (GEs) of the telencephalon in mammals. There they generate progenitor cells, which proliferate to amplify the neural precursor pool and undergo terminal mitosis before migrating to the cortex, resulting in a differentiated neuron or glial cell. A residual population of neural stem cells persists in the SVZ into adulthood. Classical cell cycle regulators are implicated in directing the proliferation, differentiation, and self-renewal of neural stem cells during neurogenesis (Yoshikawa, 2000).

1.1.2 Neurosphere assays

Unlike many other cell types, neural stem cells do not express any known definitive molecular markers. The presence and abundance of neural stem cells must instead be evaluated by unique functional criteria. This is accomplished by the neurosphere assay, previously described in detail (Chojnacki and Weiss, 2008). For this assay, putative neural stem cells are dissociated to a single cell suspension and cultured in the presence of mitogens (e.g. bFGF) with which only neural stem and progenitor cells are able to survive long-term (Reynolds and Rietze, 2005). Thus, in these conditions, only neural stem and progenitor cells will thrive and proliferate clonally, producing a sphere of cells. If the cell from which this primary neurosphere was derived is a veritable neural stem cell, the sphere should be made up of not only proliferating progenitors but also a small number of neural stem cells resulting from self-renewing divisions. The presence and abundance of neural stem cells in the primary neurosphere is then determined by its dissociation and culture, again in the presence of mitogens. Any neural stem cells within the primary neurosphere should give rise to a secondary neurosphere. Upon removal of bFGF and introduction of differentiation signals, neural stem cells should also be capable of differentiating to neurons, astrocytes, and oligodendrocytes.

Although the neurosphere assay is an indispensable tool for evaluating the presence and abundance of neural stem cells, it has limitations. Neural progenitor cells are also capable of responding to mitogens contributing to sphere formation, and so, although neurospheres are largely initiated from neural stem cells, the assay does not unequivocally differentiate stem cells from progenitor cells (Reynolds and Rietze, 2005). The initiating cell may be further evaluated by its potential to form secondary and tertiary

spheres upon the sphere's dissociation. This technique allows a greater measure of the initiating cell's stemness and function. Alternatively, in order for a neural stem cell to be identified as such, neurosphere assays must be corroborated by in vivo evidence such as long-term BrdU labelling or olfactory neurogenesis. For this reason, this thesis will refer to neural stem and progenitor cells commonly as neural precursor cells (NPCs).

1.2 pRB/E2F in cell cycle regulation

The *E2f* family is comprised of eight genes, some of which have alternative splice sites, which encode nine transcription factors known to play important roles in regulating the cell cycle at multiple points. The progression of the cell cycle from the Gap 1 (G_1) phase to the DNA synthesis (S) phase is regulated by the E2Fs through the phosphorylated state of the retinoblastoma protein (pRB) (Figure 1-1). When pRB is hypophosphorylated, it binds to E2F family members, preventing the expression of E2F target genes, and thereby arresting the cell cycle at the G_1/S phase checkpoint. In the hyperphosphorylated state, pRB dissociates from E2F, allowing expression of E2F target genes, and subsequently allowing the progression of the cell cycle into S phase. Phosphorylation of pRB occurs through the concerted action of cyclin proteins associated with cyclin dependent kinases (CDKs). pRB phosphorylation is negatively regulated during the cell cycle by CDK inhibitors (CDKIs), such as $p16^{INK4a}$ and $p21^{CIP}$.

The nine *E2f* gene products all possess at least one DNA binding domain through which they can bind to E2F-regulated promoters (Figure 1-2). E2F1-6 also have a DP dimerization domain through which E2Fs heterodimerize with one of three dimerization

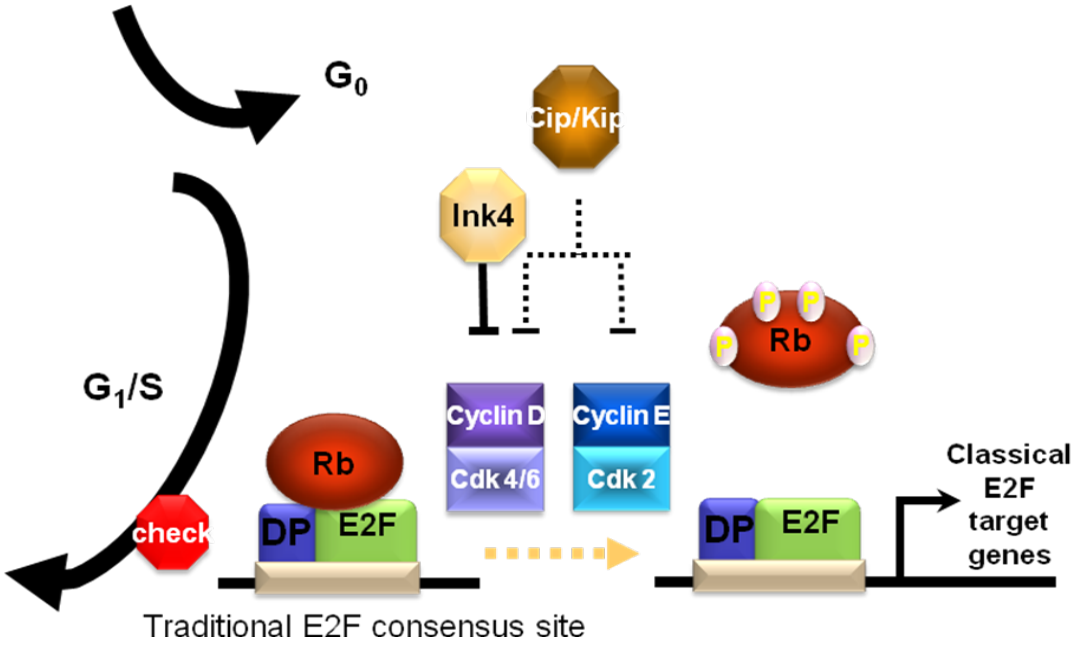

Figure 1-1. The role of E2Fs in cell cycle regulation.

Phosphorylation of pRB by cyclin-CDK complexes allows progression of the cell cycle from the G_1 phase into the S phase, via E2F-dependent transcriptional activation of pro-proliferative target genes. Modified from McClellan KA, Slack RS (2007) Specific In Vivo Roles for E2Fs in Differentiation and Development. Cell Cycle 6:2917-27.

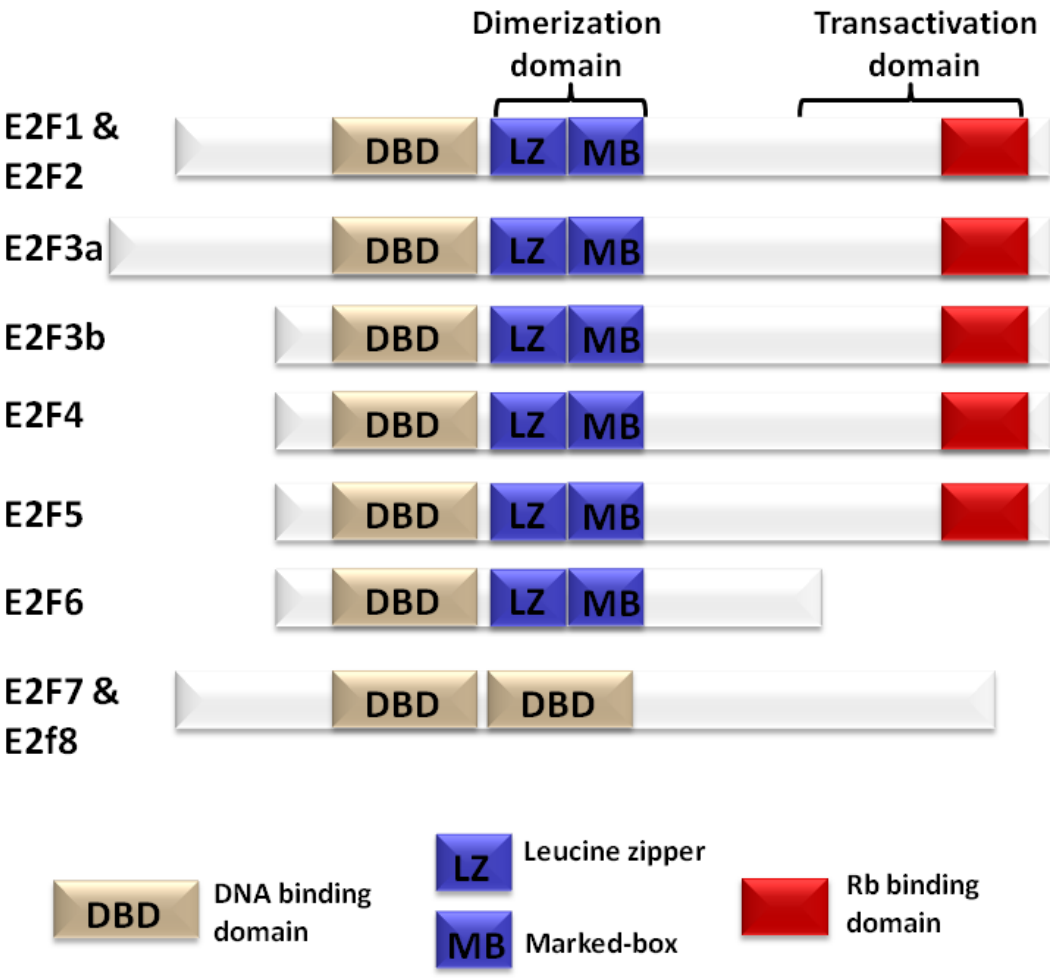

Figure 1-2. Structural similarity amongst E2F family members contributes to overlapping functions.

The E2Fs bind to DNA through the highly conserved DNA binding domain (DBD), to DP through the dimerization domain made up of leucine zipper (LZ) and marked-box (MB) motifs, and to pocket proteins through the pRB binding domain. E2F6 lacks a pRB binding domain while E2F7 and E2F8 lack both a pRB binding domain as well as a dimerization domain. Modified from DeGregori J, Johnson DG (2006) Distinct and overlapping roles for E2F family members in transcripton, proliferation and apoptosis. Curr Mol Med 6:739-748.

proteins (DP1, DP2/3, or DP4) to form a E2F-DP complex (Girling et al., 1993; Milton et al., 2006; Ormondroyd et al., 1995; Zhang and Chellappan, 1995). Heterodimerization with DP creates functional E2Fs, capable of carrying out transcriptional activities at gene targets (Krek et al., 1993; Wu et al., 1995). In addition to these domains, E2F1-5 also possess a transactivation and a pocket protein binding domain through which E2Fs associate with RB family members; RB, p107, and p130.

The E2F family members can be broadly divided into two groups. E2F1, E2F2, and E2F3a are transcriptional activators and act to induce apoptosis as well as to promote cell cycle progression through transcriptional activation of E2F target genes. In wild-type cells, these E2Fs associate uniquely with pRB and are expressed in a cell cycle-dependent manner where their highest expression occurs during late G_1 and early S phase. E2F3b, E2F4, E2F5, E2F6, E2F7, and E2F8 are transcriptional repressors and are thought to be necessary for cell cycle exit. E2F3b, E2F4, and E2F5 are expressed ubiquitously throughout the cell cycle and, although they possess a transactivation domain, they have been found to be weak activators and seem to instead act as transcriptional repressors by recruiting RB family members to E2F target genes. E2F4 can associate with all three RB family members while E2F5 has only been shown to associate with p130. E2F6, E2F7, and E2F8, on the other hand, do not possess a pocket protein binding domain and so they use alternative methods to repress E2F targets. E2F6 associates with Polycomb group proteins, which repress transcription (Attwooll et al., 2005; Ogawa et al., 2002; Trimarchi et al., 2001), while the method of repression of E2F7 and E2F8 remains to be fully elucidated. As of now, these two newest discovered members of the E2F family have been shown to repress transcription and to bind to E2F

targets through their two DNA binding domains independently of DP binding (Logan et al., 2004; 2005). It has instead been suggested that E2F7 and E2F8 form homo- (Di Stefano et al., 2003; Logan et al., 2004; Maiti et al., 2005) or heterodimers (Li et al., 2008) via their DNA binding domains which mimic E2F/DP heterodimers and that these dimers act to negatively regulate the activity of activating E2Fs (Logan et al., 2004).

Although certain E2F family members have been shown to have distinct roles, there is functional redundancy between many E2Fs. This is due to a high degree of conservation of the DNA binding domain between E2Fs. In fact, in vitro, all nine E2Fs are able to bind to the classical E2F consensus sequence TTT(c/g)(c/g)CGC (Rabinovich et al., 2008). However, specificity of E2F recruitment has been demonstrated to be determined not only by the DNA binding sequence, but also by adjacent DNA sequences which bind cooperating transcription factors (Freedman et al., 2009; Rabinovich et al., 2008; van Ginkel et al., 1997). This could explain why there is functional redundancy of E2Fs at some E2F responsive genes, while not at others.

1.3 E2F3 in neurogenesis

1.3.1 The importance of E2F3 in cell cycle regulation and development

The family member E2F3 has been shown to be required for S phase entry as well as for proper cellular proliferation (Humbert et al., 2000; Leone et al., 1998; Wu et al., 2001). Furthermore, E2F3 is critical for neonatal viability (Humbert et al., 2000). Callaghan and colleagues showed by electrophoretic mobility shift assay (EMSA) that, in

wild-type NPCs, pRB mainly associates with E2F3 and that there are only low levels of free E2F3 bound to DNA. In the absence of pRB, differentiating NPCs show delayed terminal mitosis while DNA binding activity of free E2F3 was increased resulting in increased expression of E2F target genes (Callaghan et al., 1999). This indicates that tight regulation of E2F3 by pRB is required in NPCs for proper control of the cell cycle. Our lab and others have also demonstrated cell cycle-independent functions for E2F3, such as regulating neuronal migration (McClellan et al., 2007) and differentiation (Chen et al., 2007). These findings suggest that strict regulation of E2F3 may be generally required for cell cycle-independent functions of pRB/E2F. I have thus focussed my thesis on the role of E2F3 in the developing brain.

1.3.2 E2F3 isoforms

The *E2f3* locus was believed to have only one gene product until Leone and colleagues identified a novel E2F3 product, "E2F3b", dubbing the original product "E2F3a". The E2F3a and E2F3b sequences are expressed from different promoters (Tsai et al., 2008) and although the sequences are mostly identical, the E2F3b protein lacks the N-terminal domain found in E2F3a (Figure 1-2). This portion of the N-terminus is suspected to control accumulation of E2F3a (Adams et al., 2000). The two products also differ in function. As mentioned above, E2F3a is generally thought to be a transcriptional activator while E2F3b is generally thought of as a transcriptional repressor (Adams et al., 2000; Leone et al., 2000). However, E2F3a and E2F3b seem to also have redundant functions during embryonic development since expression of at least one of the two isoforms is sufficient for fetal development in the absence of the other E2F activators, E2F1 and E2F2 (Tsai et al., 2008).

1.3.3 Cell cycle independent functions of E2F3

Our lab has recently found that E2F3 performs unique, cell cycle independent functions in the brain, including the regulation of neural precursor proliferation and stem cell self-renewal (McClellan et al., 2009). Specifically, further investigation by primary neurosphere assays suggests that in the absence of E2F3, there is a significant ($p<0.05$) increase in the number of self-renewing NPCs in the embryonic SVZ (Figure 1-3A). Furthermore, secondary neurosphere assays suggest that these NPCs also have a significantly ($p<0.02$) increased capacity for self-renewal (Figure 1-3B). In order to further investigate the possible mechanism(s) through which this deregulation of neural precursor populations may be occurring, our lab has performed ChIP-on-chip experiments to identify target genes of E2F3 in neural precursors (Julian et al., 2013). Multiple members of several gene families were identified with this technique that may explain our observed *E2f3* phenotype of increased NPCs and NPCs with an increased capacity for self-renewal. Of note, the E2F3 ChIP-on-chip identified both $p16^{INK4a}$ and *Sox2* as putative E2F3 target genes (Figure 1-4).

1.4 E2F3 ChIP-on-chip target genes

1.4.1 $p16^{INK4a}$/CDKN2A

$p16^{INK4a}$ (also known as CDKN2A) is typically associated with senescence and aging (Krishnamurthy et al., 2004; Michaloglou et al., 2005). Neural progenitors of the SVZ in particular display declining function during aging, which correlates with an increase in $p16^{INK4a}$ expression (Molofsky et al., 2006). At present, the primary function

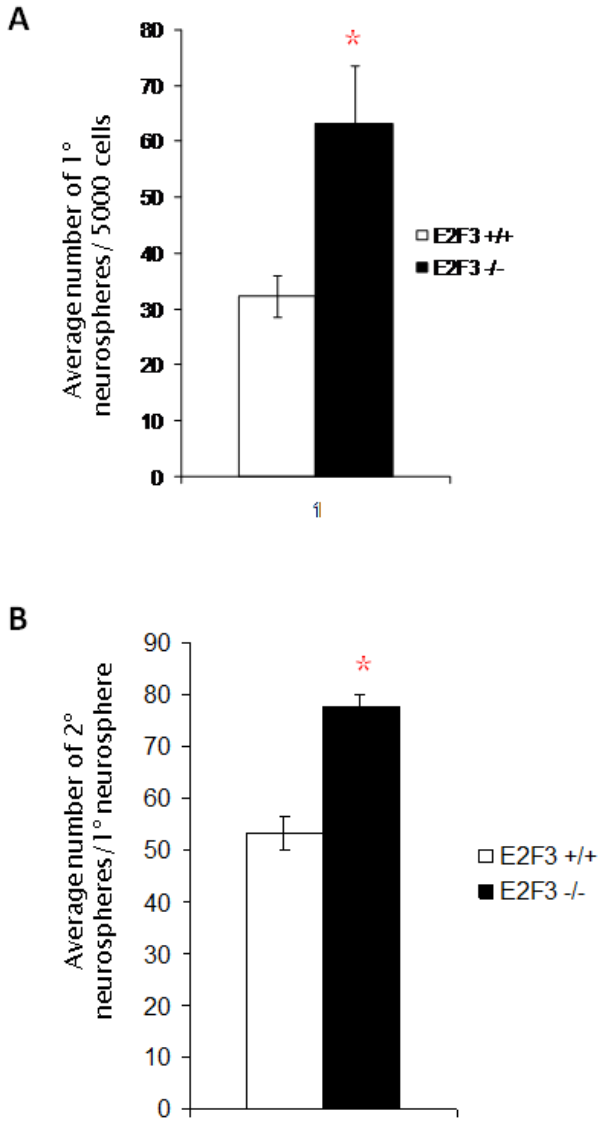

Figure 1-3. E2F3 regulates numbers of neural precursors and their capacity for self-renewal.

A) *E2f3*$^{-/-}$ GE tissue generates increased numbers of neural precursor cells compared to *E2f3*$^{+/+}$. The averages over 6 wells were calculated. B) *E2f3*$^{-/-}$ neural precursor cells have an increased capacity to self-renew compared to *E2f3*$^{+/+}$. Data courtesy of Dr. KA McClellan.

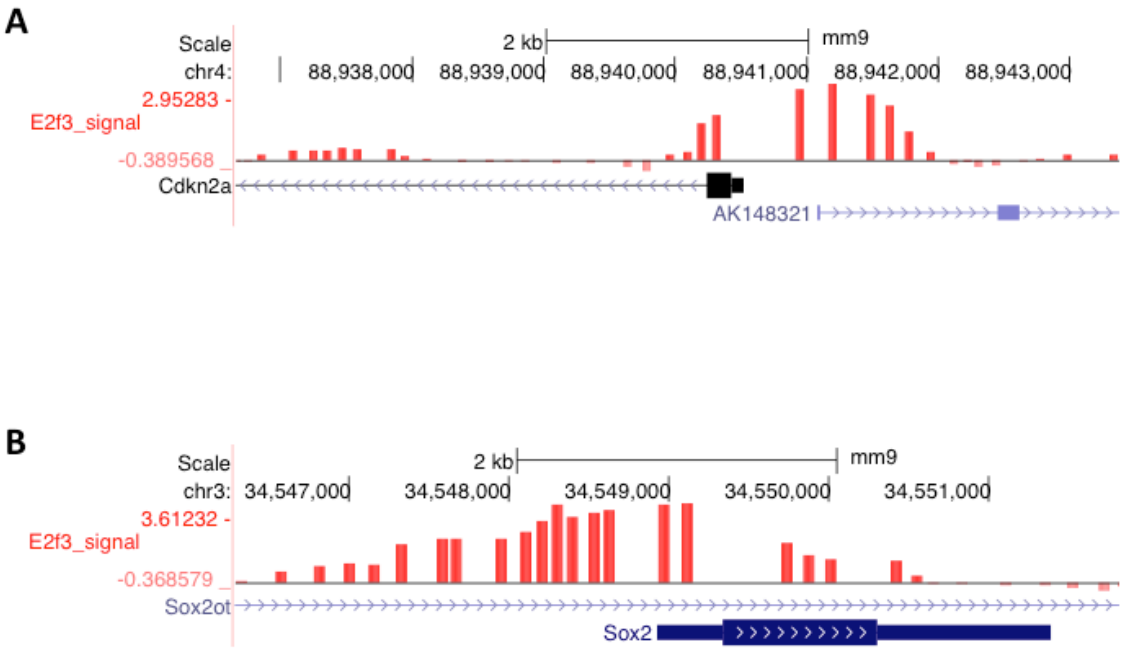

Figure 1-4. E2F3 is enriched at *p16*^{INK4a} and *Sox2* transcriptional regulatory regions.

ChIP-on-chip for E2F3 was performed using neurospheres derived from GE of E14.5 mice. Schematics represent enrichment of E2F3 binding at the promoter regions of A) *p16*^{INK4a}; and B) *Sox2*. Areas of E2F3 enrichment are indicated by red peaks. n=3. Julian et al., 2013. Generated using the UCSC Genome Browser (http://genome.ucsc.edu/).

of $p16^{INK4a}$ appears to be to induce cellular senescence in response to hyperproliferative or stress signals in order to prevent tumour formation (Gil and Peters, 2006; Kim and Sharpless, 2006). Although $p16^{INK4a}$ expression is not always easily detectable in vivo, stressing cells by placing them in culture has been shown to be sufficient to activate its expression (Zindy et al., 1997).

$p16^{INK4a}$ is an established negative regulator of the cell cycle (Serrano, 1997). Upon activation of $p16^{INK4a}$ expression, pRB is recruited to E2F-regulated promoters, causing a block of cell cycle progression from G_1 to S phase, preventing further cellular proliferation (Dahiya et al., 2001). $p16^{INK4a}$ is thus a tumour suppressor; its expression is down-regulated in a large proportion of several types of human cancers due to inactivation of the gene or to point mutations in the gene (Kamb et al., 1994; Nobori et al., 1994). Epigenetic silencing of $p16^{INK4a}$ has also been observed in multiple forms of cancer (Esteller et al., 2001). It is thought that the lack of expression of the tumour suppressor allows cells to cycle without constraint, resulting in tumour formation.

Certain cancers have been shown to exhibit an increase in $p16^{INK4a}$ expression despite its usual association with tumour suppression (Romagosa et al., 2011). High $p16^{INK4a}$ expression is often associated with high-grade malignant tumours with poor prognoses (Arifin et al., 2006; Lam et al., 2008; Milde-Langosch et al., 2001; Steigen et al., 2008). The inability of high $p16^{INK4a}$ levels to impede aberrant cellular proliferation could indicate that these tumours have an improperly functioning pRB-E2F pathway, which has been demonstrated to allow tumour cells to bypass the $p16^{INK4a}$ senescence machinery (Lukas et al., 1995).

1.4.2 SOX2

SOX2 is a transcription factor which is required to maintain pluripotent stem cell populations (Avilion et al., 2003) and is one of four transcription factors required to establish pluripotency in induced pluripotent stem cells (Takahashi and Yamanaka, 2006). SOX2 appears to be particularly important for neural stem cells as its expression is conserved in the developing central nervous system across multiple species (Collignon et al., 1996). Indeed, its expression has been demonstrated to be required for maintenance of neural stem cell identity (Ferri et al., 2004). Its expression is maintained in not only embryonic, but also adult neural progenitors (Bani-Yaghoub et al., 2006; Brazel et al., 2005; D'Amour and Gage, 2003; Ellis et al., 2004), and can be observed in postnatal neurogenic regions, namely, the subventricular zone and the dentate gyrus (Ellis et al., 2004; Ferri et al., 2004).

SOX2 expression is primarily observed in proliferating neural precursors (Pevny and Placzek, 2005) and has been shown to maintain these populations and to inhibit neuronal differentiation (Graham et al., 2003). More recently, radial glial cell populations, which have increased multipotency and self-renewal capacity compared with the intermediate progenitor populations, have also been shown to display increased SOX2 expression (Hutton and Pevny, 2011).

Given that our lab has generated data suggesting that, in the absence of E2F3 there is an increase in NPC numbers and self-renewal (Julian et al., 2013), and given the role of SOX2 in maintaining neural stem cell populations and of $p16^{INK4a}$ in tumour

formation when the pRB-E2F pathway is dysregulated, we aimed to further investigate how E2F3 could potentially regulate expression of $p16^{INK4a}$ and SOX2.

1.4.3 Polycomb Group proteins

Several members of the Polycomb Group (PcG) protein family were identified as E2F3 gene targets (Figure 1-5). PcG proteins have established roles in embryonic development as well as in differentiation (Bracken et al., 2006; Ezhkova et al., 2009; Hirabayashi et al., 2009; Pasini et al., 2007; 2004; Sher et al., 2008; Walker et al., 2010; Yadirgi et al., 2011). More recently, PcG proteins have been suggested to play a role in the maintenance of various stem cell populations (Juan et al., 2011; Kamminga et al., 2006; Molofsky et al., 2005; Román-Trufero et al., 2009; Villasante et al., 2011). The PcG protein EZH2 has specifically been implicated in preventing hematopoietic stem cell exhaustion (Kamminga et al., 2006).

PcG proteins have previously been found to function downstream of the pRB-E2F pathway (Bracken et al., 2003) and their recruitment to the $p16^{INK4a}$ locus has been suggested to be regulated by the truncated isoform of E2F3, E2F3b (Miki et al., 2007). The $p16^{INK4a}$ locus is not only a potential E2F3 gene target, but also a well-studied PcG protein target gene. Similarly, although *Sox2*, to our knowledge, has not yet been identified as a PcG gene target, PcG proteins have been shown to bind at the promoters of several members of the *Sox* family as well as other key pluripotency genes. The PcG protein family was therefore an excellent candidate for further investigation of potential downstream targets of E2F3 that could account for the perturbed regulation of neural precursors observed with E2F3 loss.

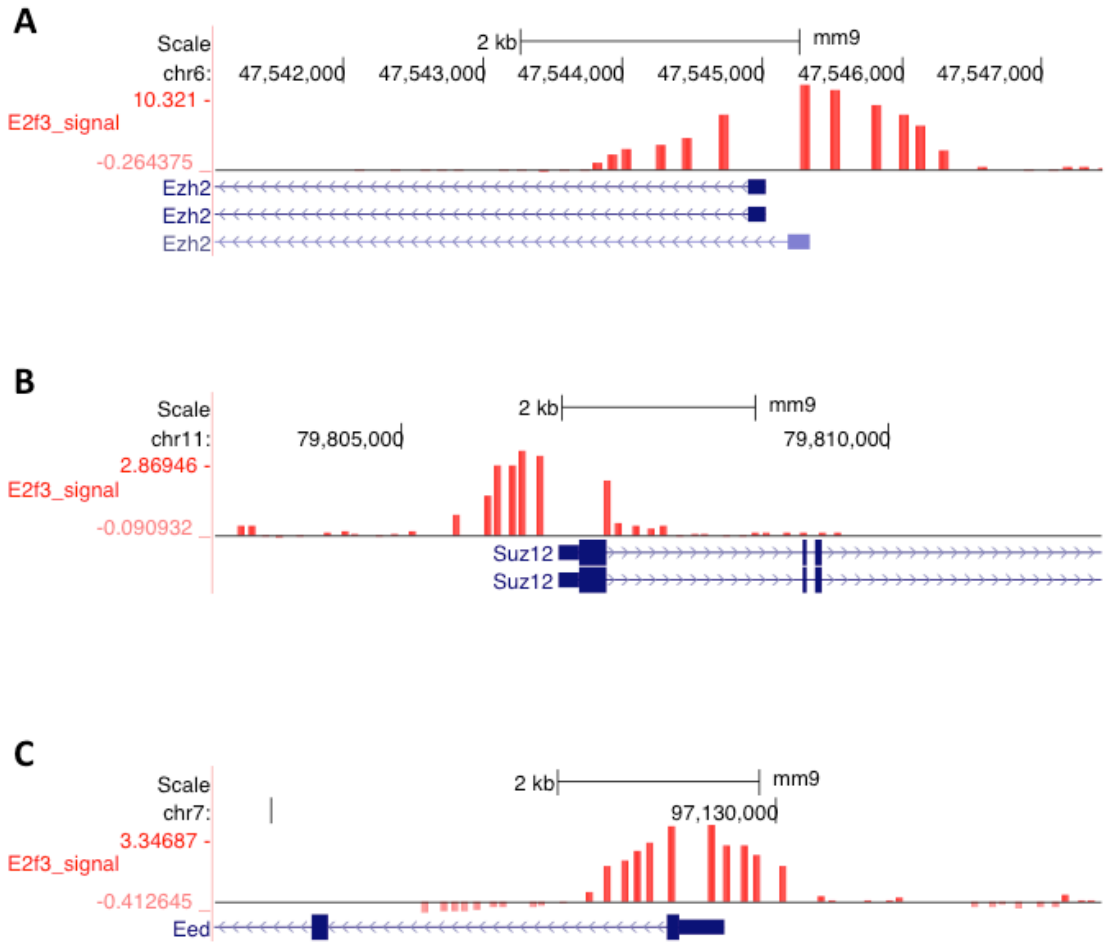

Figure 1-5. E2F3 is enriched at the promoters of the core PRC2 components.

ChIP-on-chip for E2F3 was performed using neurospheres derived from GE of E14.5 mice. Schematics represent enrichment of E2F3 binding at the promoter regions of several PRC2 components A) *Ezh2*; B) *Suz12*; and C) *Eed*. Areas of E2F3 enrichment are indicated by red peaks. n=3. Julian et al., 2013. Generated using the UCSC Genome Browser (http://genome.ucsc.edu/).

Given that the *p16*^{INK4a} and *Sox2* genes are potentially bound and regulated by both E2F3 and PcG proteins, these loci were used to further study the potential role of E2F3 in PcG protein recruitment to target genes. By comparing the presence of PcG complexes at these genes both in *E2f3*$^{+/+}$ and *E2f3*$^{-/-}$ NPCs, the potential influence of E2F3 on recruitment of PcG proteins to E2F-responsive genes may be further investigated.

1.5 The function of Polycomb Group proteins

1.5.1 Polycomb Repressive Complex 2

The proteins of which the PcG family is comprised form two distinct protein complexes, Polycomb Repressive Complex 2 (PRC2), and Polycomb Repressive Complex 1 (PRC1). The current model suggests that PRC2, composed mainly of enhancer of zeste homologue 2 (EZH2), suppressor of zeste homologue 12 (SUZ12), and embryonic ectoderm development (EED), is first recruited to the chromatin-histone complex at the target gene. EZH2 contains a SET domain, which confers histone methyltransferase (HMTase) activity (Kuzmichev et al., 2002). Thus, once PRC2 is recruited to the target gene, it deacetylates and trimethylates histone H3, imparting the H3K27me3 chromatin mark (Müller et al., 2002). This histone modification has been demonstrated by several groups to be associated with an inactive chromatin state (Cao et al., 2002; Papp and Müller, 2006).

Although SUZ12 and EED do not have HMTase activity, they are essential for the formation of a functional PRC2 (Cao and Zhang, 2004; Pasini et al., 2004). Of particular interest, EED has recently been shown to be the component responsible for the binding of PRC2 to pre-established H3K27me3 marks (Margueron et al., 2009; Xu et al., 2010). PRC2 binding to pre-established H3K27me3 is thought to further stabilize repression by physically blocking the site from demethylases or activating histone modifications. EED can also bind to methylated or unmethylated lysine 26 of histone H1 (H1K26) (Xu et al., 2010). Similar to H3K27, H1K26 is methylated by PRC2 (Kuzmichev et al., 2004). While binding of EED to H3K27me3 activates PRC2 HMTase activity and acts to propagate the H3K27me3 modification to daughter DNA strands, binding of EED to H1K26 inhibits HMTase activity of PRC2 (Xu et al., 2010).

1.5.2 Polycomb Repressive Complex 1

Cao and colleagues demonstrated that the deposition of the H3K27me3 mark at target genes facilitates the recruitment of PRC1 (Cao et al., 2002). PRC1 acts to further stabilize transcriptional repression of target genes. The components of this complex are more variable but typically include a chromobox homologue (CBX2, CBX4, or CBX8), a polyhomeotic homologue (PHC1, PHC2, or PHC3), BMI1 or its homologue MEL18, and a ring finger protein (RING1 or RNF2). It is the chromobox homologue that binds the H3K27me3 mark, while the polyhomeotic homologue prevents chromatin from being remodelled by PcG-opposing ATP-dependent remodelling factors (Francis et al., 2001; Shao et al., 1999). The ring finger proteins contain zinc fingers that are required for the mono-ubiquitylation of lysine 119 of histone H2A (H2AK119Ub) (Wang et al., 2004) which has been shown to prevent transcriptional elongation by RNA polymerase II

(RNAP) (Zhou et al., 2008). Although the theory that PcG complexes are sequentially recruited has been well supported, this theory does not always hold true; many gene targets have been found to be bound by PRC2 alone and lacked H2AK119Ub (Ku et al., 2008). The nucleosomes of these targets were shown to retain the H3K27me3 mark less well compared to targets bound by both PRC2 and PRC1. There is also evidence of targets bound only by PRC1 (Schoeftner et al., 2006). These targets also lack trimethylation of H3K27. Taken together, recent studies demonstrate the complexity of PRC2 and PRC1 recruitment and the heterogeneity of this recruitment across different targets.

1.6 Other Important Histone Modifications

1.6.1 Trithorax Group Proteins

The tritothorax group (TrxG) proteins are thought to antagonize the actions of the PcG proteins by trimethylating histone H3 at lysine 4 (H3K4me3) and by di- or tri-methylating histone H3 at lysine 36 (H3K36me2/3) (Beisel et al., 2002; Byrd and Shearn, 2003; Gregory et al., 2007; Schmitges et al., 2011; Tanaka et al., 2007; Yuan et al., 2011). These histone modifications, contrary to H3K27me3, have been shown to be associated with active chromatin structure (Santos-Rosa et al., 2002; Xu et al., 2008).

1.6.2 Bivalent domains

Despite the antagonistic nature of H327me3 and H3K4me3, these two histone modifications can exist at the same PcG target. This creates a bivalent domain. Bivalent

domains are thought to exist as a method of maintaining plasticity of expression of PcG target genes in pluripotent cells (Bernstein et al., 2006). The presence of both activating and repressive histone modifications results in sporadic or low levels of gene expression and allows the gene to be poised for further activation or repression cues upon commitment or differentiation of the cell. When this occurs, H3K27me3 may be lost, resulting in the potential for the recruitment of transcription complexes and gene activation. Conversely, H3K4me3 may be lost instead, resulting in the potential for recruitment of more repressive marks and complexes, and subsequent gene repression (Mikkelsen et al., 2007). Although bivalent domains are typically found at, and associated with, PcG target genes in embryonic stem cells (Bernstein et al., 2006; Pan et al., 2007; Zhao et al., 2007), these domains have also been found in more committed cell types and even in terminally differentiated cells (Mikkelsen et al., 2007; Mohn et al., 2008).

1.6.3 Histone acetylation

Histone acetylation is also associated with transcriptionally active chromatin and has been shown to antagonize transcriptional repression by PcG proteins (Tie et al., 2009). Histones are acetylated by histone acetyltransferases (HATs) and deacetylated by histone deacetylases (HDACs). Demethylation and acetylation of PcG target genes at H3K27 has been shown to be associated with a switch from repressed to active chromatin (Pasini et al., 2010). Histone H3 and H4 acetylation is generally associated with active chromatin (Szutorisz et al., 2005), and has been demonstrated as being important for transcriptional activation (Lee et al., 2007). Acetylation of histones H3 and H4 may be regulated by the presence or absence of H3K4me3 (Guillemette et al., 2011).

1.7 Recruitment of PcG complexes

In *D. melanogaster*, PcG proteins are recruited to target genes via a Polycomb Response Element (PRE) (Simon et al., 1993). PREs are chromatin sites that are necessary and sufficient for the recruitment of PcG complexes and thus for the repression of PcG target genes.

In mammals, a PRE unique to all PcG target genes has yet to be identified. Although a potential vertebrate PRE has been proposed for the mouse *MafB/Kreisler* gene (Sing et al., 2009), this element has yet to be identified at other loci. Alternatively, based on genome-wide ChIP-Seq arrays of several PcG proteins, as well as histone modifications, Ku and colleagues have suggested that large CpG islands lacking activating factor motifs are sufficient for the recruitment of both PRC1 and PRC2 in pluripotent cells (Ku et al., 2008). Given the extent to which PREs have evolved between *D. melanogaster* species alone (Hauenschild et al., 2008), a mammalian PRE is likely quite different from that found in *D. melanogaster* and quite different between mammalian species. A mechanism for PcG recruitment in mammals therefore remains elusive.

1.8 Potential regulation of Polycomb Group proteins by pRB-E2F3

1.8.1 Regulation of PcG genes by hypophosphorylated pRB

The histone methyltransferase *Ezh2* has been previously shown to be a regulatory target of the pRB-E2F pathway in human fibroblasts (Bracken et al., 2003). Furthermore, in multipotent stem cells, hypophosphorylated pRB has been shown to bind at the *Ezh2*

and *Suz12* genes, presumably through E2F (Jung et al., 2010). Interestingly, the authors also showed that the phosphorylation status of pRB was dependent on HDAC activity. HDAC inhibitors have been suggested to differently affect G_1-specific cell cycle proteins by decreasing G_1-specific CDKs while increasing CDKIs (Mathew et al., 2010), specifically $p21^{CIP1}$ (Noro et al., 2010), preventing the phosphorylation of pRB. Thus, by inhibiting HDAC activity, pRB became hypophosphorylated. Subsequently, EZH2 and SUZ12 became downregulated and the abundance of H3K27me3 decreased at the $p16^{INK4a}$ promoter (Jung et al., 2010). Taken together, these data suggest that upon its hypophosphorylation, pRb associates with E2Fs at its target genes *Ezh2* and *Suz12* and represses their transcription. Consequently, fewer PRC2 complexes are formed and recruited to the $p16^{INK4a}$ promoter.

1.8.2 E(Z) expression is dE2F1 dependent

Further supporting these data, in *D. melanogaster*, E(Z) (*D. melanogaster Ezh2* homologue) protein levels and H3K27me2 levels decreased in dE2F1 (the activator E2F in *D. melanogaster*)-depleted cells (Lee et al., 2010). These authors also co-immunoprecipitated E(Z) with both RBF (*D. melanogaster* RB family members) proteins. They found the interaction to be DNA independent, and suggested a direct physical link between the two proteins.

1.8.3 pRB binds components of PRC2

The possibility that the recruitment of PcG proteins is regulated by the pRB-E2F3 pathway is further strengthened through the existence of the retinoblastoma-binding

proteins 4 and 7 (RBBP4 and RBBP7, respectively). These histone chaperones bind pRB (Qian et al., 1993) and have been shown to complex with multiple chromatin remodelling complexes including HDACs (Philpott et al., 2000). Importantly, these proteins have also been shown to be components of PRC2 (Cao et al., 2002; Kuzmichev et al., 2002; Tie et al., 2001). Although they are not required for the HMTase activity of PRC2 (Cao et al., 2002; Pasini et al., 2004), they have been suggested to play a role in the recruitment of PRC2 to histones H3 and H4 (Song et al., 2008). Given that RBBP4/7 have been shown to bind both pRB and PRC2, these histone chaperones could act as a link through which pRB-E2F could associate with PRC2 to potentially regulate its recruitment.

1.8.4 pRB is required for H3K27me3 deposition at *p16^{INK4a}*

pRB has also been shown to have an important function in the deposition and maintenance of H3K27me3 at *p16^{INK4a}* as well as at other cell cycle genes. Kotake et al. demonstrated in human fibroblasts that, in the absence of functional RB family proteins, binding of BMI1 and SUZ12, as well as H3K27me3, is no longer found at the *p16^{INK4a}* locus, resulting in derepression of p16^{INK4a} expression (Kotake et al., 2007). Similarly, Blais and colleagues showed in myotubes that knock-down of pRB, specifically, resulted in decreased H3K27me3 at the promoters of cell cycle regulatory genes, resulting in re-expression of these genes and re-entry of the cell cycle (Blais et al., 2007). Taken together, these studies suggest that pRB is required for recruitment of PRC1 and PRC2 as well as the deposition of H3K27me3 at genes involved in cell cycle regulation.

1.8.5 pRB associates with E2Fs

While pRB has been shown to have an essential and well supported role in the recruitment of PcG complexes to target genes, it is important to note that pRB functions primarily through association with E2Fs at E2F responsive genes (Blais et al., 2007; Nielsen et al., 2001). Given the established and conserved association between pRB and E2F family members, we asked how E2F family members could be attributing to the recruitment of PcG proteins. As mentioned above, Miki and colleagues looked at the role of E2F3 in the recruitment of the PRC1 complex specifically at the $p16^{INK4a}$ locus in MEFs (Miki et al., 2007). By artificially senescing MEFs in culture, the authors investigated binding at the $p16^{INK4a}$ locus. They found that both E2F3 and RING1B bind at this locus and are both eluted upon senescence. They therefore suggested that E2F3 may be required for PRC1 to properly repress expression at this locus.

Taken together, PcG proteins have not only been shown to be transcriptionally regulated through the phosphorylation status of pRB and the presence of activating E2Fs, but their recruitment has also been suggested to be modulated through direct or indirect interactions with pRB/E2F. In order to further understand how this may be occurring, further investigation is necessary.

1.9 Hypotheses

Based on 1) recent studies implicating pRB/E2F in the regulation of PcG protein expression and recruitment to target genes, 2) chromatin immunoprecipitation (ChIP)-on-

chip data from our lab (Julian et al., 2013) suggesting that E2F3 is involved in the transcriptional regulation of multiple PcG proteins in NPCs 3) increased NPC numbers and self-renewal capacity in the absence of E2F3, and 4) modified recruitment of PcG protein complexes in the absence of E2F3 and subsequent deregulated expression of PcG targets, the following hypotheses will be tested:

1) E2F3 regulates NPC self-renewal though regulation of PcG protein expression,

2) E2F3 regulates PcG recruitment to target genes to co-regulate gene expression.

In order to test the first hypothesis, I first examined transcriptional regulation of various PcG genes by E2F3 in NPCs. This was accomplished by examining recruitment of E2F3 at genomic sites by ChIP techniques and protein expression by western blot. NPC self-renewal was then examined in *E2f3*$^{-/-}$ NPCs in which PcG protein expression has been restored to *E2f3*$^{+/+}$ levels using a lentivirus.

The second hypothesis was tested using the key NPC self-renewal regulators *p16*^{INK4a} and *Sox2* as representative gene targets. Binding of both E2F3 and PcG proteins was first verified at these loci by ChIP experiments, and dysregulation of their expression was examined in the absence of E2F3 by western blot experiments. Further ChIP experiments were then used to investigate potential changes in PcG protein enrichment and histone modifications at the *p16*^{INK4a} and *Sox2* transcriptional regulatory regions in the absence of E2F3. Finally, expression of PcG proteins was restored to *E2f3*$^{+/+}$ levels in *E2f3*$^{-/-}$ NPCs using a lentivirus to examine its effect in regulating p16^{INK4a} and SOX2 expression in the absence of E2F3.

Chapter 2 - Materials and Methods

2.1 Mouse colonies

E2F3-/- mice were generated previously by Dr. Gustavo Leone (Leone et al., 2001) and maintained as described previously (McClellan et al., 2007). E2F3a-/- and E2F3b-/- mice were also obtained from Dr. Gustavo Leone (Tsai et al., 2008). Genotypes were verified by PCR as well as by Western blot using an antibody directed against E2F3 (Santa Cruz sc-878) (Figure 2-1). For neurosphere cultures, knock-out embryos and littermate *E2f3*$^{+/+}$ controls were harvested at embryonic day 14.5 (E14.5). DNA was extracted from adult ear clips and embryonic tail clips using Extraction (Sigma E7526) and Tissue Preparation (Sigma T3073) Solutions to extract DNA, and Neutralization B (Sigma N3910) Solution to neutralize the reaction. Genotyping was performed by polymerase chain reaction (PCR) using REDExtract-N-Amp™ PCR Ready Mix™ (Sigma R4775) and primers designed around the *E2f3* locus (Table 1) according to the manufacturer's protocol.

2.2 EZH2 Lentivirus

2.2.1 EZH2 plasmid generation

The MIEV-EZH2A plasmid was generously provided by Dr. de Haan (Kamminga et al., 2006). cDNA of the EZH2 coding DNA sequence (CDS) was amplified by PCR

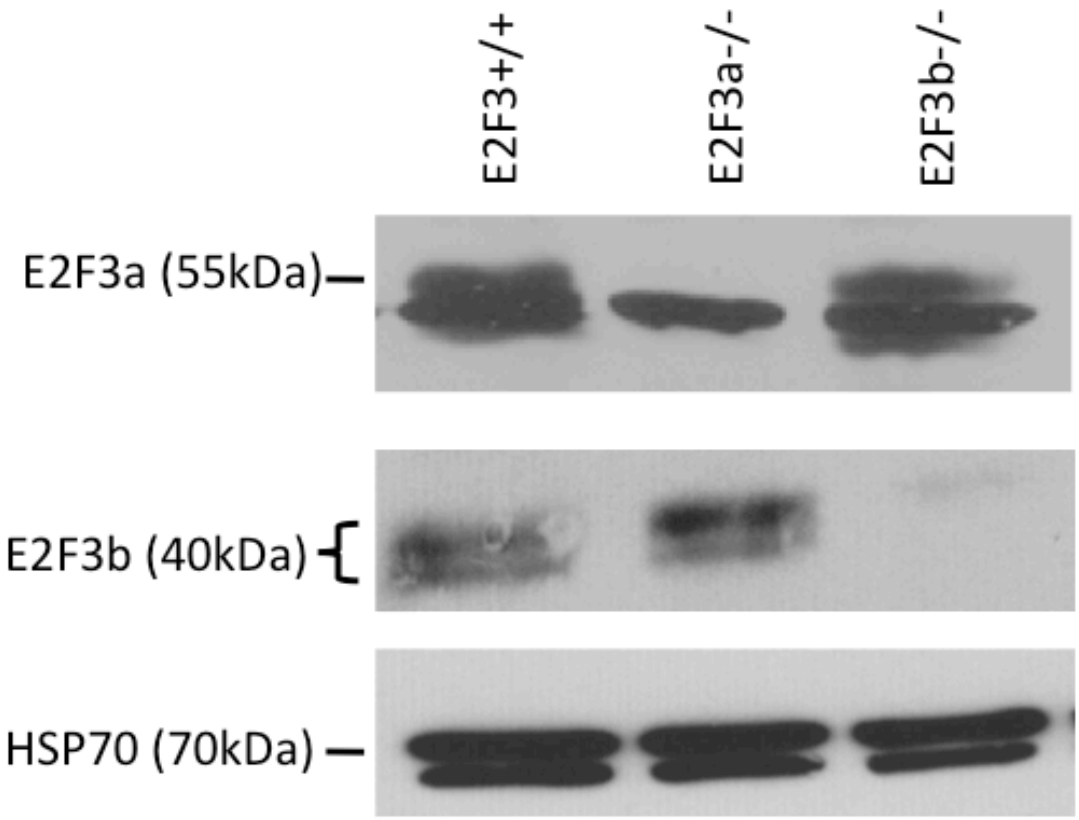

Figure 2-1. E2F3 genotyping verified by western blots.

Western blots were performed on protein extracted from *E2f3*$^{+/+}$, *E2f3a*$^{-/-}$, and *E2f3b*$^{-/-}$ neurospheres derived from GE of E14.5 mice. Equal amounts of protein were loaded in each lane and probed with an antibody directed against E2F3. HSP70 was used as a loading control. Data courtesy of LM Julian.

using primers listed in Table 1. The cDNA PCR fragment was purified with the GFX kit and a poly-A tail was added by incubation at 70ºC with dATPs and Taq DNA Polymerase. The cDNA product of the tailing reaction was then inserted into the AmpR domain-containing pGEM®-T Easy Vector by ligation with T4 DNA Ligase. The product of the ligation reaction was amplified by transformation with JM109 cells and screened on LB-AMP plates in order to select for Amp resistant-, and therefore ligation positive, colonies. Resulting colonies were screened for insertion of the *Ezh2* cDNA fragment by digestion with NotI. Colonies with successful insertion of *Ezh2* cDNA were used to insert the *Ezh2* CDS into the pLVX-CMV-IRES-ZsGreen vector (Clontech Laboratories Inc.) to create pLVX-CMV-EZH2-IRES-ZsGreen. The final pLVX-CMV-EZH2-IRES-ZsGreen was verified by sequencing.

2.2.2 Lentivirus production and live titre

Lentivirus production and titration was modified from the Trono Lab's previously described protocol (Barde et al., 2010); 293T cells were transfected with either an empty pLVX-CMV-IRES-ZsGreen vector or a pLVX-CMV-EZH2-IRES-ZsGreen vector as well as the pMD2G envelop plasmid, the psPAX2 packaging plasmid, 1.5M NaCl, Dulbecco's Modified Eagle Medium (DMEM), and polyethylene imine (PEI). Supernatants from transfected plates were collected 48 hours post-transfection and filtered with a 0.45µm HV Durapore® low protein binding filter (Millipore SCHVU01RE) to remove cell debris. Supernatants were concentrated by ultracentrifugation with 20% sucrose in a Beckman SW28 Ti swinging rotor at 20,000 RPM for 2 hours at 6ºC. The resulting pellet was dried and resuspended in phosphate buffered saline (PBS). 293T cells were plated at a density of 125,000 cells per well of a

24 well plate in complete medium; DMEM, 5% fetal bovine serum (FBS), and antibiotics. The purified lentivirus was serially diluted with DMEM to dilution factors 10^{-2}, 10^{-4}, and 10^{-6}. Each viral dilution was added to two wells of 293T cells each. After 48 hours in a humidified incubator at 37ºC with 5% CO_2, 5-6 fields of green fluorescent cells were counted with a 20X objective. The mean of the 5-6 fields was used to determine the infectious viral particles (IVP)/mL with the following calculation;

$$\text{IVP/mL} = \frac{\text{(infected cells/field) x (fields/well)}}{\text{(volume virus (mL)) x (dilution factor)}}$$

2.3 Cell culture

All cells were derived from ganglionic eminences dissected from knock-out and wild-type littermates at E14.5. Cells were cultured according to a modified previously published protocol (Reynolds and Weiss, 1992). Briefly, tissue was dissociated to a single cell suspension and grown in stem cell medium; Dulbecco's Modified Eagle Medium/F12 (DMEM/F12) supplemented with B27 supplement, antibiotic/antimycotic, basic fibroblast growth factor (bFGF) (12.5mg/mL), and heparin (2mg/mL). Cells were maintained in a humidified incubator at 37ºC with 5% CO_2.

2.3.1 Neurosphere assays

Dissociated *E2f3*$^{+/+}$ and *E2f3*$^{-/-}$ cells from murine E14.5 GE were plated at 5000 cells/well and 6 wells per embryo in 0.5mL stem cell medium per well (Figure 2-2).

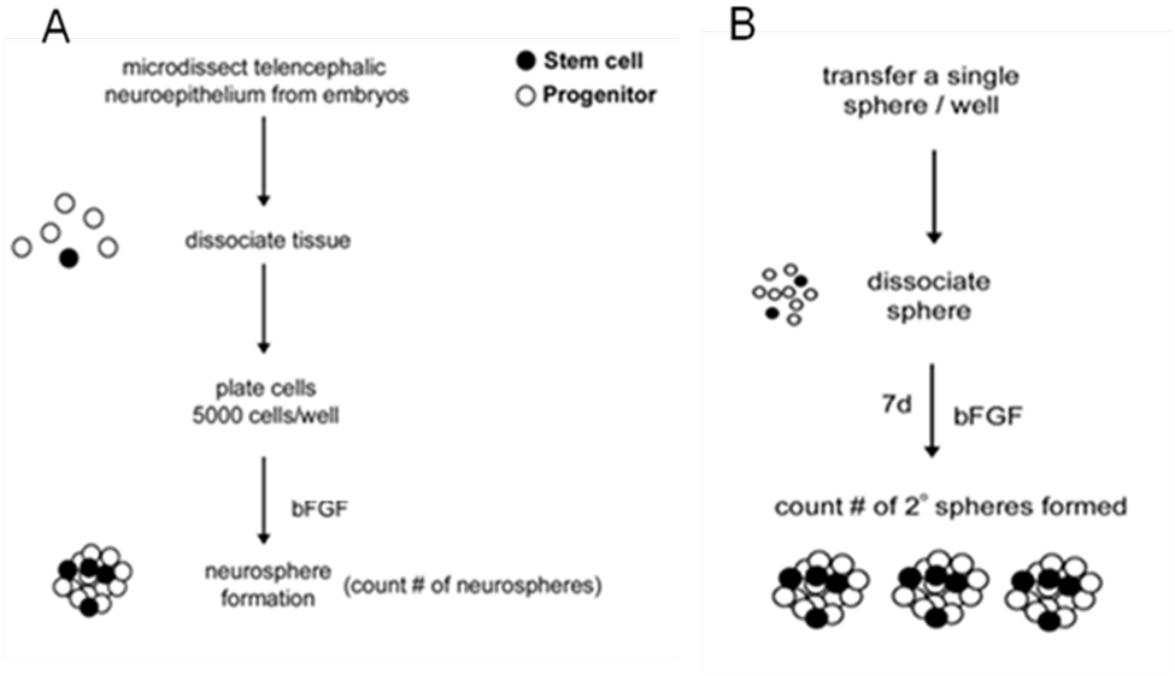

Figure 2-2. Methodology of primary and secondary neurosphere assays.

A) Primary neurosphere assay: Ganglionic eminences were dissected, dissociated and plated at 5000 cells/well. Primary neurospheres were counted after 7 days in vitro. B) Secondary neurosphere assay: After 7 days, primary neurospheres of 150um +/- 10um diameter were resuspended to a single cell suspension and plated in a well of a 96 well dish. Secondary neurospheres were counted after 7 days in vitro. Modified from Weiss et al., 1996.

Primary neurospheres were counted after 7 days in vitro. After 7 days in culture, bulk-plated wild-type and *E2f3*$^{-/-}$ primary neurospheres of 150μm +/- 10μm diameter were individually plucked and dissociated to a single cell suspension and plated in stem cell medium in a well of a 96 well plate; 12 spheres per embryo were plated. Secondary neurospheres were counted after 7 days in vitro.

2.3.2 Lentivirus-infected secondary neurosphere assays

Dissociated *E2f3*$^{+/+}$ and *E2f3*$^{-/-}$ cells were incubated with either LVX-ZsGreen or LVX-EZH2 at 37ºC with 5% CO_2 at a density of 1 million cells/mL stem cell medium in a 24 well plate. Cells incubated without virus were plated in the same way for an uninfected control. After 3 hours, cells were diluted into 5mL stem cell medium in 6cm plates. After 7 days in vitro, green primary neurospheres at 150um +/- 10um diameter were individually plucked and dissociated to a single cell suspension and plated in stem cell medium in a well of a 96 well plate; 12 spheres per embryo were plated. Uninfected primary neurospheres of the same size were also plucked, dissociated, and plated for an uninfected control. Secondary neurospheres were counted after 7 days in vitro.

2.3.3 Neurosphere differentiation

Neurospheres were induced to differentiate according to a previously published protocol (Chojnacki and Weiss, 2008). Briefly, neurospheres from *E2f3*$^{+/+}$ and *E2f3*$^{-/-}$ embryos at E14.5 were cultured as described above for 7 days. Neurospheres were then dissociated and plated in 10 or 15cm plates in differentiation medium; Neurobasal medium supplemented with antibiotic/antimycotic, 1% heat-inactivated non-dialysed

fetal bovine serum (FBS), L-glutamine, 1% N2 supplement, and 2% B27 supplement. Cells were harvested 1, 3, 5, or 7 days later; medium was removed and Trypl-E was added to the plates. Plates were incubated at 37ºC with 5% CO_2 for 3 minutes. Cells were scraped into a Falcon tube and centrifuged to collect the cell pellet. The pellet was washed once in 1X PBS and stored at -80 ºC.

2.4 Western blots

Passaged wild-type and knock-out neurospheres were harvested after 10 days in vitro (passage 1, day 3) and protein was extracted using a lysis buffer comprised of 10mM Tris pH 7.4, 150mM NaCl, 0.5% Triton, and 1mM EDTA, as well as protease inhibitors. Protein extracts were quantified by Bradford assay. Western blots were performed as previously described (Cregan et al., 1999). Briefly, equal amounts of total protein per sample were electrophoresed through 10% SDS-PAGE and blotted on a nitrocellulose membrane. Immunoblotting was performed with incubation of primary antibodies directed against proteins of interest (EZH2, BD Transduction Laboratories 612666; SUZ12, Abcam ab12073; EED, Santa Cruz sc30812; MEL18, Santa Cruz sc-10744; BMI1, Upstate 05-637; RING1B, hybridoma received from Dr. Jeff Dilworth's lab, H3K27me3, Millipore ABE44; SOX2, Santa Cruz sc17320; $p16^{INK4a}$, Santa Cruz sc-1661) for 1 hour at room temperature or overnight at 4ºC. Secondary antibodies were used at 1:2000 for 1 hour at room temperature. GAPDH (Chemicon AB9132) and HSP70 (ABR Bioreagents MA3-028) were used as loading controls. Membranes were incubated with primary antibodies and subsequently incubated with the appropriate secondary

antibody for 1 hour at room temperature. Blots were developed by chemiluminescence according to manufacturer's instructions (ECL; Amersham Biosciences).

2.5 Chromatin Immunoprecipitation

Neurospheres from wild-type and *E2f3*$^{-/-}$ embryos at E14.5 were cultured as described above for 7 days. Neurospheres were subsequently dissociated to a single cell suspension and infected with either no virus (uninfected), LVX-ZsGreen, or LVX-EZH2. After 5 or 7 days in stem cell medium, cells were collected and fixed with an 11% formaldehyde solution for 20 minutes. Resultant cell pellets were either stored at -80ºC or immediately lysed. Cell lysates were sonicated in an ice-cold water bath at 40% amplitude for 4 minutes pulsing 1second on and 1second off, resulting in chromatin fragments of approximately 300-400bp. Sheared chromatin with bound protein was separated from cellular debris by centrifugation. Chromatin immunoprecipitation was performed as described (Blais et al., 2005). Briefly, chromatin was cleared with either blocked A/G agarose beads (H3K27me3, H3K4me3, H3Ac, and H4Ac ChIPs) or blocked protein A magnetic Dynabeads® (SUZ12 and MEL18 ChIPs) for 3 hours at 4ºC. After removing the beads, a 10% input sample was removed and stored at -20ºC. The remaining sample was incubated with 2µg antibody directed against the protein of interest (E2F3, Santa Cruz sc-878; SUZ12, Abcam ab12073; MEL18, Santa Cruz sc-10744; H3K4me3, Millipore 17-614; H3K27me3, Millipore ABE44) or against the antibody host IgG (normal mouse IgG, Santa Cruz sc-2025; normal rabbit IgG, Millipore 12-370) as a negative control. Antibody-bound chromatin fragments were

immunoprecipitated with beads. Crosslinks were reversed by incubation with 1% SDS overnight at 65ºC and resulting DNA fragments were isolated and resuspended in 100µL water each. DNA samples were amplified by Real-Time PCR using the Mx3000P thermocycler and Quanta SYBR Green Fast mix with low ROX (Quanta 95074-250) as an internal reference dye to which detection of SYBR Green fluorescence was normalized. Primers were specifically designed to amplify the promoter of *Sox2* and first exon of $p16^{INK4a}$ (Table 1). Immunoprecipitated samples were run alongside a standard curve derived from serial dilutions of the 10% input samples. Immunoprecipitated samples and IgG samples were normalized to the standard curve of input samples. Normalized IgG values acted as a baseline for non-specific binding and were thus subtracted from the normalized IP values in order to obtain normalized and corrected IP values.

Gene	Forward	Reverse
Primers for genotyping		
E2f3	GTGGCTGGAAGGGTGCCAAG	TGAATCATGGACAGAGCCAGG
	GATTGATTCTGGGTTGTCAGG	
E2f3a	CTCCAGACCCCCGATTATTT	TCCAGTGCACTACTCCCTCC
	GCTAGCAGTGCCCTTTTGTC	
E2f3b	TGTTAGACTCGGGGTGCTTT	CCCCATTTCCCAAAGTCCTA
	AAAGCGCCTTTGAGAGATGA	
Primers for *Ezh2* cloning		
Ezh2	GGGACGAAGAATAATCATGGGCCAGACTG	TCAAGGGATTTCCATTTCTCGTTCGATGCC
Primers for ChIP		
Ezh2	GTGCGGTACCTCTCAGGAAA	GCGGTTAAGACCGTTACCAA
$p16^{INK4a}$	AAAACTCGATGCCAAAATGG	TCGTACCCCGATTCAGGTAG
Sox2	GAGTTCCAGCTTTGCCTTTG	GAGTCCTCTGCCCATGTAGC

Table 1. Primers used for genotyping, cloning, and ChIP Real-Time PCR.

Forward and reverse primers used for genotyping purposes to amplify regions unique to the *E2f3*, *E2f3a*, or *E2f3b* loci, for cloning of the *Ezh2* CDS, and for amplifying the *Ezh2*, $p16^{INK4a}$, and *Sox2* loci from ChIP products by Real-Time PCR.

Chapter 3 - Results

3.1 E2F3 regulates NPC self-renewal through transcriptional regulation of EZH2

3.1.1 E2F3 binds to the promoter regions of PRC2 genes and regulates expression of EZH2

Our lab has previously demonstrated an increase in both primary and secondary neurospheres in the absence of E2F3 (Figure 1-3). To initiate my studies, I first verified these data and was able to confirm the result (Figure 3-1). Dissociated ganglionic eminences from *E2f3*$^{-/-}$ mouse embryos (n=12, where n represents an independent experiment with 6 replicate wells) were found to produce 1.5-fold more neurospheres compared to *E2f3*$^{+/+}$ littermate controls (n=14) (p=0.042) suggesting an increase in numbers of NPCs. A 1.5-fold increase in *E2f3*$^{-/-}$ over WT littermate control secondary neurospheres was also observed, although statistical significance could not be determined due to low n (n=2, where n represents an independent experiment with 12 replicate wells), suggesting that *E2f3*$^{-/-}$ NPCs have an increase in self-renewal capacity. Given that E2F3 is a transcription factor, we sought to identify downstream target genes of E2F3 that could account for the increased numbers and increased self-renewal capacity of neural precursor cells.

As discussed briefly above, in order to identify potential E2F3 target genes in NPCs, our lab performed ChIP-on-chip experiments to identify promoter regions bound by E2F3 in an unbiased fashion (Julian et al., 2013). Chromatin from *E2f3*$^{+/+}$ neurospheres derived from E14.5 GE tissue from our E2F3a colony (FVBN background) was

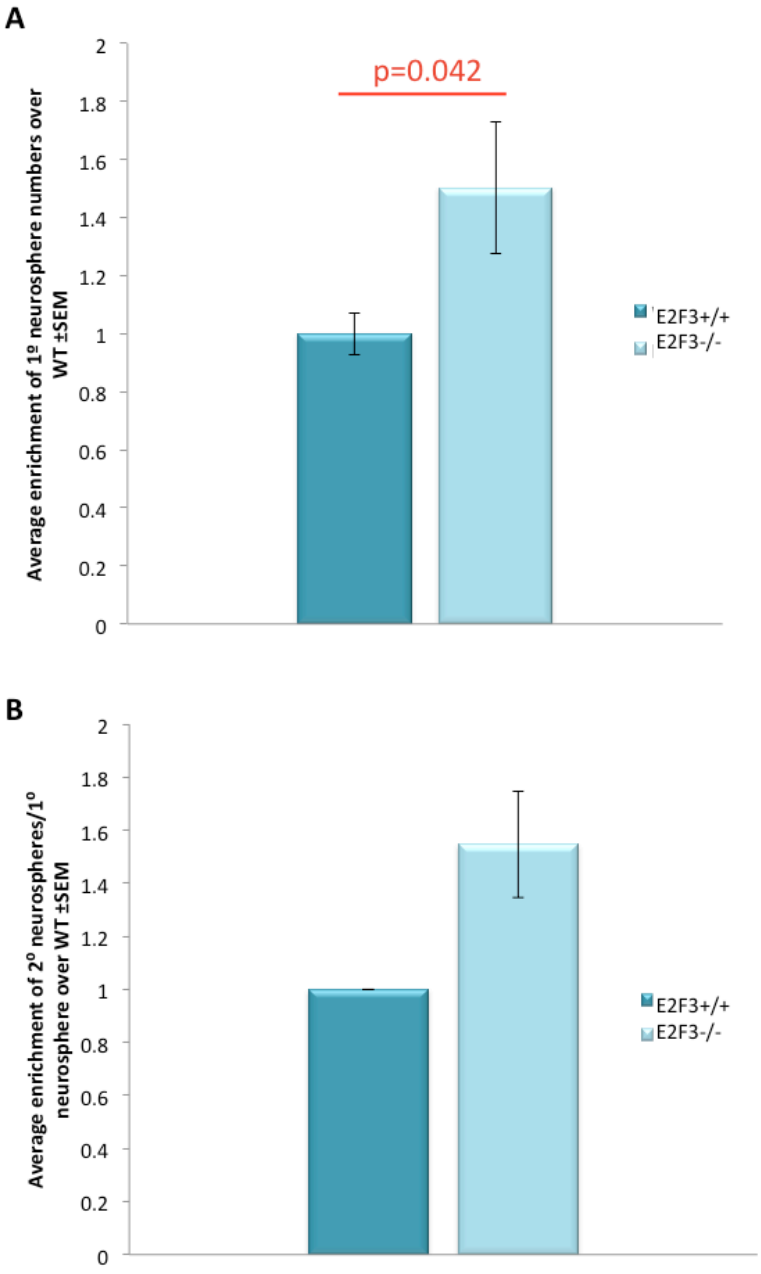

Figure 3-1. E2F3 regulates numbers of neural precursors and their capacity for self-renewal.

A) *E2f3*$^{-/-}$ ganglionic eminences have increased numbers of neural precursor cells compared to *E2f3*$^{+/+}$ controls. Primary neurosphere assays were performed, and the average number of neurospheres after 7 days was normalized so that all *E2f3*$^{+/+}$ values are equal to 1. n=14 (*E2f3*$^{+/+}$) n=12 (*E2f3*$^{-/-}$). B) *E2f3*$^{-/-}$ neural precursor cells have an increased capacity to self-renew compared to *E2f3*$^{+/+}$. Averages were normalized so that *E2f3*$^{+/+}$ values are equal to 1. n=2.

sonicated to approximately 200-350bp fragments. After immunoprecipitation with an antibody directed against E2F3 (Santa Cruz sc-878), resultant isolated chromatin fragments were hybridized to a DNA microarray (Agilent Technologies). The genome coverage of the microarray was -5.5kb to +2kb relative to the transcriptional start site of all known genes in the mouse genome, with probes of 60 nucleotides in length spaced approximately 200bp apart (resultant probe coverage was approximately 5 probes per kb of DNA). From these experiments, performed in triplicate, numerous genes were identified as putative E2F3 targets. We focused on target genes through which E2F3 may control neural precursor self-renewal. Notably, E2F3 was enriched at the promoter regions of all three essential core components of PRC2: *Ezh2*, *Suz12*, and *Eed* (Figure 1-5). The ChIP-on-chip data demonstrated an E2F3 binding peak centered close to the transcription start site of each of these three genes, suggesting that E2F3 binds at, or near, the transcription start site. These findings may suggest a regulatory role for E2F3 at these genes in NPCs.

To ask if E2F3 is involved in the regulation of expression of these genes in neural precursor cells, their expression was examined by Western blot using protein extracts from $E2f3^{+/+}$ and $E2f3^{-/-}$ neurospheres cultured for ten days in vitro. Blots were probed with antibodies directed against EZH2, SUZ12, and EED, as well as several key members of PRC1, namely MEL18, BMI1, and RING1B (Figure 3-2A&B). Although ChIP-on-chip experiments did not demonstrate E2F3 binding at any PRC1 genes, expression of these PRC1 components was also investigated in order to fully understand the effects of E2F3 loss on PcG gene expression. A decrease in EZH2 expression was consistently observed in the absence of E2F3 (Figure 3-2A) while expression of all other examined PcG proteins remained

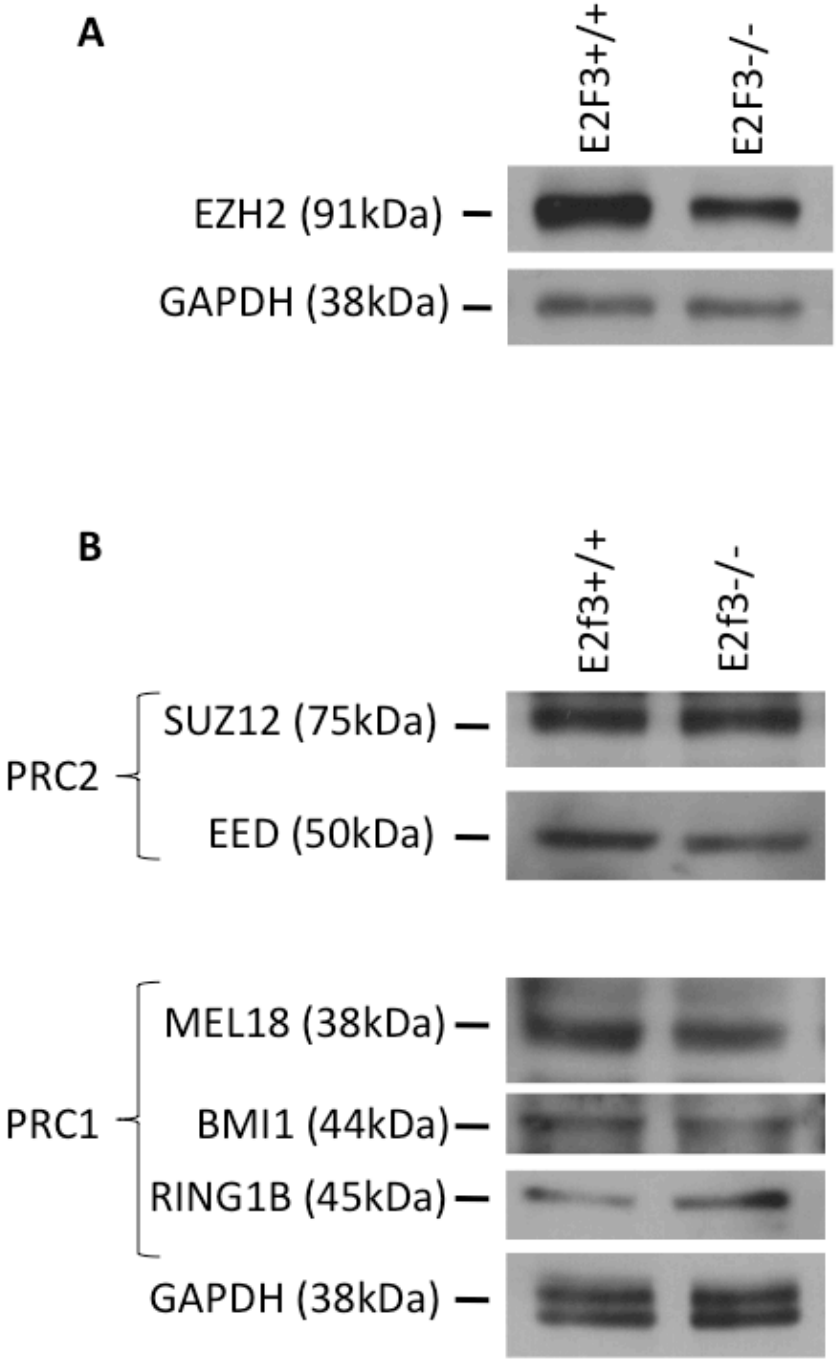

Figure 3-2. PcG protein expression in E2F3 deficient neural precursor cells.

Western blots were performed on protein extracted from *E2f3*$^{+/+}$ and *E2f3*$^{-/-}$ neurospheres derived from GE of E14.5 mice. Equal amounts of protein were loaded in each lane and probed for A) EZH2, and B) other indicated components of PRC2 and PRC1. GAPDH was used as a loading control.

constant (Figure 3-2B). These findings further suggest that E2F3 does not transcriptionally control PRC1 genes and suggest that, despite also binding at the transcriptional start sites of *Eed* and *Suz12*, E2F3 is involved in the proper transcriptional control of EZH2 only.

Given that ChIP experiments demonstrated that both E2F3 isoforms bind at the *Ezh2* promoter and that EZH2 expression is dysregulated in the absence of E2F3, I asked whether the individual E2F3 isoforms differentially regulate EZH2 expression. To address this question, Western blots were performed with protein extracts from *E2f3a*$^{-/-}$ and *E2f3b*$^{-/-}$ neurospheres, as well as from their respective WT littermate controls (Figure 3-3). EZH2 expression is typically associated with stem cell maintenance and tumourigenesis, and is thought to be down-regulated upon cellular differentiation, aging, or senescence (Bracken et al., 2003; Margueron et al., 2008; Suvà et al., 2009). Furthermore, EZH2 expression has specifically been found to decrease upon differentiation of neural stem cells (Hirabayashi et al., 2009; Sher et al., 2008). I thus explored how EZH2 expression may be regulated in both proliferating neurospheres (D0) and in NSCs one day following induction of differentiation (D1) in order to examine how EZH2 may be dysregulated not only in cycling cells, but also in cells that (should) have been cued to begin to down-regulate EZH2 in order to differentiate. As was observed in *E2f3*$^{-/-}$ neurospheres, *E2f3a*$^{-/-}$ proliferating neurospheres show a decrease in EZH2 expression (n=3) (Figure 3-3A). Interestingly, upon induction of differentiation, EZH2 expression increases compared to *E2f3a*$^{+/+}$. These results suggest that E2F3a activates EZH2 expression in NPCs but represses it in differentiating cells. Given that E2F3a expression peaks at the end of G_1 phase for transcriptional activation of E2F-responsive

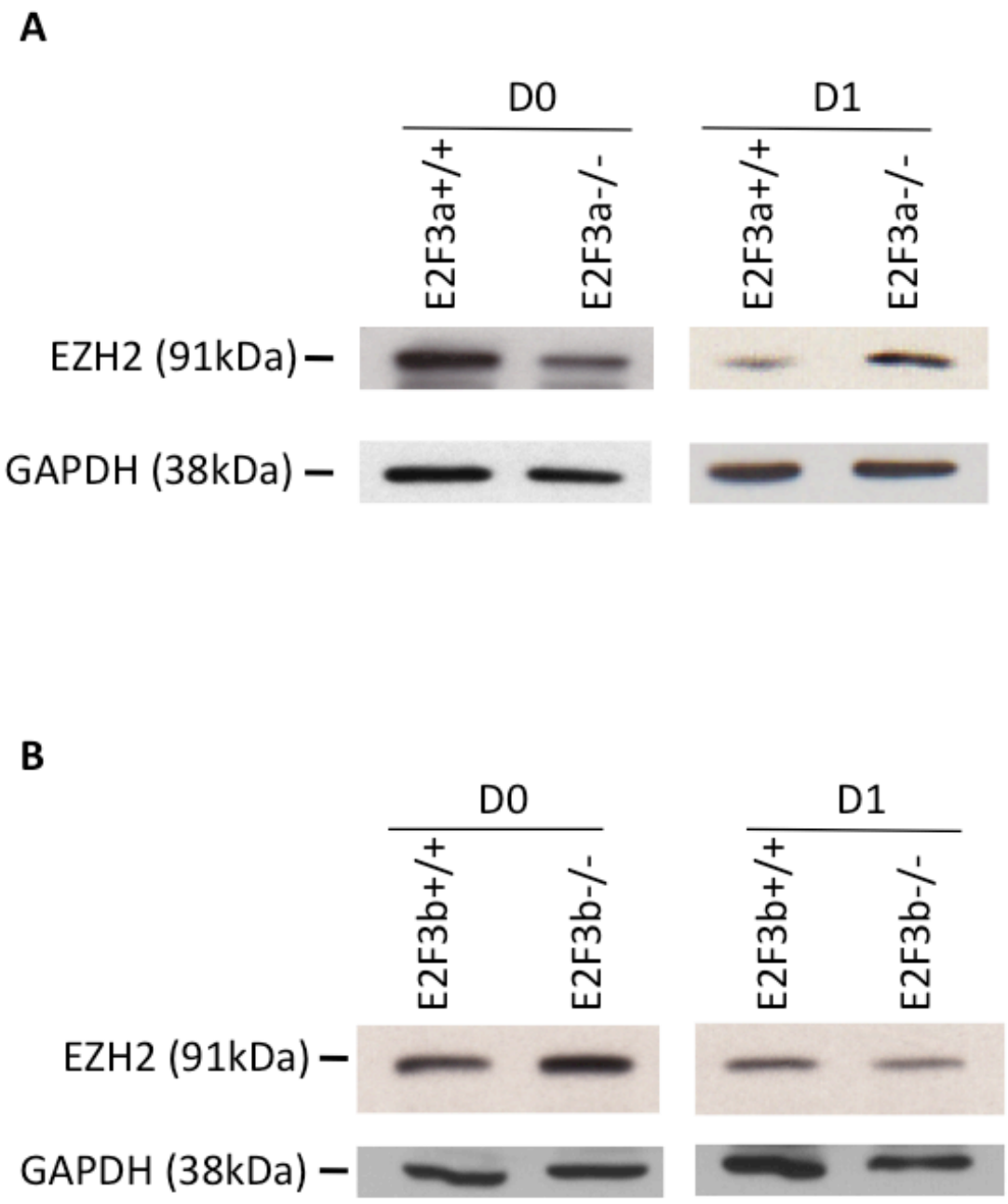

Figure 3-3. E2F3 isoforms differentially affect EZH2 expression.

Equal amounts of protein extracts from proliferating progenitors (D0) and from one day post-induction of differentiation (D1) were run on a 10% SDS-PAGE and transferred to a nitrocellulose membrane and probed for the indicated proteins. WT cells from littermate controls were compared against A) *E2f3a*$^{-/-}$ cells (n=3) and B) *E2f3b*$^{-/-}$ cells (n=3). GAPDH was used as a loading control.

genes (Leone et al., 1998; 2000), a time point at which a cell can decide to either enter or exit the cell cycle, E2F3a could potentially mediate a balance between self-renewal and differentiation of NPCs through regulation of EZH2. Conversely, EZH2 expression increases in *E2f3b*$^{-/-}$ proliferating neurospheres and decreases upon differentiation (n=3) compared to WT neurospheres (Figure 3-3B). These results suggest that E2F3b opposes the transcriptional regulation of E2F3a, potentially to ensure the tight regulation of EZH2.

In order to verify our ChIP-on-chip findings, classical ChIP experiments were performed using chromatin from *E2f3*$^{+/+}$ and *E2f3*$^{-/-}$ neurospheres from our E2F3 colony (C57BL6 background). The resulting chromatin fragments were amplified by PCR with primers designed specifically around the regions identified as potentially bound by E2F3 in our ChIP-on-chip studies. This region is within the *Ezh2* promoter, which surrounds the *Ezh2* transcription start site from -1095→+48, where 1 is the transcription start site and <1 is upstream of the transcription start site (Bracken et al., 2003). Figure 3-4A demonstrates binding of E2F3 at the *Ezh2* promoter at -496→-254 in *E2f3*$^{+/+}$ neurospheres, which is consistent with our E2F3 ChIP-on-chip experiments. To better understand how E2F3 may be regulating expression of EZH2, ChIP experiments designed to evaluate specific binding by E2F3a or E2F3b were also carried out (Figure 3-4B). Due to structural overlap between E2F3a and E2F3b, there is no commercially available antibody specific to E2F3b. Thus, to examine binding of the individual isoforms, neurospheres derived from *E2f3a*$^{-/-}$ and *E2f3b*$^{-/-}$ embryos and a pan-E2F3 antibody were used. ChIP experiments using *E2f3a*$^{-/-}$ neurospheres thus specifically identify binding of E2F3b, while ChIP experiments using *E2f3b*$^{-/-}$ neurospheres

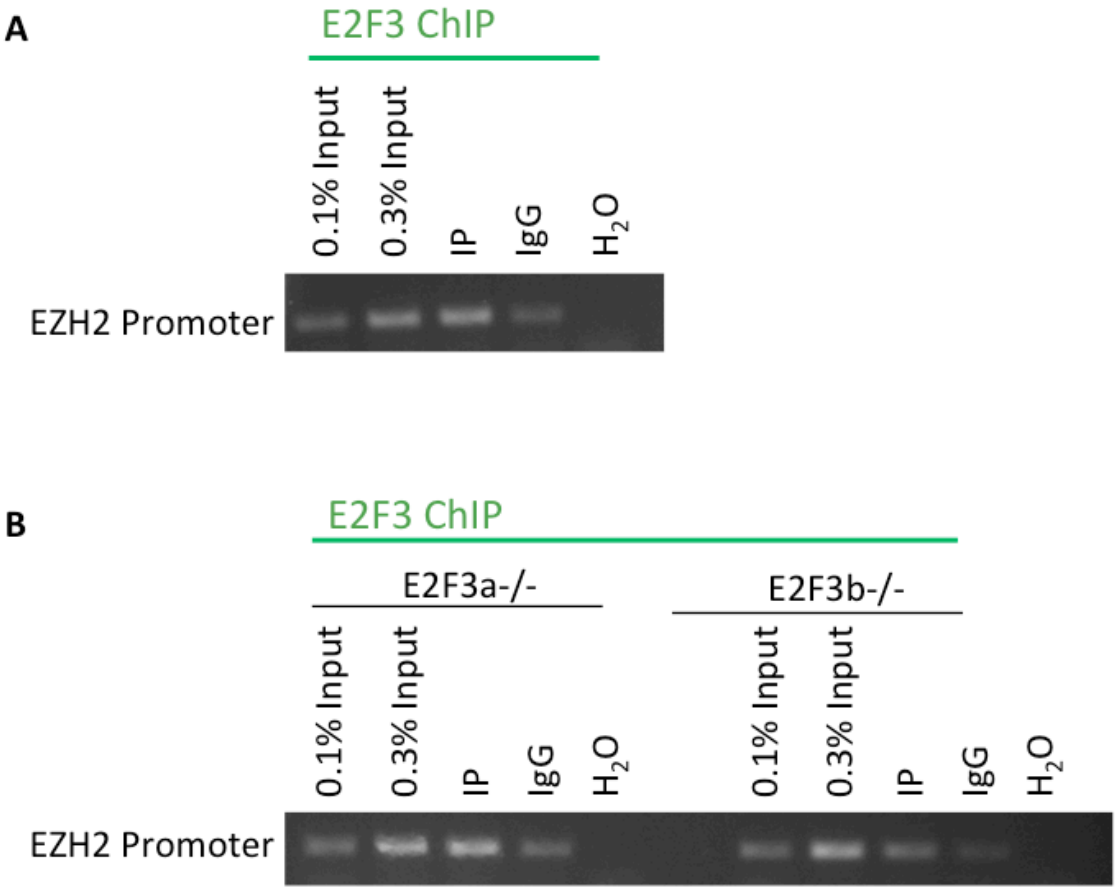

Figure 3-4. E2F3a and E2F3b bind at the *Ezh2* promoter.

E2F3 ChIP experiments were performed on A) *E2f3*$^{+/+}$ and B) *E2f3a*$^{-/-}$ and *E2f3b*$^{-/-}$ neurospheres. 10% Input samples diluted to 0.1% and 0.3% were used as standards. IPs performed with an antibody against E2F3 (IP) were compared against IPs performed with normal IgG of the E2F3 antibody host (IgG) to gauge antibody specificity. Samples were amplified by PCR with primers designed around the *Ezh2* promoter. A PCR product performed with H_2O instead of IP was loaded as a negative control. Images are representative of 4 separate experiments.

specifically identify binding of E2F3a. These ChIPs indicate that both E2F3 isoforms bind at the *Ezh2* promoter.

Taken together, these data suggest that expression of EZH2 is directly regulated by both E2F3 isoforms in proliferating and differentiating NPCs. EZH2 expression is dysregulated in the absence of either E2F3 isoform, although in an opposing manner. In proliferating NPCs lacking both E2F3 isoforms, EZH2 expression mimics that which is seen in *E2f3a*$^{-/-}$ cells. This indicates that E2F3a may play a more predominant role than E2F3b in the regulation of EZH2 expression in NPCs.

3.1.2 Re-expression of EZH2 partially restores secondary neurosphere numbers

As discussed above, PcG proteins have been implicated in the maintenance of stem cell populations. Given that EZH2 expression is dysregulated in the absence of E2F3, we asked if insufficient levels of EZH2 could contribute to the increased numbers of NPCs and their increased capacity for self-renewal observed by neurosphere assays (Figure 3-1). We thus hypothesized that if we restored EZH2 expression to wild-type levels in *E2f3*$^{-/-}$ neurospheres, this may rescue the observed NPC self-renewal defects. This hypothesis was tested with the use of an EZH2-expressing lentivirus engineered to over-express EZH2, which was prepared using the MIEV-EZH2A vector generously provided by Dr. de Haan (Kamminga et al., 2006). The EZH2-expressing virus (LVX-EZH2) and a control virus (LVX-ZsGreen) were used to infect primary cells cultured from the GEs of *E2f3*$^{+/+}$ and *E2f3*$^{-/-}$ E14.5 mice to assess their ability to overexpress EZH2. Western blots of protein extracts from these cells 4 days post-infection show that EZH2 is indeed overexpressed and that *E2f3*$^{+/+}$ levels of EZH2 expression are restored in *E2f3*$^{-/-}$ neurospheres (Figure 3-5A). To determine when EZH2 overexpression begins,

protein extracts from neurospheres were examined by Western blot 1, 3, 5 and 7 days post-infection (Figure 3-5B). The blot shows that overexpression of EZH2 was not observed until after day 3 post-infection despite appearance of ZsGreen fluorescence by day 3 post-infection (Figure 3-5C). Based on these results, it was determined that the LVX-EZH2 could be used to attempt a rescue of the increased self-renewal defect observed in E2F3-/- NPCs.

In order to adequately observe the effects of EZH2 over-expression on neurosphere numbers, wild-type levels of EZH2 would have to be reached in *E2f3*$^{-/-}$ LVX-EZH2 infected NPCs at the onset of neurosphere formation, i.e. in the first 24 hours after plating. Due to the observed delay in overexpression of EZH2 following LVX-EZH2 infection, it was not feasible to use this virus to attempt a rescue experiment in a primary neurosphere assay. However, it was reasonable to use the virus in a secondary neurosphere assay, since neurospheres are dissociated and plated for this assay on day 7 post-infection, individual fluorescent primary spheres of standard width were then individually plucked, dissociated, and plated in single wells in the presence of bFGF. After seven days, the number of neurospheres per well were counted (Figure 3-6). *E2f3*$^{-/-}$ spheres infected with the control LVX-ZsGreen maintained increased numbers compared to their wild-type counterparts as observed in the uninfected secondary neurosphere assay (Figure 3-1). Specifically, *E2f3*$^{-/-}$ neurospheres infected with LVX-ZsGreen displayed a 1.9 fold increase over *E2f3*$^{+/+}$ neurospheres infected with the same virus. *E2f3*$^{-/-}$ spheres infected with LVX-EZH2, although still in greater numbers compared to the E2F3+/+ LVX-ZsGreen-infected spheres, displayed a partial rescue, displaying only a 1.5 fold increase over E2F3+/+ LVX-ZsGreen-infected spheres.

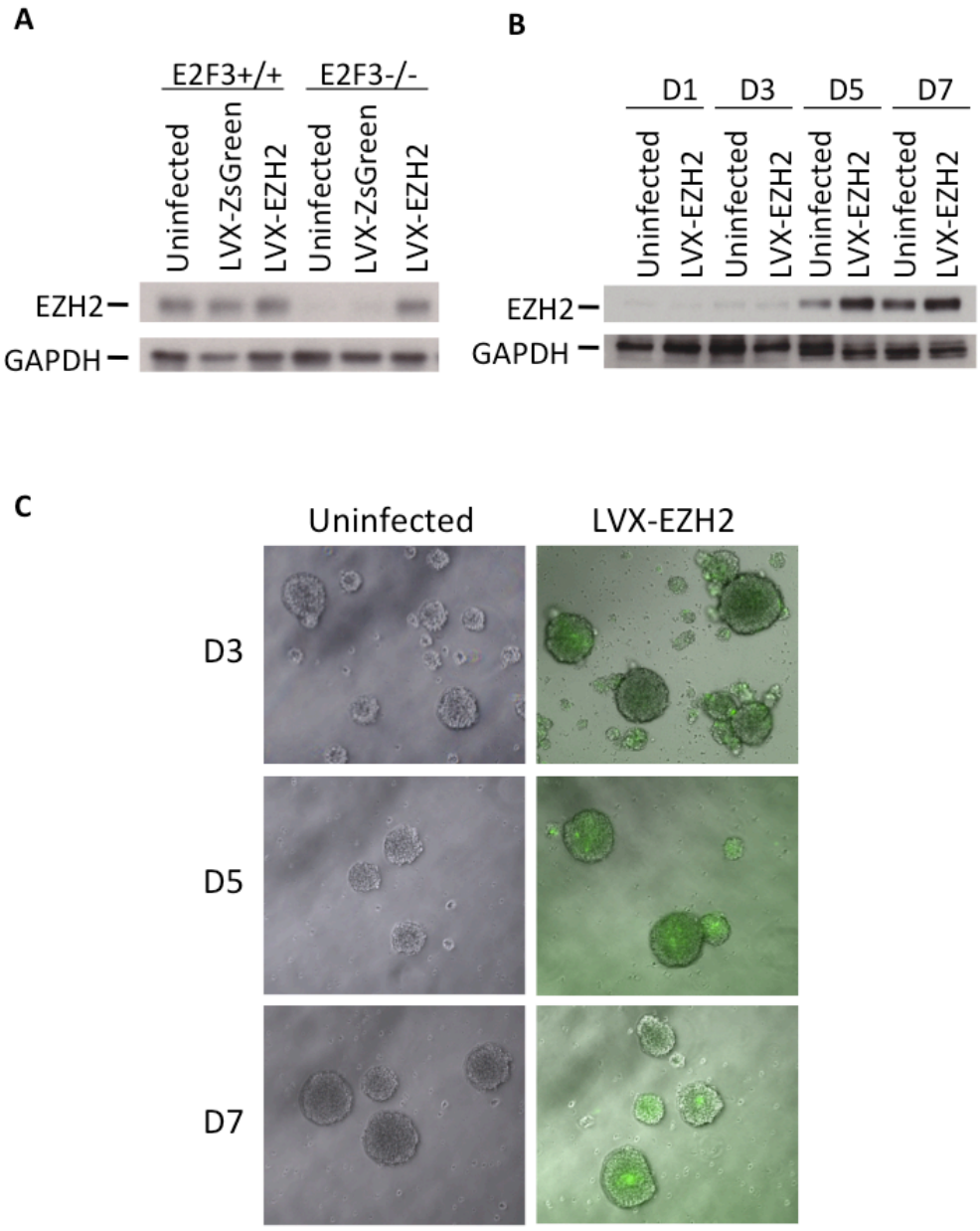

Figure 3-5. LVX-EZH2 recapitulates E2F3+/+ EZH2 levels.

Neurospheres derived from GE of E14.5 mice were incubated with LVX-ZsGreen, LVX-EZH2, or no virus (uninfected) for 3 hours before being diluted with stem cell medium. A) Protein extracts from *E2f3*$^{+/+}$ and *E2f3*$^{-/-}$ neurospheres 4 days post-infection were evaluated for EZH2 (91kDa) overexpression by Western blot; n=3. B) Protein extracts from *E2f3*$^{+/-}$ neurospheres 1 (D1), 3 (D3), 5 (D5), and 7 (D7) days post-infection were evaluated for optimal Ezh2 overexpression.: n=1. GAPDH (38kDa) was used as a loading control. C) Neurospheres infected with LVX-EZH2 and uninfected controls were evaluated for EZH2 overexpression 3 (D3), 5 (D5), and 7 (D7) days post-infection by detection of fluorescence; n=2.

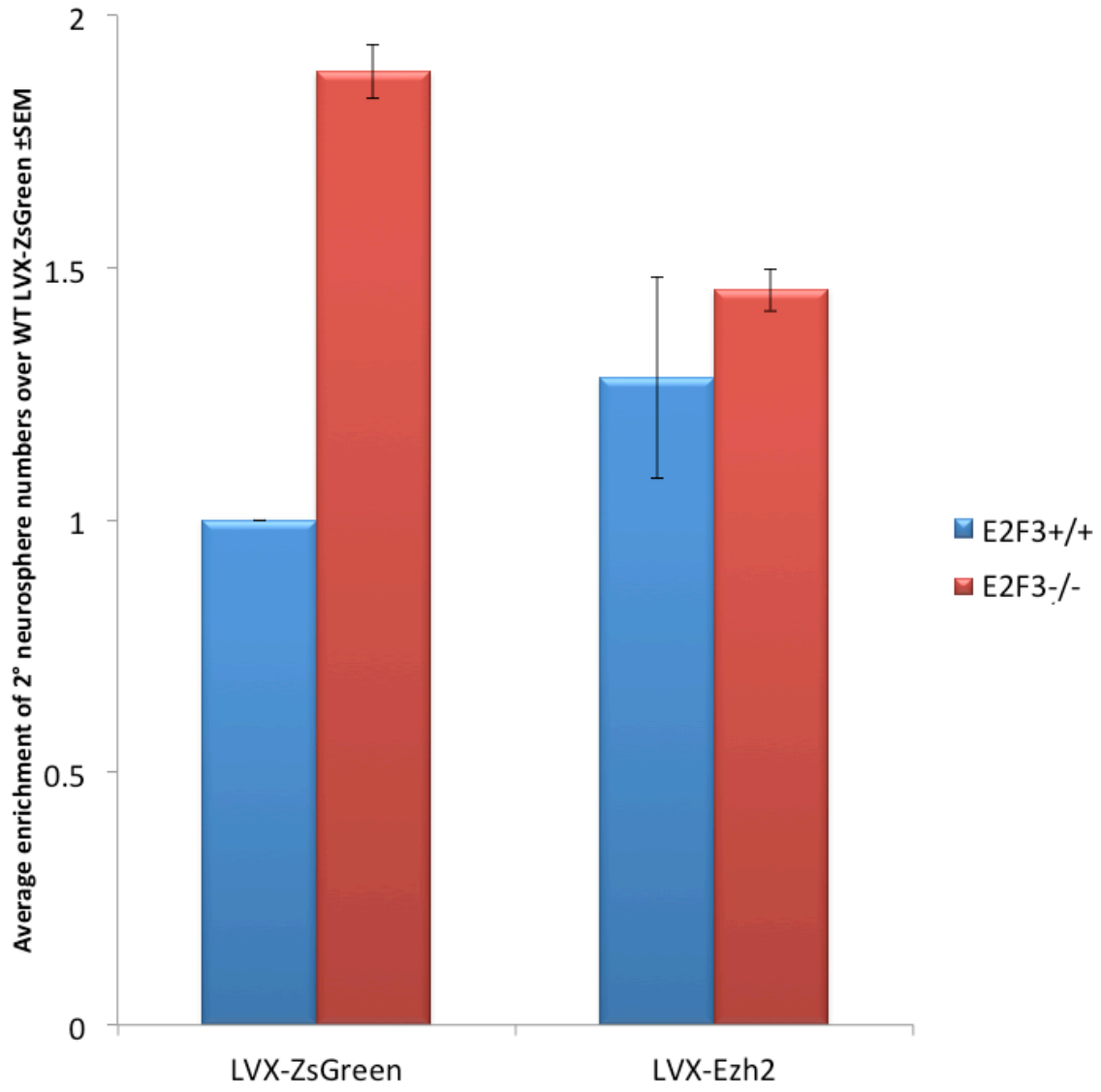

Figure 3-6. Infection with LVX-EZH2 reduces numbers of secondary neurospheres.

E2f3$^{+/+}$ and *E2f3*$^{-/-}$ GE of E14.5 mice was infected with LVX-ZsGreen as a control or with LVX-EZH2. After 7 days in vitro, green spheres of 150±10µm were individually plucked, dissociated, and plated in a 96 well dish. After 7 days, spheres were counted. *E2f3*$^{+/+}$ LVX-ZsGreen averages were normalized to 1. Averages over 12 wells are presented ± SEM. n=2, where n represents an individual experiment with 12 replicate wells.

Although a small sample size (n=2) prevented statistical analyses from being carried out, these results suggest that recapitulating EZH2 expression to wild-type levels may at least partially restore proper maintenance of self-renewal in *E2f3*$^{-/-}$ NPCs.

3.2 E2F3 transcriptionally regulates SOX2 and p16^{INK4a}, key regulators of self-renewal

E2F3 ChIP-on-chip experiments identified numerous potential E2F3 target genes in proliferating NPCs (Julian et al., 2013). Given the observed increase in NPC numbers and their increased capacity to self-renew in the absence of E2F3, I investigated the ChIP-on-chip targets *p16*^{INK4a} and *Sox2* as potential regulatory targets of E2F3, as they have previously been identified as key regulators of neural precursor populations, as discussed in detail above. Figure 1-4 demonstrates the binding sites of E2F3 at these gene targets as determined by E2F3 ChIP-on-chip experiments (Julian et al., 2013). By performing classical ChIP experiments, binding of E2F3 at the first exon of *p16*^{INK4a} and at the *Sox2* promoter was verified (Figure 3-7). Specifically, E2F3 was shown to bind at +289→+492 downstream of the *p16*^{INK4a} transcription start site, which overlaps with its first exon. This first exon has been demonstrated to be a regulatory site for *p16*^{INK4a} transcription (Carragher et al., 2010) and was chosen in order to avoid regulatory regions of *p19*^{Arf} that may be present upstream of *p16*^{INK4a}. E2F3 was also specifically demonstrated to bind at -811→-635 upstream of the *Sox2* transcription start site, a region which overlaps with the *Sox2* promoter (Wiebe et al., 2000).

I next asked whether E2F3 could be directly regulating expression of these two genes through its interaction with their regulatory regions. To answer this question, Western blots were performed to evaluate expression of p16^{INK4a} and SOX2 in the

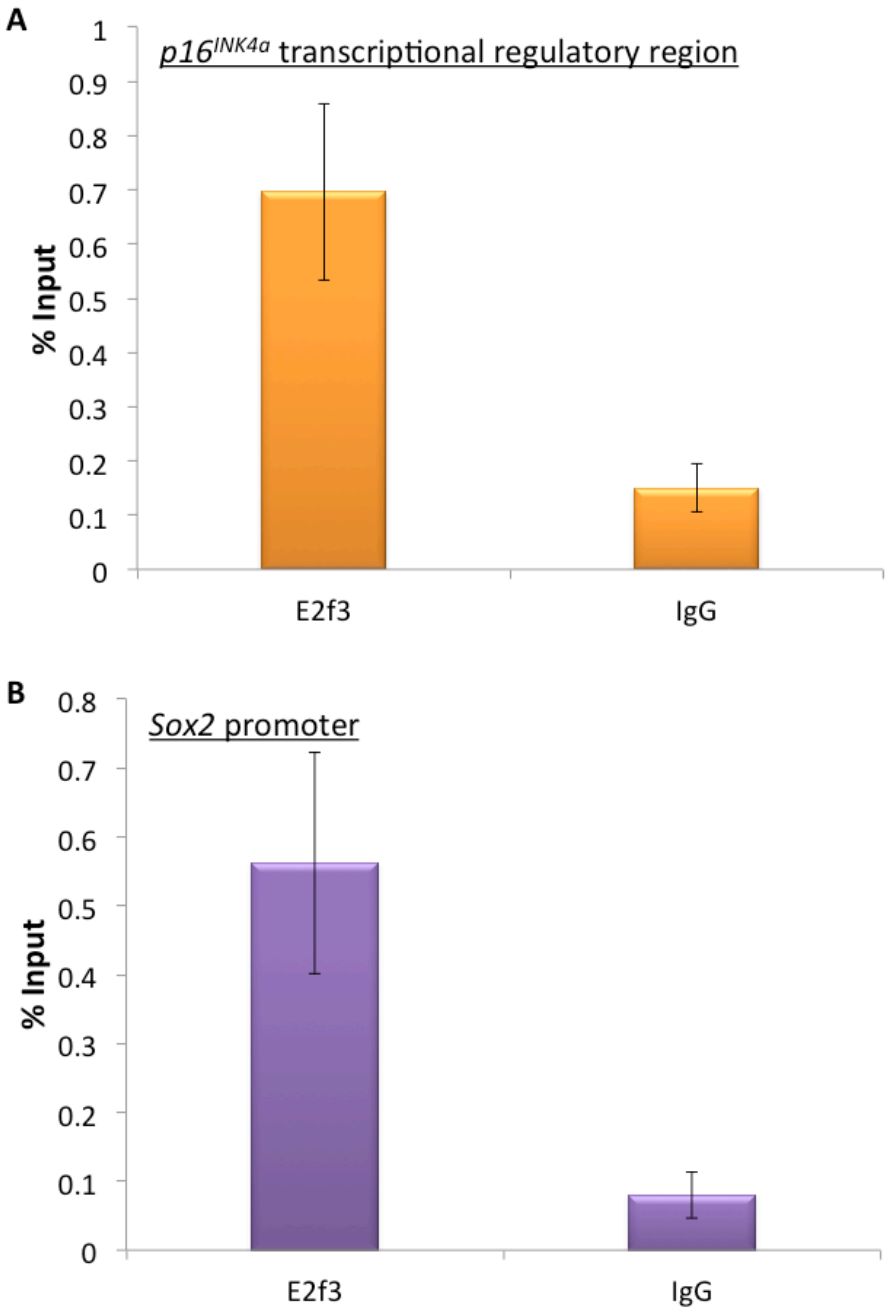

Figure 3-7. E2F3 binds at the transcriptional regulatory regions of *p16*^{INK4a} and *Sox2*.

Chromatin was immunoprecipitated with an antibody directed against E2F3. Input samples along with the immunoprecipitated (IP) sample, and sample incubated with an anti-rabbit IgG antibody (IgG) were amplified by Real-Time PCR using primers specifically designed to amplify the transcriptional regulatory regions of A) *p16*^{INK4a} (n=3) or B) *Sox2* (n=4); data courtesy LM Julian. Julian et al., 2013.

presence and in the absence of E2F3 in proliferating neurosphere cultures. These blots demonstrate that expression of both $p16^{INK4a}$ and SOX2 increase in NPCs in the absence of E2F3 compared to $E2f3^{+/+}$ littermate controls (Figure 3-8). Taken together, ChIP and Western blot data suggest that E2F3 directly and negatively regulates expression of $p16^{INK4a}$ and SOX2 in proliferating NPCs.

3.3 E2F3 may regulate PcG recruitment to target genes

3.3.1 E2F3 and PcG proteins bind overlapping regions of *Sox2* and $p16^{INK4a}$

ChIP-on-chip studies in various cell types have suggested that E2Fs and PcG proteins may regulate similar families of target genes. E2F3 in particular has been suggested to play a role in regulating the recruitment of PRC1 to the $p16^{INK4a}$ locus in MEFs (Miki et al., 2007). We sought to determine whether E2F3 regulates the recruitment of PcG proteins to target genes in neural precursor cells. In order to address this question, we performed ChIP experiments with antibodies directed against a component of the PRC2 complex (SUZ12), a component of the PRC1 complex (MEL18), and the repressive H3K27me3 mark deposited by PRC2. EZH2 would have been used to evaluate the presence of PRC2 at different loci since it is this component of the complex that is down-regulated in the absence of E2F3, but no suitable ChIP antibodies directed against EZH2 were available for these experiments, while ChIP-grade antibodies directed against SUZ12 were commercially available. Since SUZ12 has been demonstrated to be required for EZH2 histone methyltransferase activity and for the structural integrity of PRC2 (Pasini et al., 2004), SUZ12 ChIPs were performed in order to infer the locations

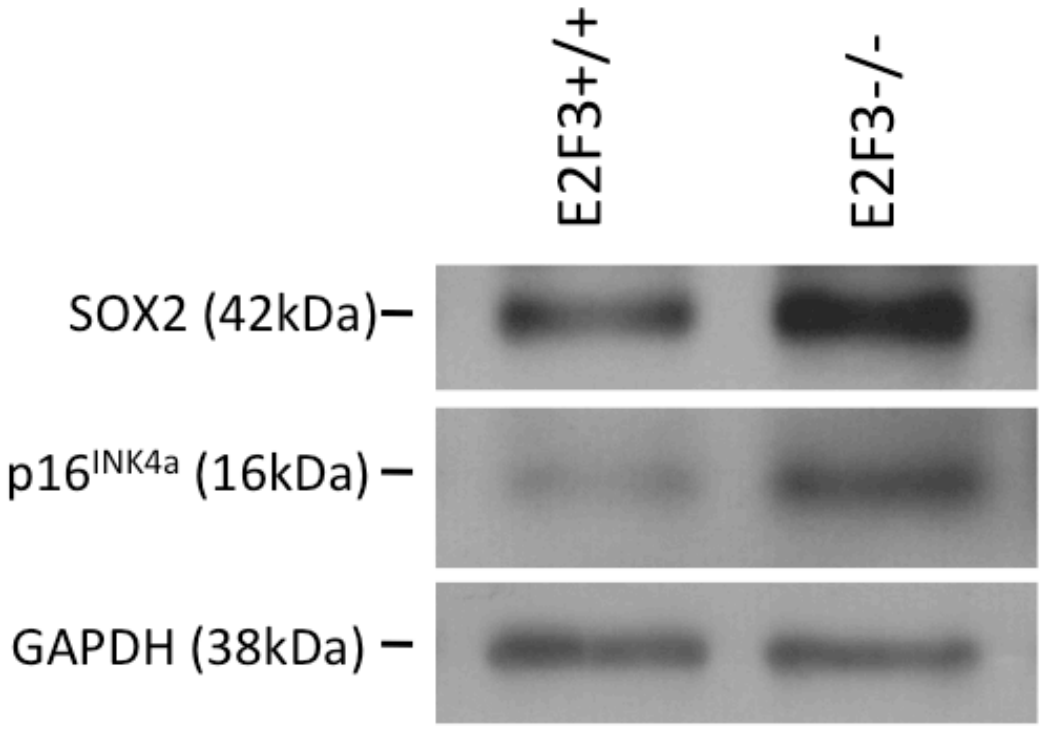

Figure 3-8. SOX2 and p16^{INK4a} expression in E2F3 deficient neural precursors.

Equal amounts of protein extracts from WT and *E2f3*$^{-/-}$ neurospheres derived from GE of E14.5 mice were run on a 10% SDS-PAGE and transferred to a nitrocellulose membrane and probed for the indicated proteins. GAPDH was used as a loading control. Blots are representative of 3 separate experiments.

of PRC2 binding.

To determine whether PRC2 and PRC1 are recruited to the *p16*^{INK4a} and *Sox2* regulatory regions in NPCs, ChIP experiments were first performed with *E2f3*$^{+/+}$ neurospheres. SUZ12, MEL18, and H3K27me3 ChIPs were performed alongside an IgG control and the resultant chromatin fragments for each ChIP were used to run Real-Time PCR with primers designed around the *p16*^{INK4a} (Figure 3-9) and *Sox2* (Figure 3-10) transcriptional regulatory regions, the same regions where E2F3 was demonstrated to bind (Figure 3-7). Each ChIP was performed in triplicate and ChIP IP samples were each normalized to their input values. Normalized SUZ12 IP samples were enriched at least 3.7 fold over IgG, MEL18 IP samples were enriched at least 8.7 fold over IgG, and H3K27me3 IP samples were enriched at least 13.1 fold over IgG. Replicates were not combined, but instead presented individually in Figures 3-9 and 3-10. Although each ChIP IP was enriched at least 3.7 fold above its respective IgG, considerable variability between experiments confounded statistical analysis.

This data confirms previous publications, which demonstrate binding of PRC2 (Bracken et al., 2007; Ezhkova et al., 2009; Kotake et al., 2007) and PRC1 (Bruggeman et al., 2005; Jacobs et al., 1999; Molofsky et al., 2005) at the *p16*^{INK4a} promoter. Although indirect connections have recently been made between *Sox2* regulation and both PRC2 and PRC1 (Marson et al., 2008; Seo et al., 2011; Walker et al., 2011), to our knowledge this is the first time direct binding of either PcG complex has been demonstrated at the *Sox2* promoter.

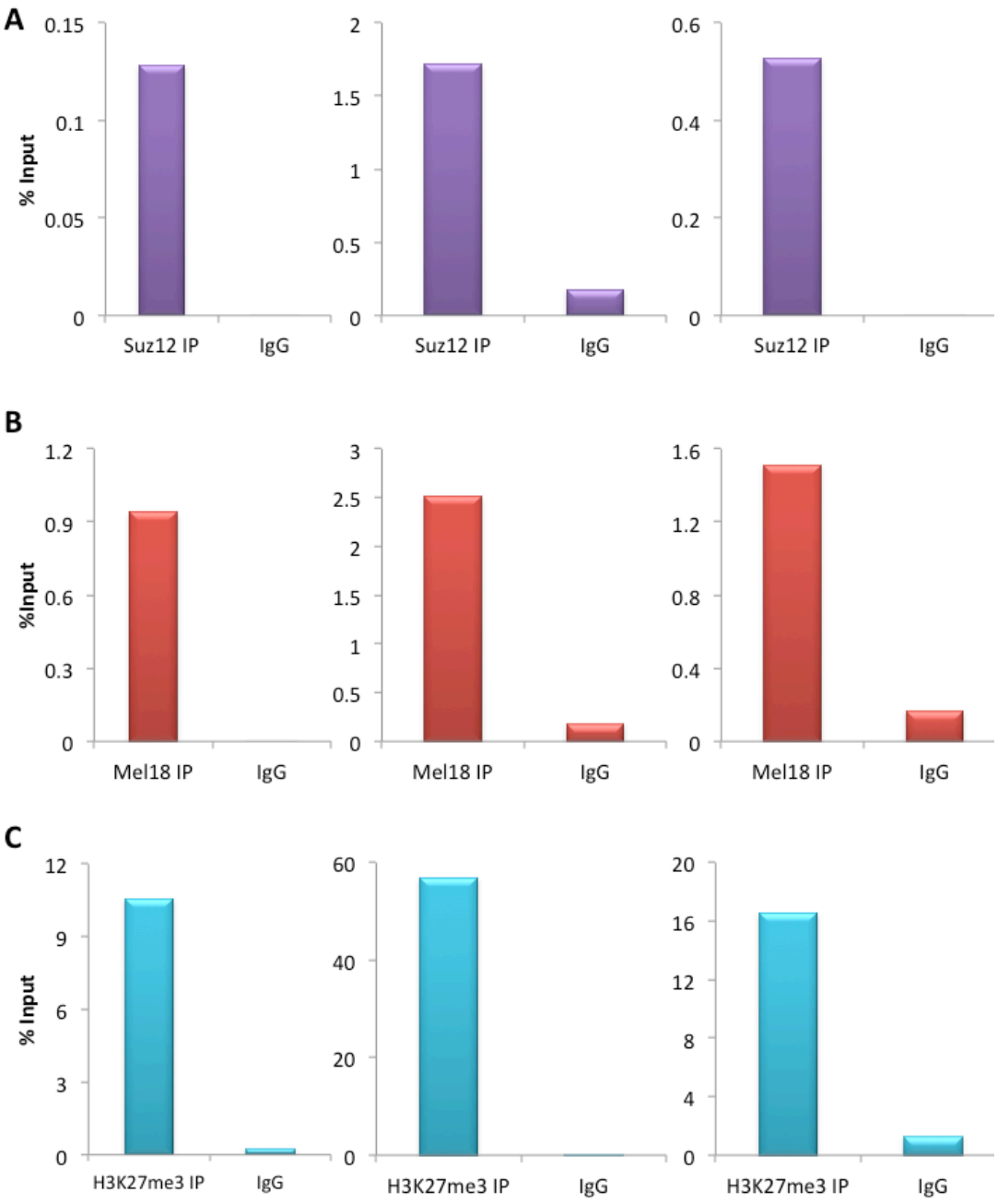

Figure 3-9. Enrichment of PcG proteins at the *p16*^{INK4a} transcription regulatory region.

A) SUZ12 (SUZ12 IP), B) MEL18 (MEL18 IP), and C) H3K27me3 (H3K27me3 IP) ChIPs were performed on *E2f3*$^{+/+}$ neurospheres derived from GE of E14.5 mice. ChIP was also performed with normal IgG of the SUZ12, MEL18, and H3K27me3 antibody hosts (IgG) to gauge antibody specificity. Real-Time PCR was performed using primers designed at the *p16*^{INK4a} transcription regulatory region. SUZ12 IP, MEL18 IP, H3K27me3, and IgG samples were normalized against a standard curve of input sample dilutions. Graphs demonstrate results of 3 separate ChIP experiments.

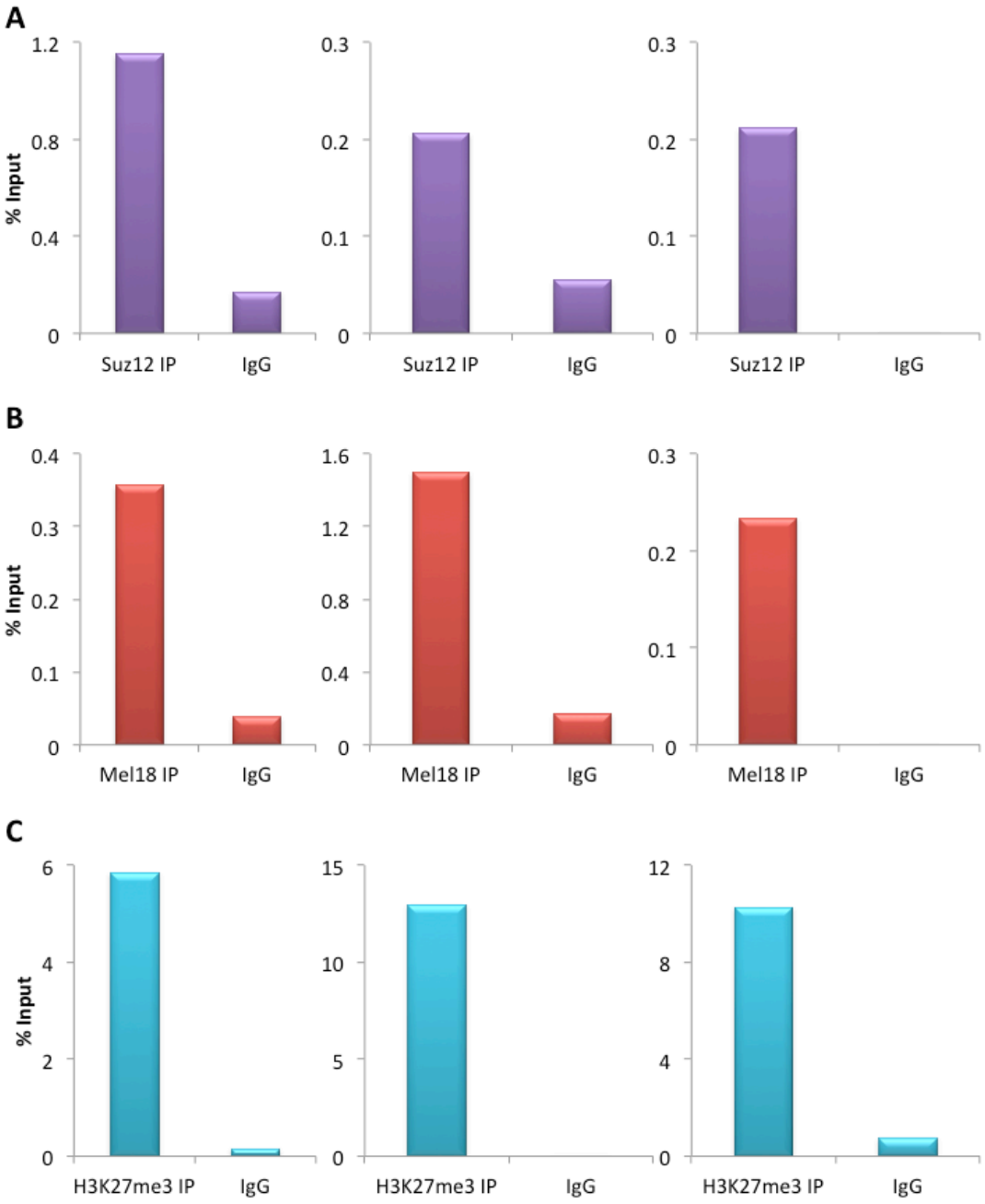

Figure 3-10. Enrichment of PcG proteins at the *Sox2* promoter.

A) SUZ12 (SUZ12 IP), B) MEL18 (MEL18 IP), and C) H3K27me3 (H3K27me3 IP) ChIPs were performed on *E2f3*$^{+/+}$ neurospheres derived from GE of E14.5 mice. ChIP was also performed with normal IgG of the SUZ12, MEL18, and H3K27me3 antibody hosts (IgG) to gauge antibody specificity. Real-Time PCR was performed using primers designed at the *Sox2* transcription regulatory region. SUZ12 IP, MEL18 IP, H3K27me3, and IgG samples were normalized against a standard curve of input sample dilutions. Graphs demonstrate results of 3 separate ChIP experiments.

3.3.2 E2F3 loss affects recruitment of PcG proteins to target genes

Next, we asked whether the absence of E2F3 would disrupt the recruitment of functional PcG complexes to the regulatory regions of *p16*^{INK4a} and *Sox2*. In order to determine if, in the absence of E2F3, functional PRC2 complexes continue to be recruited to target genes, H3K27me3 ChIP experiments were performed with an antibody against trimethylated H3K27. These ChIPs indicated that, in the absence of E2F3, the presence of H3K27me3 decreased by an average of 58.8% at the *p16*^{INK4a} transcriptional regulatory region (p=0.397) (Figure 3-11C) and by an average of 35.4% at the *Sox2* promoter (p=0.012) (Figure 3-11D).

Similarly, MEL18 ChIPs performed with an antibody against MEL18 in *E2f3*$^{+/+}$ and *E2f3*$^{-/-}$ neurospheres demonstrate that in the absence of E2F3, binding of MEL18 to the *p16*^{INK4a} locus decreases by an average of 57.7% (p=0.004) (Figure 3-11A). These data support previously reported findings (Miki et al., 2007), discussed above, which suggest that E2F3 may be involved in the recruitment of PRC1 to the *p16*^{INK4a} locus. Furthermore, binding of MEL18 was also shown to decrease at the *Sox2* promoter in the absence of E2F3, although to a lesser extent and with greater variability (average decrease of 19.2%; p=0.227) (Figure 3-11B). These data indicate that, in the absence of E2F3, the ability of PRC1 to be recruited to, or to remain at, the *p16*^{INK4a} locus is reduced. Potentially due to a low number of repeats (n=3) and variability between ChIP experiments, two-tailed t tests did not reach statistical significance for the *Sox2* locus. However, the trend demonstrated in Figure 3-11B suggests that binding of PRC1 at the *Sox2* locus may also be decreased in the absence of E2F3.

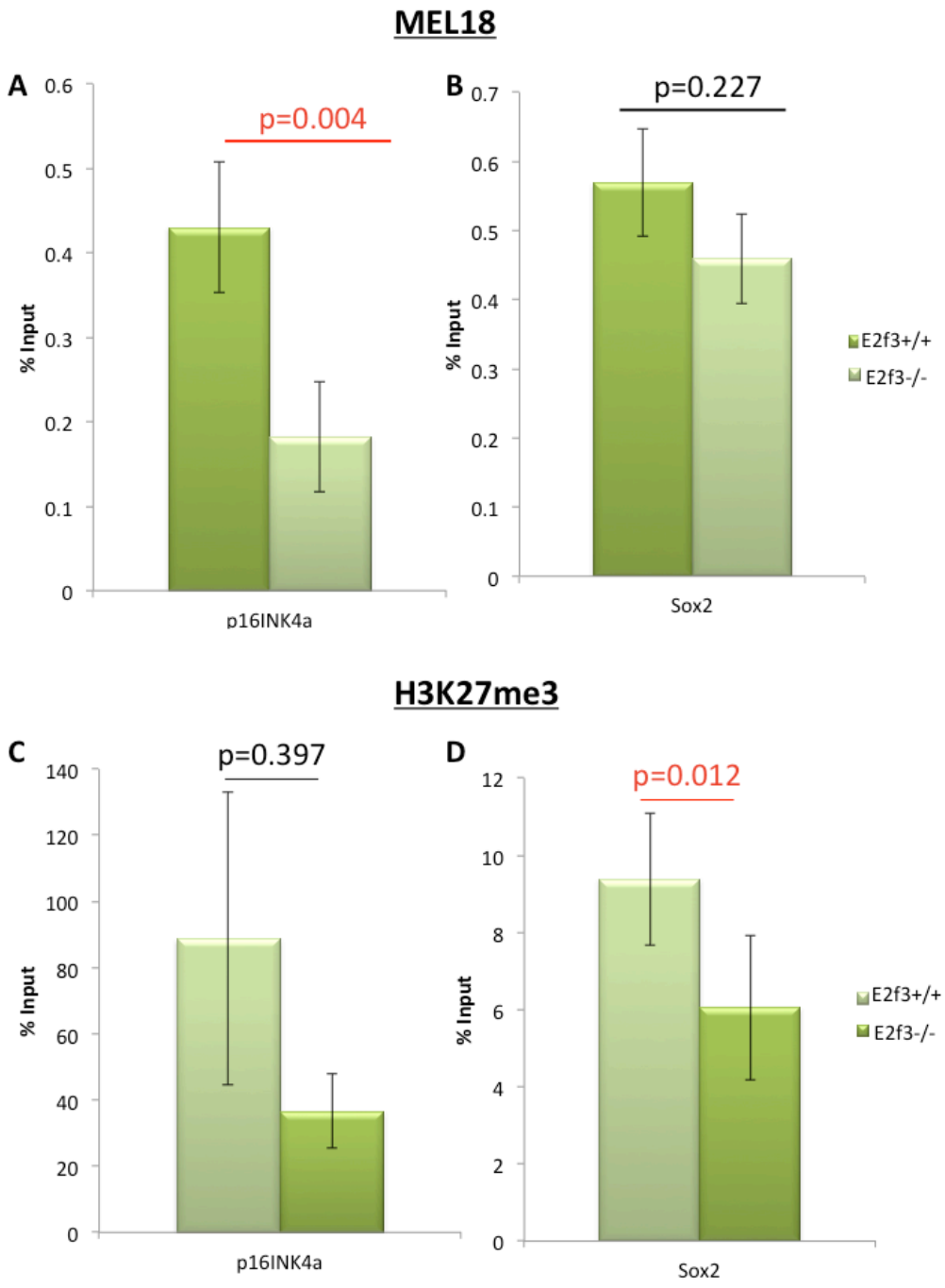

Figure 3-11. Enrichment of PcG proteins at target genes in the absence of E2F3.

MEL18 (A&B) and H3K27me3 (C&D) ChIPs were performed with *E2f3*$^{+/+}$ and *E2f3*$^{-/-}$ neurospheres derived from GE of E14.5 mice. Real-Time PCR was performed using primers designed at the A&C) *p16*^{INK4a} and B&D) *Sox2* transcription regulatory regions. MEL18 IP, H3K27me3 IP, and IgG samples were normalized against a standard curve of input sample dilutions. Normalized IgG values were then subtracted from IP values to account for non-specific binding. Averages of these values are presented ± SEM. n=3.

Although conclusive statements about these results cannot be made due to a lack of statistical significance, taken together, these results demonstrate a trend that in the absence of E2F3, the deposition of the repressive H3K27me3 mark compromised at PcG targets. This defect in H3K27me3 deposition in the absence of E2F3 could subsequently result in the observed decreased recruitment of PRC1 to these targets.

These results present two possibilities: The first is that E2F3 is required to activate sufficient transcription of EZH2 for the formation of PRC2 complexes so that H3K27me3 can be deposited and subsequently recruit PRC1. The second possibility is that E2F3 is required for the recruitment of PRC2 and/or PRC1 to target genes independent of its transcriptional effects on EZH2.

3.3.3 Restoring *E2f3*$^{+/+}$ EZH2 levels in *E2f3*$^{-/-}$ NPCs reduces aberrant target gene expression

To determine if loss of EZH2 in *E2f3*$^{-/-}$ NPCs accounts for deregulated p16^{INK4a} and SOX2 expression, neurospheres infected with LVX-EZH2 were also examined by western blot (Figure 3-12). Following overexpression of EZH2 (day 5 post-infection) in *E2f3*$^{-/-}$ cultures, expression of both p16^{INK4a} and SOX2 was decreased. These data indicate that restoring EZH2 expression is sufficient to repress expression of p16^{INK4a} and SOX2 in the absence of E2F3. These results also suggest that the increase in SOX2 protein levels and the subsequent increase in primary and secondary neurospheres observed in the absence of E2F3 can be attributed, at least in part, to insufficient levels of EZH2. Thus, E2F3 is essential for the regulation of EZH2 in NPCs to ensure the proper regulation of p16^{INK4a} and SOX2.

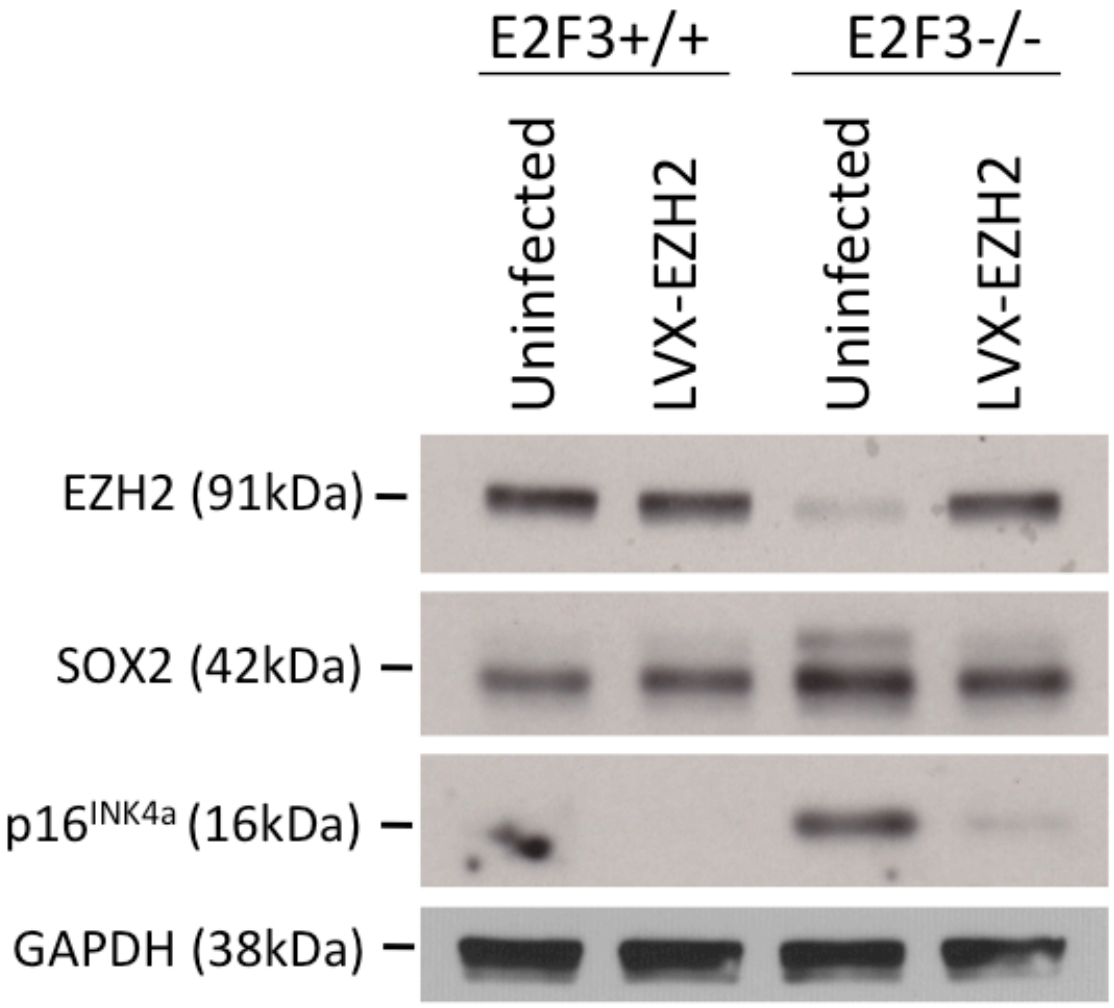

Figure 3-12. SOX2 and p16^{INK4a} expression upon restoration of EZH2 expression.

Equal amounts of protein extracts from *E2f3*$^{+/+}$ and *E2f3*$^{-/-}$ neurospheres 5 days post-infection with LVX-EZH2 were run on a 10% SDS-PAGE and transferred to a nitrocellulose membrane and probed for the indicated proteins. Equal amounts of protein extracts from *E2f3*$^{+/+}$ and *E2f3*$^{-/-}$ uninfected neurospheres were also loaded for comparison. GAPDH was used as a loading control. Blot is representative of two separate experiments.

Chapter 4 - Discussion

4.1 Summary of results

In summary, I have verified previous data from our lab which suggest that NPCs from E14.5 *E2f3*$^{-/-}$ GE are found in greater numbers and have a greater capacity for self-renewal compared to *E2f3*$^{+/+}$ littermate controls. I have also validated E2F3 ChIP-on-chip data from our lab by performing conventional ChIP experiments to demonstrate binding of both E2F3 isoforms at the *Ezh2* promoter as well as western blot experiments, which demonstrated that EZH2 is differentially regulated by E2F3a and E2F3b. In the absence of both isoforms, EZH2 expression is decreased while expression of two other E2F3 targets, p16^{INK4a} and SOX2, is increased. Given the repressive effects of PcG proteins and the potential result of SOX2 overexpression on regulation of neural precursor populations, we hypothesized that recapitulation of EZH2 expression to *E2f3*$^{+/+}$ levels may rescue the aforementioned defects observed in NPC regulation. Restoration of EZH2 was able to at least partly rescue these defects as well as to re-repress p16^{INK4a} and SOX2 expression, demonstrating that E2F3 controls PcG activity at these loci, in part, via transcriptional activity of EZH2.

4.2 E2F3 regulates NPC populations

Our lab has previously demonstrated that E2F3 plays an important role in regulating NPC populations and their capacity for self-renewal; by primary and

secondary neurosphere assays, *E2f3*$^{-/-}$ NPCs were found to be in greater numbers and to have an increased capacity for self-renewal, respectively, when compared to *E2f3*$^{+/+}$ NPCs (Figures 1-3 & 3-1). This was a surprising result, since E2F3 has been previously shown to be required for proliferation in other cell types (Humbert et al., 2000; Leone et al., 1998), while loss of all three activator E2Fs in MEFs resulted in cell cycle arrest (Wu et al., 2001). More recently, however, retinal progenitor cells and embryonic stem cells lacking all three activator E2Fs were reported to be capable of division (Chen et al., 2009; Chong et al., 2009), indicating that the role of E2F3 in regulation of proliferation may be tissue-specific. Additionally, Wenzel and colleagues found that, although E2F3 loss suppresses ectopic proliferation in pRB mutant lenses, proliferation does not decrease below what is observed in WT lenses (Wenzel et al., 2011), indicating that E2F3 may regulate proliferation in a pRB-dependent manner.

In order to better understand how E2F3 may be regulating properties of NPCs, E2F3 ChIP-on-chip experiments were carried out (Julian et al., 2013). These experiments demonstrated that E2F3 binds at the promoter region of, and potentially regulates, multiple genes which have been implicated in neural stem cell maintenance (Julian et al., 2013). The putative targets *p16*^{INK4a}, *Sox2* and several PcG proteins were of particular interest.

4.3 E2F3 regulates transcription of EZH2

Although E2F3 ChIP-on-chip data suggested that E2F3 may regulate all three core components of PRC2 (Figure 1-5), and data from other labs demonstrated that

expression of both EZH2 and EED is regulated by E2F transcription factors (Bracken et al., 2003), EZH2 is the only PRC2 protein to demonstrate dysregulated expression in the absence of E2F3 in NPCs (Figure 3-2). These data suggest that in NPCs, E2F3 is required for the proper transcriptional regulation of only EZH2, and not EED or SUZ12. Given the similar structure and compensatory nature of E2F1-3 (Tsai et al., 2008; Rabinovich et al., 2008), it is reasonable that E2F1, E2F2, or both, may be compensating for loss of E2F3 at the *Eed* and *Suz12* loci, therefore preventing their dysregulation in the absence of E2F3. E2F1 and/or E2F2 may also partially compensate for loss of E2F3 at the *Ezh2* promoter; expression of EZH2 is decreased, but still present, in the absence of E2F3 (Figure 3-2), suggesting that other activating factors may be present.

EZH2 had been previously established as a target of the pRB/E2F pathway (Bracken et al., 2003), and the transcriptional activation of EZH2 by E2F3 has received much attention in recent cancer studies, as both E2F3 and EZH2 were overexpressed in aggressive forms of prostate cancer (Stanbrough et al., 2006; Foster et al., 2004). This indicates that, at least in some cell types, E2F3 may trigger overexpression of EZH2, resulting in hyper-proliferation or tumours. Although E2F3 is generally considered an activating E2F, this view does not always hold true; Figure 3-3 demonstrates the different regulatory effects of the two E2F3 isoforms on EZH2. In Figure 3-3A, EZH2 expression decreases in the absence of E2F3a in proliferating cells, however, its expression increases in the absence of E2F3a upon induction of differentiation. This suggests that E2F3a acts as a transcriptional activator at the *Ezh2* locus during proliferation, but becomes a repressor during differentiation. Indeed, Chong and colleagues compared proliferating cells of the gut crypts to the differentiating cells of the gut villi and determined that

E2F1-3, the classical E2F activators, act as activators only in proliferating cells and switch to a repressive role upon hypophosphorylation of pRB and induction of differentiation (Chong et al., 2009). Conversely, Figure 3-3B shows that E2F3b, generally thought of as a transcriptional repressor, acts as a repressor at the EZH2 promoter only in proliferating cells. Upon induction of differentiation, E2F3b acts as a transcriptional activator. Although not explored by Chong and colleagues, our data could indicate that while E2F activators become repressors upon differentiation, the opposite could be true for E2F repressors.

As previously discussed, despite previous publications reporting that EZH2 positively regulates stem cell maintenance (Juan et al., 2011; Kamminga et al., 2006; Molofsky et al., 2005; Román-Trufero et al., 2009; Villasante et al., 2011), we have observed the opposite effect; E2F3-/- NPCs exhibited decreased expression of EZH2 (Figure 3-2) and had an increased capacity for self-renewal compared with *E2f3*$^{+/+}$ NPCs (Figures 1-3 & 3-1). Furthermore, upon restoring EZH2 expression to *E2f3*$^{+/+}$ levels, numbers of secondary neurospheres generated from *E2f3*$^{-/-}$ NPCs decreased towards *E2f3*$^{+/+}$ levels (Figure 3-6). Much has been published regarding dysregulation of EZH2 and subsequent tumour formation due to p16^{INK4a} repression. Our counter-intuitive results, however, suggest an additional function for EZH2 in stem cell maintenance outside of p16^{INK4a} transcriptional regulation. We have thus demonstrated that the E2F3-EZH2 transcriptional regulatory mechanism is important for the proper regulation of NPC self-renewal.

In separate experiments, our lab has found that E2F3 also regulates NPC self-renewal through transcriptional control of the essential self-renewal gene *Sox2* (Julian et

al., 2013). Based on our own E2F3 ChIP-on-chip studies (Julian et al., 2013) as well as previous studies which suggest that E2F3 and EZH2 may have overlapping target genes (Miki et al., 2007), we next asked whether E2F3 may play a role in recruitment of PcG proteins to target genes. The genes $p16^{INK4a}$ and *Sox2* were chosen due to enrichment of both E2F3 and PcG proteins at these loci, as well as their transcriptional dysregulation in the absence of E2F3.

4.4 EZH2 regulates SOX2 expression

Increased SOX2 expression in $E2f3^{-/-}$ NPCs compared to $E2f3^{+/+}$ (Figure 3-8) was not surprising, given the established positive role of SOX2 in neural stem cell maintenance (Ellis et al., 2004; Graham et al., 2003); as numbers of NPCs increase and as the proportion of self-renewing NPCs in a neurosphere increase, one would also expect to observe an increase in factors that positively govern these cells' multipotent identity. It was surprising, however, for our data to indicate that, in addition to E2F3, PcG proteins also bind at the *Sox2* promoter (Figures 3-10). In ChIP-on-chip and classical ChIP studies performed in embryonic stem cells, the *Sox2* promoter has not been reported to be bound by any PcG protein nor does it have any repressive chromatin marks (Bracken et al., 2006; Ku et al., 2008; Mikkelsen et al., 2007; Pan et al., 2007; Squazzo et al., 2006; Villasante et al., 2011; Zhao et al., 2007). Figure 3-10, however, demonstrates the presence of SUZ12, MEL18, and H3K27me3 at the *Sox2* promoter, indicating that both PRC2 and PRC1 bind at this locus in NPCs.

Furthermore, recapitulation of EZH2 expression to *E2f3*$^{+/+}$ levels in *E2f3*$^{-/-}$ NPCs is sufficient to restore SOX2 expression to near *E2f3*$^{+/+}$ levels (Figure 3-12). Recent literature has suggested that SOX2 expression decreases as NPCs become committed and lose their capacity to self-renew (Hutton and Pevny, 2011). A mechanism for repressing SOX2 expression must therefore exist. Given ChIP data demonstrating the presence of PRC2 and PRC1 at the *Sox2* promoter (Figure 3-10), as well as rescue of SOX2 expression upon recapitulation of EZH2 *E2f3*$^{+/+}$ expression levels (Figure 3-12), PcG proteins may be at least one method used by the neural precursor cell to repress SOX2 expression. Additionally, Figure 3-6 demonstrates that restoring EZH2 expression to *E2f3*$^{+/+}$ levels decreases *E2f3*$^{-/-}$ NPC self-renewal capacity towards that of *E2f3*$^{+/+}$ NPCs. Taken together, our data suggest that EZH2 is an important regulator of SOX2 expression and thus of NPC self-renewal properties, and that its transcriptional regulation by E2F3 is a key aspect of this function.

4.5 EZH2 regulates p16^{INK4a} expression

Increased levels of EZH2 have been found in multiple forms of human cancer (Li et al., 2010; Pietersen et al., 2008; Rao et al., 2010; Taniguchi et al., 2012; Varambally et al., 2002), while loss or down-regulation of EZH2 typically results in decreased stem cell self-renewal (Aoki et al., 2010; Chang et al., 2011; Juan et al., 2011; Luis et al., 2011). These effects are thought to be due to repression of p16^{INK4a} by PcG protein complexes in stem cells and proliferating precursor cells (Bracken et al., 2007; Ezhkova et al., 2009; Kotake et al., 2007; Maertens et al., 2009). Typically, increased p16^{INK4a} expression is

indicative of senescence (Michaloglou et al., 2005) and is turned on in response to cellular stress or oncogenic signals to prevent aberrant proliferation and tumour formation. As cells age and senesce, expression of PcG proteins decreases, allowing de-repression of $p16^{INK4a}$, and thus preventing further cell cycling.

Our findings are therefore counter-intuitive: in the absence of E2F3, we have found a decrease in EZH2 expression (Figure 3-2A) and a concurrent increase in $p16^{INK4a}$ expression (Figure 3-8). Since $p16^{INK4a}$ is a CDKI, its overexpression in *E2f3*$^{-/-}$ NPCs should cause cell cycle arrest (Serrano, 1997). Instead, there are increased numbers of *E2f3*$^{-/-}$ NPCs compared to *E2f3*$^{+/+}$ NPCs, and these cells have demonstrated an increased capacity for self-renewal (Figures 1-3 & 3-1). This apparent contradiction could indicate that this population of cells is receiving hyper-proliferative signals and is simultaneously increasing its $p16^{INK4a}$ expression in attempts to prevent tumour formation. Yet, based on neurosphere assay data, increased expression of this CDKI in *E2f3*$^{-/-}$ NPCs appears to be insufficient to impede an increase in NPC numbers. An interesting further study would be to determine if the dysregulation of embryonic NPC populations leads to an eventual depletion of NPCs in the adult brain.

When considering these data, one must be aware that protein from whole cell lysates was used to evaluate protein expression levels. Haller and colleagues, however, have examined both cytoplasmic and nuclear expression levels of $p16^{INK4a}$ in gastrointestinal stromal tumours and have found that tumour progression is associated with low levels of nuclear and high levels of cytoplasmic $p16^{INK4a}$ (Haller et al., 2010). Nuclear $p16^{INK4a}$ is thought to regulate the cell cycle (Adams, 2001), while cytoplasmic $p16^{INK4a}$ has no known function as of yet. Still, expression of cytoplasmic $p16^{INK4a}$ has

been found to correlate with poor prognosis in several tumour types (Emig et al., 1998; Evangelou et al., 2004; Milde-Langosch et al., 2001), including high-grade astrocytomas (Arifin et al., 2006). High levels of cytoplasmic $p16^{INK4a}$ may be responsible for low levels of nuclear $p16^{INK4a}$ due to a negative feedback loop, allowing cells to continue to proliferate (Haller et al., 2010). A second possibility could be that the cell is attempting to silence the effects of $p16^{INK4a}$ by sequestering the CDKI to the cytoplasm where it cannot regulate the cell cycle (Evangelou et al., 2004). A third possibility is that inadequate levels of newly synthesized $p16^{INK4a}$ are being shuttled into the nucleus after translation due to defects in nuclear chaperone proteins (Evangelou et al., 2004). Regardless of the mechanism by which it functions, given the correlation between high levels of cytoplasmic $p16^{INK4a}$ and poor tumour prognosis, the cellular localization of $p16^{INK4a}$ in *E2f3*$^{+/+}$ and *E2f3*$^{-/-}$ NPCs should be evaluated to better understand how $p16^{INK4a}$ overexpression could coincide with increased numbers of NPCs with increased capacity for self-renewal.

Alternatively, specific defects in the pRB-E2F pathway have been shown to allow cells to bypass induction of cell cycle arrest despite increased $p16^{INK4a}$ expression (Lukas et al., 1996). For instance, cells overexpressing E2F1, E2F2, or E2F3 are capable of bypassing the cell cycle arrest and entering S phase (Lukas et al., 1996). Although it has not yet been fully examined, the absence of E2F3 may cause an up-regulation of other cell cycle proteins. Expression levels of other E2Fs and many other important cell cycle genes remain to be evaluated. Additionally, other E2Fs may demonstrate compensatory binding at specific genomic sites in the absence of E2F3, regardless of a potential dysregulation in their expression. If, and how, changes in expression of cell cycle

proteins contribute to the observed increase in primary and secondary neurospheres (Figures 1-3 & 3-1) remains to be elucidated.

4.6 PcG protein enrichment changes in the absence of E2F3

In order to further elucidate the repressive effects of PcG proteins at both *Sox2* and $p16^{INK4a}$ as well as the potential role of E2F3 in this process, ChIP experiments were carried out with antibodies directed against either MEL18 or H3K27me3. Enrichment of MEL18 at both $p16^{INK4a}$ and *Sox2* decreased in the absence of E2F3 compared to $E2f3^{+/+}$, although to a lesser extent and with greater variability at the *Sox2* promoter (Figures 3-11A&B). Enrichment of H3K27me3 also decreased at these target genes in the absence of E2F3, although to a lesser extent and with greater variability at the $p16^{INK4a}$ regulatory region (Figure 3-11C&D). Given that PRC1 is thought to be recruited to target genes following the deposition of H3K27me3 by PRC2 (Cao et al., 2002), decreased trimethylation of H3K27 would explain the decreased binding of PRC1 observed in the absence of E2F3. These results suggest that PRC2 has decreased ability to trimethylate H3K27 at the $p16^{INK4a}$ and *Sox2* transcriptional regulatory regions in the absence of E2F3.

Decreased enrichment of PRC1 and PRC2 at these target genes in the absence of E2F3 could result from several possibilities: first, down-regulation of EZH2 expression in the absence of E2F3 may limit the number of functional PRC2 complexes, leading to a global decrease in H3K27 methylation. Secondly, E2F3 may be required for proper

recruitment of PRC2, and subsequent recruitment of PRC1, to the *p16*^{INK4a} and *Sox2* genes. It is important to note that these two possibilities are not necessarily mutually exclusive. In order to further explore these two possibilities, *E2f3*$^{+/+}$ and *E2f3*$^{-/-}$ NPCs were infected with a lentivirus that overexpresses EZH2 (LVX-EZH2). The resultant *E2f3*$^{-/-}$ neurospheres not only exhibited EZH2 expression restored to near *E2f3*$^{+/+}$ levels, but also demonstrated p16^{INK4a} and SOX2 expression levels that approached *E2f3*$^{+/+}$ levels (Figure 3-12). This finding suggests that restoring EZH2 expression to *E2f3*$^{+/+}$ levels in NPCs lacking E2F3 is sufficient to re-repress p16^{INK4a} and SOX2 expression. Therefore, the dysregulation of p16^{INK4a} and SOX2 in the absence of E2F3 appears to be largely due to the transcriptional effect of E2F3 on EZH2.

However, since increased capacity for self-renewal in *E2f3*$^{-/-}$ NPCs is not completely rescued upon restoration of EZH2 expression (Figure 3-6), this indicates that E2F3 contributes to regulation of neural precursor populations independently of its transcriptional effects on EZH2 expression. E2F3 could have transcriptional effects on other genes essential for proper regulation of NPC self-renewal. Furthermore, a potential role for E2F3 in recruiting PcG proteins to target genes cannot be ruled out. Despite restoration of EZH2 expression, in the absence of E2F3, proper recruitment of PcG proteins to target genes may remain dysregulated. Further studies are required to examine the effects of restoring EZH2 expression in *E2f3*$^{-/-}$ NPCs on PcG recruitment to target genes.

4.7 Future Directions

Although restoring *E2f3*$^{+/+}$ EZH2 expression levels in *E2f3*$^{-/-}$ NPCs is sufficient to largely rescue dysregulated expression of p16^{INKa} and SOX2, it remains insufficient to rescue the increased capacity for self-renewal of *E2f3*$^{-/-}$ NPCs. By comparing our E2F3 ChIP-on-chip data to PcG ChIP-on-chip or ChIP-Seq data from other labs, a large overlap between gene targets is observable. One possible explanation for this observation is that E2F3 plays a role in recruiting PcG proteins to its gene targets. To further explore the potential role of E2F3 in regulating recruitment of EZH2, it is important to elucidate whether recruitment of PcG proteins is dysregulated in the absence of E2F3. In order to do this, enrichment of multiple PcG gene targets would have to be examined both in the presence and in the absence of E2F3. This could be accomplished by performing a series of ChIP-on-chip or ChIP-Seq experiments in parallel with antibodies directed against components of both PRC1 and PRC2 as well as the repressive H3K27me3 histone modification deposited by EZH2. Of course, we would have to account for the decreased expression of EZH2 in *E2f3*$^{-/-}$ NPCs. This would be accomplished by using the LVX-EZH2 virus to restore *E2f3*$^{+/+}$ EZH2 expression levels to *E2f3*$^{-/-}$ NPCs. We could therefore examine changes in EZH2 recruitment in the absence of E2F3, independent of the effects of E2F3 on EZH2 expression, on a large scale. Using microarray data, it would also be possible to examine the resultant changes in gene expression in the absence of E2F3 as well as changes when EZH2 expression has been restored to *E2f3*$^{+/+}$ levels.

Another aspect of this research that warrants further investigation is the effect of dysregulated EZH2 expression on differentiation of *E2f3*$^{-/-}$ NPCs. A role for PcG proteins in differentiation of various tissues has been well established (Bracken et al.,

2006; Sher et al., 2008; Hirabayashi et al., 2009; Sher et al., 2012). Specific to differentiation of neural precursor cells, EZH2 expression levels have been demonstrated to influence cell fate choices. Sher and colleagues demonstrated that EZH2, which is highly expressed in proliferating NPCs, shows markedly decreased expression upon differentiation to neurons, is completely repressed upon differentiation to astrocytes, but remains highly expressed upon differentiation to oligodendrocytes (Sher et al., 2008). Additionally, NPCs lacking EZH2 have been shown to have an increased neurogenic phase with a resulting delayed astrogenic phase, indicating a temporal regulatory role for EZH2 (Hirabayashi et al., 2009). Given that we have demonstrated dysregulated expression of EZH2 in the absence of either E2F3 isoform upon induction of differentiation (Figure 3-3), potential effects of E2F3 loss on differentiating NPCs should be examined by differentiation assay.

It would also be interesting to explore the possibility of rescuing any potential dysregulation of differentiating *E2f3*$^{-/-}$ NPCs by restoring EZH2 to *E2f3*$^{+/+}$ expression levels. As previously discussed, several groups have suggested that EZH2 expression fluctuates throughout proliferation and differentiation to regulate cell fate choice of NPCs (Sher et al., 2008; Hirabayashi et al., 2009). However, upon differentiation, PcG complexes have been shown to dissociate from target genes which are only activated during differentiation, but remain consistently bound to target genes that are activated during proliferation and repressed during differentiation (Bracken et al., 2006). The latter group of target genes continue to be expressed during proliferation, despite PcG protein binding at these sites. Thus, restoring *E2f3*$^{+/+}$ expression levels of EZH2 in *E2f3*$^{-/-}$ NPCs

during proliferation may be sufficient to correct potential dysregulation of differentiation in these cells.

4.8 Conclusions

The work presented in this thesis has verified previous findings from our lab, which suggest that in the absence of E2F3, numbers of NPCs increase along with their capacity for self-renewal. It also supports previous work done by Bracken and colleagues, which demonstrates that expression of EZH2 is regulated by the pRB-E2F pathway (Bracken et al., 2006). Furthermore, this work has demonstrated a novel function for E2F3, specifically the transcriptional regulation of EZH2 in regulating NPC self-renewal (Figure 4-1). Additionally, I have demonstrated that both E2F3 and EZH2 bind at the transcriptional regulatory regions of two key regulators of stem cell populations; $p16^{INK4a}$ and *Sox2* (Figure 4-1). E2F3 appears to regulate expression of these target genes through transcriptional regulation of EZH2. However, a role for E2F3 in recruiting PcG proteins to target genes cannot be refuted as of yet and will require future investigations to further explore this possibility. The implications of these findings contribute to the on-going research of how expression and recruitment of PcG proteins is regulated, both spatially and temporally, as well as which target genes E2F3 and PcG proteins regulate to control stem cell functions. Elucidation of these mechanisms will be essential in the design of future cancer therapeutics aimed at correcting dysregulation of PcG proteins.

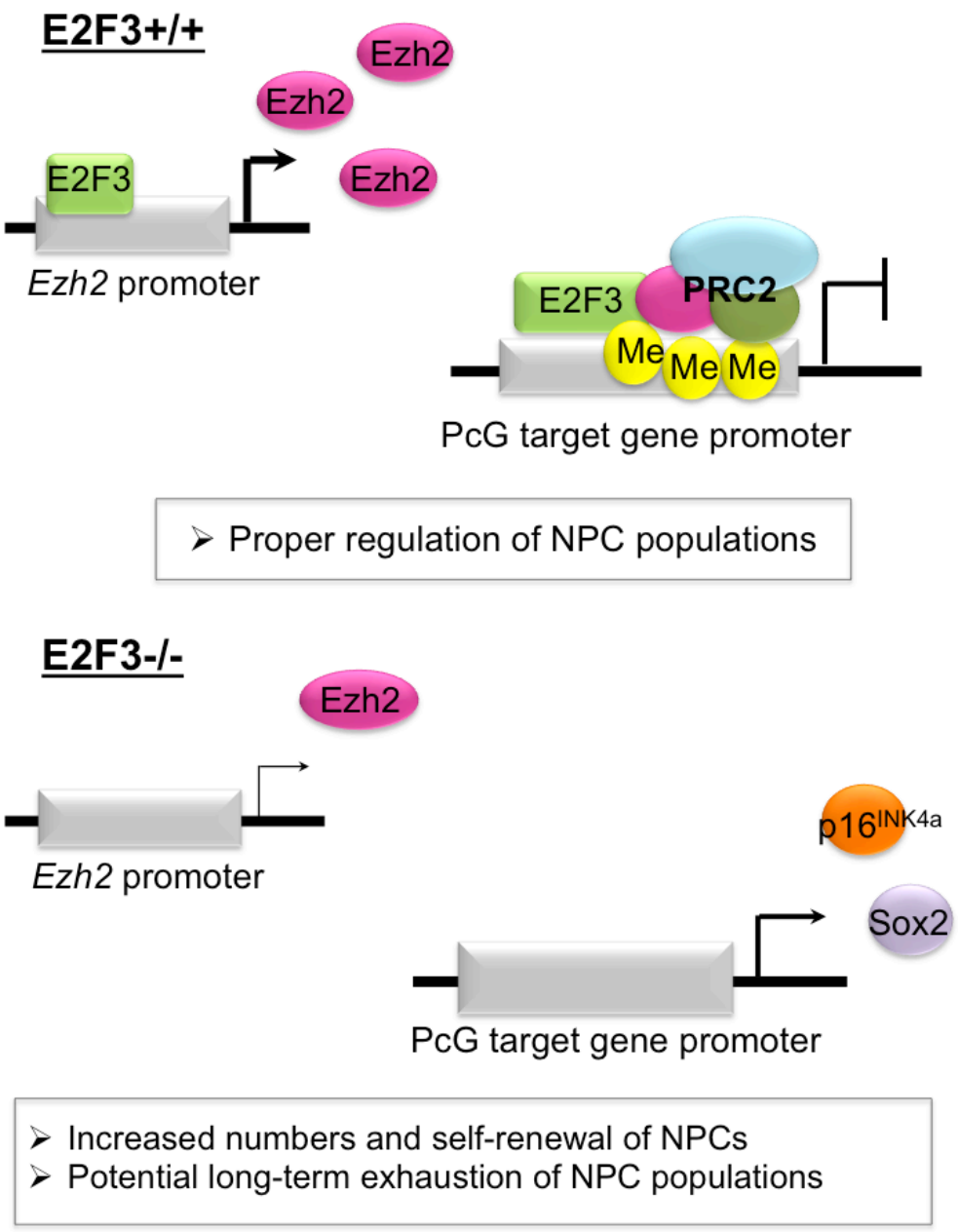

Figure 4-1. Model of the role of E2F3 and PRC2 in regulating target gene expression.

In *E2f3*$^{+/+}$ NPCs, E2F3 binds at the *Ezh2* promoter, activating expression of EZH2. Both E2F3 and PRC2 can then bind at the transcriptional regulatory regions of target genes with the resulting effect of repressing target gene expression. In the absence of E2F3 (*E2f3*$^{-/-}$), EZH2 expression is downregulated and enrichment of PRC2 at target genes is decreased, resulting in derepression of target gene expression, such as p16^{INK4a} and SOX2.

Chapter 5 - References

Adams, M.R., R. Sears, F. Nuckolls, G. Leone, and J.R. Nevins. 2000. Complex transcriptional regulatory mechanisms control expression of the E2F3 locus. *Mol. Cell. Biol.* 20:3633–3639.

Adams, P.D. 2001. Regulation of the retinoblastoma tumor suppressor protein by cyclin/cdks. *Biochim. Biophys. Acta*. 1471:M123–33.

Aoki, R., T. Chiba, S. Miyagi, M. Negishi, T. Konuma, H. Taniguchi, M. Ogawa, O. Yokosuka, and A. Iwama. 2010. The polycomb group gene product Ezh2 regulates proliferation and differentiation of murine hepatic stem/progenitor cells. *J. Hepatol.* 52:854–863.

Arifin, M.T., S. Hama, Y. Kajiwara, K. Sugiyama, T. Saito, S. Matsuura, F. Yamasaki, K. Arita, and K. Kurisu. 2006. Cytoplasmic, but not nuclear, p16 expression may signal poor prognosis in high-grade astrocytomas. *J. Neurooncol.* 77:273–277.

Attwooll, C., S. Oddi, P. Cartwright, E. Prosperini, K. Agger, P. Steensgaard, C. Wagener, C. Sardet, M.C. Moroni, and K. Helin. 2005. A novel repressive E2F6 complex containing the polycomb group protein, EPC1, that interacts with EZH2 in a proliferation-specific manner. *J. Biol. Chem.* 280:1199–1208.

Avilion, A.A., S.K. Nicolis, L.H. Pevny, L. Perez, N. Vivian, and R. Lovell-Badge. 2003. Multipotent cell lineages in early mouse development depend on SOX2 function. *Genes Dev.* 17:126–140.

Bani-Yaghoub, M., R.G. Tremblay, J.X. Lei, D. Zhang, B. Zurakowski, J.K. Sandhu, B. Smith, M. Ribecco-Lutkiewicz, J. Kennedy, P.R. Walker, and M. Sikorska. 2006. Role of Sox2 in the development of the mouse neocortex. *Dev. Biol.* 295:52–66.

Barde, I., P. Salmon, and D. Trono. 2010. Production and titration of lentiviral vectors. *Curr Protoc Neurosci*. Chapter 4:Unit 4.21.

Beisel, C., A. Imhof, J. Greene, E. Kremmer, and F. Sauer. 2002. Histone methylation by the Drosophila epigenetic transcriptional regulator Ash1. *Nature*. 419:857–862.

Bernstein, B.E., T.S. Mikkelsen, X. Xie, M. Kamal, D.J. Huebert, J. Cuff, B. Fry, A. Meissner, M. Wernig, K. Plath, R. Jaenisch, A. Wagschal, R. Feil, S.L. Schreiber, and E.S. Lander. 2006. A bivalent chromatin structure marks key developmental genes in embryonic stem cells. *Cell*. 125:315–326.

Blais, A., C.J.C. van Oevelen, R. Margueron, D. Acosta-Alvear, and B.D. Dynlacht. 2007. Retinoblastoma tumor suppressor protein-dependent methylation of histone H3 lysine 27 is associated with irreversible cell cycle exit. *J. Cell Biol.* 179:1399–1412.

Blais, A., M. Tsikitis, D. Acosta-Alvear, R. Sharan, Y. Kluger, and B.D. Dynlacht. 2005. An initial blueprint for myogenic differentiation. *Genes Dev.* 19:553–569.

Bracken, A.P., D. Kleine-Kohlbrecher, N. Dietrich, D. Pasini, G. Gargiulo, C. Beekman, K. Theilgaard-Mönch, S. Minucci, B.T. Porse, J.-C. Marine, K.H. Hansen, and K. Helin. 2007. The Polycomb group proteins bind throughout the INK4A-ARF locus and are disassociated in senescent cells. *Genes Dev.* 21:525–530.

Bracken, A.P., D. Pasini, M. Capra, E. Prosperini, E. Colli, and K. Helin. 2003. EZH2 is downstream of the pRB-E2F pathway, essential for proliferation and amplified in cancer. *EMBO J.* 22:5323–5335.

Bracken, A.P., N. Dietrich, D. Pasini, K.H. Hansen, and K. Helin. 2006. Genome-wide mapping of Polycomb target genes unravels their roles in cell fate transitions. *Genes Dev.* 20:1123–1136.

Brazel, C.Y., T.L. Limke, J.K. Osborne, T. Miura, J. Cai, L. Pevny, and M.S. Rao. 2005. Sox2 expression defines a heterogeneous population of neurosphere-forming cells in the adult murine brain. *Aging Cell*. 4:197–207.

Bruggeman, S.W.M., M.E. Valk-Lingbeek, P.P.M. van der Stoop, J.J.L. Jacobs, K. Kieboom, E. Tanger, D. Hulsman, C. Leung, Y. Arsenijevic, S. Marino, and M. van Lohuizen. 2005. Ink4a and Arf differentially affect cell proliferation and neural stem cell self-renewal in Bmi1-deficient mice. *Genes Dev.* 19:1438–1443.

Byrd, K.N., and A. Shearn. 2003. ASH1, a Drosophila trithorax group protein, is required for methylation of lysine 4 residues on histone H3. *Proc. Natl. Acad. Sci. U.S.A.* 100:11535–11540.

Callaghan, D.A., L. Dong, S.M. Callaghan, Y.X. Hou, L. Dagnino, and R.S. Slack. 1999. Neural precursor cells differentiating in the absence of Rb exhibit delayed terminal mitosis and deregulated E2F 1 and 3 activity. *Dev. Biol.* 207:257–270.

Cao, R., and Y. Zhang. 2004. SUZ12 is required for both the histone methyltransferase activity and the silencing function of the EED-EZH2 complex. *Mol. Cell*. 15:57–67.

Cao, R., L. Wang, H. Wang, L. Xia, H. Erdjument-Bromage, P. Tempst, R.S. Jones, and Y. Zhang. 2002. Role of histone H3 lysine 27 methylation in Polycomb-group silencing. *Science*. 298:1039–1043.

Carragher, L.A.S., K.R. Snell, S.M. Giblett, V.S.S. Aldridge, B. Patel, S.J. Cook, D.J. Winton, R. Marais, and C.A. Pritchard. 2010. V600EBraf induces gastrointestinal crypt senescence and promotes tumour progression through enhanced CpG methylation of p16INK4a. *EMBO Mol Med*. 2:458–471.

Chang, C.-J., J.-Y. Yang, W. Xia, C.-T. Chen, X. Xie, C.-H. Chao, W.A. Woodward, J.-M. Hsu, G.N. Hortobagyi, and M.-C. Hung. 2011. EZH2 promotes expansion of breast tumor initiating cells through activation of RAF1-β-catenin signaling. *Cancer Cell*.

19:86–100.

Chen, D., M. Pacal, P. Wenzel, P.S. Knoepfler, G. Leone, and R. Bremner. 2009. Division and apoptosis of E2f-deficient retinal progenitors. *Nature*. 462:925–929.

Chen, D., R. Opavsky, M. Pacal, N. Tanimoto, P. Wenzel, M.W. Seeliger, G. Leone, and R. Bremner. 2007. Rb-mediated neuronal differentiation through cell-cycle-independent regulation of E2f3a. *PLoS Biol.* 5:e179.

Chojnacki, A., and S. Weiss. 2008. Production of neurons, astrocytes and oligodendrocytes from mammalian CNS stem cells. *Nat Protoc*. 3:935–940.

Chong, J.-L., P.L. Wenzel, M.T. Sáenz-Robles, V. Nair, A. Ferrey, J.P. Hagan, Y.M. Gomez, N. Sharma, H.-Z. Chen, M. Ouseph, S.-H. Wang, P. Trikha, B. Culp, L. Mezache, D.J. Winton, O.J. Sansom, D. Chen, R. Bremner, P.G. Cantalupo, M.L. Robinson, J.M. Pipas, and G. Leone. 2009. E2f1-3 switch from activators in progenitor cells to repressors in differentiating cells. *Nature*. 462:930–934.

Collignon, J., S. Sockanathan, A. Hacker, M. Cohen-Tannoudji, D. Norris, S. Rastan, M. Stevanovic, P.N. Goodfellow, and R. Lovell-Badge. 1996. A comparison of the properties of Sox-3 with Sry and two related genes, Sox-1 and Sox-2. *Development*. 122:509–520.

Cregan, S.P., J.G. MacLaurin, C.G. Craig, G.S. Robertson, D.W. Nicholson, D.S. Park, and R.S. Slack. 1999. Bax-dependent caspase-3 activation is a key determinant in p53-induced apoptosis in neurons. *J. Neurosci.* 19:7860–7869.

D'Amour, K.A., and F.H. Gage. 2003. Genetic and functional differences between multipotent neural and pluripotent embryonic stem cells. *Proc. Natl. Acad. Sci. U.S.A.* 100 Suppl 1:11866–11872.

Dahiya, A., S. Wong, S. Gonzalo, M. Gavin, and D.C. Dean. 2001. Linking the Rb and polycomb pathways. *Mol. Cell*. 8:557–569.

Di Stefano, L., M.R. Jensen, and K. Helin. 2003. E2F7, a novel E2F featuring DP-independent repression of a subset of E2F-regulated genes. *EMBO J.* 22:6289–6298.

Ellis, P., B.M. Fagan, S.T. Magness, S. Hutton, O. Taranova, S. Hayashi, A. McMahon, M. Rao, and L. Pevny. 2004. SOX2, a persistent marker for multipotential neural stem cells derived from embryonic stem cells, the embryo or the adult. *Dev. Neurosci.* 26:148–165.

Emig, R., A. Magener, V. Ehemann, A. Meyer, F. Stilgenbauer, M. Volkmann, D. Wallwiener, and H.P. Sinn. 1998. Aberrant cytoplasmic expression of the p16 protein in breast cancer is associated with accelerated tumour proliferation. *Br. J. Cancer*. 78:1661–1668.

Esteller, M., P.G. Corn, S.B. Baylin, and J.G. Herman. 2001. A gene hypermethylation

profile of human cancer. *Cancer Res.* 61:3225–3229.

Evangelou, K., J. Bramis, I. Peros, P. Zacharatos, D. Dasiou-Plakida, N. Kalogeropoulos, P.J. Asimacopoulos, C. Kittas, E. Marinos, and V.G. Gorgoulis. 2004. Electron microscopy evidence that cytoplasmic localization of the p16(INK4A) "nuclear" cyclin-dependent kinase inhibitor (CKI) in tumor cells is specific and not an artifact. A study in non-small cell lung carcinomas. *Biotech Histochem*. 79:5–10.

Ezhkova, E., H.A. Pasolli, J.S. Parker, N. Stokes, I.-H. Su, G. Hannon, A. Tarakhovsky, and E. Fuchs. 2009. Ezh2 orchestrates gene expression for the stepwise differentiation of tissue-specific stem cells. *Cell*. 136:1122–1135.

Ferri, A.L.M., M. Cavallaro, D. Braida, A. Di Cristofano, A. Canta, A. Vezzani, S. Ottolenghi, P.P. Pandolfi, M. Sala, S. DeBiasi, and S.K. Nicolis. 2004. Sox2 deficiency causes neurodegeneration and impaired neurogenesis in the adult mouse brain. *Development*. 131:3805–3819.

Foster, C.S., A. Falconer, A.R. Dodson, A.R. Norman, N. Dennis, A. Fletcher, C. Southgate, A. Dowe, D. Dearnaley, S. Jhavar, R. Eeles, A. Feber, and C.S. Cooper. 2004. Transcription factor E2F3 overexpressed in prostate cancer independently predicts clinical outcome. *Oncogene*. 23:5871–5879.

Francis, N.J., A.J. Saurin, Z. Shao, and R.E. Kingston. 2001. Reconstitution of a functional core polycomb repressive complex. *Mol. Cell*. 8:545–556.

Freedman, J.A., J.T. Chang, L. Jakoi, and J.R. Nevins. 2009. A combinatorial mechanism for determining the specificity of E2F activation and repression. *Oncogene*. 28:2873–2881.

Gil, J., and G. Peters. 2006. Regulation of the INK4b-ARF-INK4a tumour suppressor locus: all for one or one for all. *Nat. Rev. Mol. Cell Biol.* 7:667–677.

Girling, R., J.F. Partridge, L.R. Bandara, N. Burden, N.F. Totty, J.J. Hsuan, and N.B. La Thangue. 1993. A new component of the transcription factor DRTF1/E2F. *Nature*. 362:83–87.

Graham, V., J. Khudyakov, P. Ellis, and L. Pevny. 2003. SOX2 functions to maintain neural progenitor identity. *Neuron*. 39:749–765.

Gregory, G.D., C.R. Vakoc, T. Rozovskaia, X. Zheng, S. Patel, T. Nakamura, E. Canaani, and G.A. Blobel. 2007. Mammalian ASH1L is a histone methyltransferase that occupies the transcribed region of active genes. *Mol. Cell. Biol.* 27:8466–8479.

Guillemette, B., P. Drogaris, H.-H.S. Lin, H. Armstrong, K. Hiragami-Hamada, A. Imhof, E. Bonneil, P. Thibault, A. Verreault, and R.J. Festenstein. 2011. H3 lysine 4 is acetylated at active gene promoters and is regulated by H3 lysine 4 methylation. *PLoS Genet.* 7:e1001354.

Haller, F., A. Agaimy, S. Cameron, M. Beyer, B. Gunawan, N. Happel, C. Langer, G. Ramadori, A. von Heydebreck, and L. Füzesi. 2010. Expression of p16INK4A in gastrointestinal stromal tumours (GISTs): two different forms exist that independently correlate with poor prognosis. *Histopathology*. 56:305–318.

Hauenschild, A., L. Ringrose, C. Altmutter, R. Paro, and M. Rehmsmeier. 2008. Evolutionary plasticity of polycomb/trithorax response elements in Drosophila species. *PLoS Biol.* 6:e261.

Hirabayashi, Y., N. Suzki, M. Tsuboi, T.A. Endo, T. Toyoda, J. Shinga, H. Koseki, M. Vidal, and Y. Gotoh. 2009. Polycomb limits the neurogenic competence of neural precursor cells to promote astrogenic fate transition. *Neuron*. 63:600–613.

Humbert, P.O., R. Verona, J.M. Trimarchi, C. Rogers, S. Dandapani, and J.A. Lees. 2000. E2f3 is critical for normal cellular proliferation. *Genes Dev.* 14:690–703.

Hutton, S.R., and L.H. Pevny. 2011. SOX2 expression levels distinguish between neural progenitor populations of the developing dorsal telencephalon. *Dev. Biol.* 352:40–47.

Jacobs, J.J., K. Kieboom, S. Marino, R.A. DePinho, and M. van Lohuizen. 1999. The oncogene and Polycomb-group gene bmi-1 regulates cell proliferation and senescence through the ink4a locus. *Nature*. 397:164–168.

Juan, A.H., A. Derfoul, X. Feng, J.G. Ryall, S. Dell'Orso, A. Pasut, H. Zare, J.M. Simone, M.A. Rudnicki, and V. Sartorelli. 2011. Polycomb EZH2 controls self-renewal and safeguards the transcriptional identity of skeletal muscle stem cells. *Genes Dev.* 25:789–794.

Julian LM, Vandenbosch R, Pakenham CA, Andrusiak MG, Nguyen AP, McClellan KA, Svoboda DS, Lagace DC, Park DS, Leone GE, Blais A, Slack RS. 2013. Opposing regulation of Sox2 by cell cycle effectors E2f3a&b in neural stem cells. *Cell Stem Cell*, in press.

Jung, J.-W., S. Lee, M.-S. Seo, S.-B. Park, A. Kurtz, S.-K. Kang, and K.-S. Kang. 2010. Histone deacetylase controls adult stem cell aging by balancing the expression of polycomb genes and jumonji domain containing 3. *Cell. Mol. Life Sci.* 67:1165–1176.

Kamb, A., N.A. Gruis, J. Weaver-Feldhaus, Q. Liu, K. Harshman, S.V. Tavtigian, E. Stockert, R.S. Day, B.E. Johnson, and M.H. Skolnick. 1994. A cell cycle regulator potentially involved in genesis of many tumor types. *Science*. 264:436–440.

Kamminga, L.M., L.V. Bystrykh, A. de Boer, S. Houwer, J. Douma, E. Weersing, B. Dontje, and G. de Haan. 2006. The Polycomb group gene Ezh2 prevents hematopoietic stem cell exhaustion. *Blood*. 107:2170–2179.

Kim, W.Y., and N.E. Sharpless. 2006. The regulation of INK4/ARF in cancer and aging. *Cell*. 127:265–275.

Kotake, Y., R. Cao, P. Viatour, J. Sage, Y. Zhang, and Y. Xiong. 2007. pRB family proteins are required for H3K27 trimethylation and Polycomb repression complexes binding to and silencing p16INK4alpha tumor suppressor gene. *Genes Dev.* 21:49–54.

Krek, W., D.M. Livingston, and S. Shirodkar. 1993. Binding to DNA and the retinoblastoma gene product promoted by complex formation of different E2F family members. *Science*. 262:1557–1560.

Krishnamurthy, J., C. Torrice, M.R. Ramsey, G.I. Kovalev, K. Al-Regaiey, L. Su, and N.E. Sharpless. 2004. Ink4a/Arf expression is a biomarker of aging. *J. Clin. Invest.* 114:1299–1307.

Ku, M., R.P. Koche, E. Rheinbay, E.M. Mendenhall, M. Endoh, T.S. Mikkelsen, A. Presser, C. Nusbaum, X. Xie, A.S. Chi, M. Adli, S. Kasif, L.M. Ptaszek, C.A. Cowan, E.S. Lander, H. Koseki, and B.E. Bernstein. 2008. Genomewide analysis of PRC1 and PRC2 occupancy identifies two classes of bivalent domains. *PLoS Genet.* 4:e1000242.

Kuzmichev, A., K. Nishioka, H. Erdjument-Bromage, P. Tempst, and D. Reinberg. 2002. Histone methyltransferase activity associated with a human multiprotein complex containing the Enhancer of Zeste protein. *Genes Dev.* 16:2893–2905.

Kuzmichev, A., T. Jenuwein, P. Tempst, and D. Reinberg. 2004. Different EZH2-containing complexes target methylation of histone H1 or nucleosomal histone H3. *Mol. Cell*. 14:183–193.

Lam, A.K.-Y., K. Ong, M.J. Giv, M.J. Giv, and Y.-H. Ho. 2008. p16 expression in colorectal adenocarcinoma: marker of aggressiveness and morphological types. *Pathology*. 40:580–585.

Lee, E.R., F.E. Murdoch, and M.K. Fritsch. 2007. High histone acetylation and decreased polycomb repressive complex 2 member levels regulate gene specific transcriptional changes during early embryonic stem cell differentiation induced by retinoic acid. *Stem Cells*. 25:2191–2199.

Lee, H., K. Ohno, Y. Voskoboynik, L. Ragusano, A. Martinez, and D.K. Dimova. 2010. Drosophila RB proteins repress differentiation-specific genes via two different mechanisms. *Mol. Cell. Biol.* 30:2563–2577.

Leone, G., F. Nuckolls, S. Ishida, M. Adams, R. Sears, L. Jakoi, A. Miron, and J.R. Nevins. 2000. Identification of a novel E2F3 product suggests a mechanism for determining specificity of repression by Rb proteins. *Mol. Cell. Biol.* 20:3626–3632.

Leone, G., J. DeGregori, Z. Yan, L. Jakoi, S. Ishida, R.S. Williams, and J.R. Nevins. 1998. E2F3 activity is regulated during the cell cycle and is required for the induction of S phase. *Genes Dev.* 12:2120–2130.

Leone, G., R. Sears, E. Huang, R. Rempel, F. Nuckolls, C.H. Park, P. Giangrande, L. Wu, H.I. Saavedra, S.J. Field, M.A. Thompson, H. Yang, Y. Fujiwara, M.E. Greenberg,

S. Orkin, C. Smith, and J.R. Nevins. 2001. Myc requires distinct E2F activities to induce S phase and apoptosis. *Mol. Cell*. 8:105–113.

Li, H., Q. Cai, A.K. Godwin, and R. Zhang. 2010. Enhancer of zeste homolog 2 promotes the proliferation and invasion of epithelial ovarian cancer cells. *Mol. Cancer Res.* 8:1610–1618.

Li, J., C. Ran, E. Li, F. Gordon, G. Comstock, H. Siddiqui, W. Cleghorn, H.-Z. Chen, K. Kornacker, C.-G. Liu, S.K. Pandit, M. Khanizadeh, M. Weinstein, G. Leone, and A. de Bruin. 2008. Synergistic function of E2F7 and E2F8 is essential for cell survival and embryonic development. *Dev. Cell*. 14:62–75.

Logan, N., A. Graham, X. Zhao, R. Fisher, B. Maiti, G. Leone, and N.B. La Thangue. 2005. E2F-8: an E2F family member with a similar organization of DNA-binding domains to E2F-7. *Oncogene*. 24:5000–5004.

Logan, N., L. Delavaine, A. Graham, C. Reilly, J. Wilson, T.R. Brummelkamp, E.M. Hijmans, R. Bernards, and N.B. La Thangue. 2004. E2F-7: a distinctive E2F family member with an unusual organization of DNA-binding domains. *Oncogene*. 23:5138–5150.

Luis, N.M., L. Morey, S. Mejetta, G. Pascual, P. Janich, B. Kuebler, L. Cozutto, G. Roma, E. Nascimento, M. Frye, L. Di Croce, and S.A. Benitah. 2011. Regulation of human epidermal stem cell proliferation and senescence requires polycomb- dependent and -independent functions of Cbx4. *Cell Stem Cell*. 9:233–246.

Lukas, J., B.O. Petersen, K. Holm, J. Bartek, and K. Helin. 1996. Deregulated expression of E2F family members induces S-phase entry and overcomes p16INK4A-mediated growth suppression. *Mol. Cell. Biol.* 16:1047–1057.

Lukas, J., D. Parry, L. Aagaard, D.J. Mann, J. Bartkova, M. Strauss, G. Peters, and J. Bartek. 1995. Retinoblastoma-protein-dependent cell-cycle inhibition by the tumour suppressor p16. *Nature*. 375:503–506.

Maertens, G.N., S. El Messaoudi-Aubert, T. Racek, J.K. Stock, J. Nicholls, M. Rodriguez-Niedenführ, J. Gil, and G. Peters. 2009. Several distinct polycomb complexes regulate and co-localize on the INK4a tumor suppressor locus. *PLoS ONE*. 4:e6380.

Maiti, B., J. Li, A. de Bruin, F. Gordon, C. Timmers, R. Opavsky, K. Patil, J. Tuttle, W. Cleghorn, and G. Leone. 2005. Cloning and characterization of mouse E2F8, a novel mammalian E2F family member capable of blocking cellular proliferation. *J. Biol. Chem.* 280:18211–18220.

Margueron, R., G. Li, K. Sarma, A. Blais, J. Zavadil, C.L. Woodcock, B.D. Dynlacht, and D. Reinberg. 2008. Ezh1 and Ezh2 maintain repressive chromatin through different mechanisms. *Mol. Cell*. 32:503–518.

Margueron, R., N. Justin, K. Ohno, M.L. Sharpe, J. Son, W.J. Drury, P. Voigt, S.R.

Martin, W.R. Taylor, V. De Marco, V. Pirrotta, D. Reinberg, and S.J. Gamblin. 2009. Role of the polycomb protein EED in the propagation of repressive histone marks. *Nature*. 461:762–767.

Marson, A., S.S. Levine, M.F. Cole, G.M. Frampton, T. Brambrink, S. Johnstone, M.G. Guenther, W.K. Johnston, M. Wernig, J. Newman, J.M. Calabrese, L.M. Dennis, T.L. Volkert, S. Gupta, J. Love, N. Hannett, P.A. Sharp, D.P. Bartel, R. Jaenisch, and R.A. Young. 2008. Connecting microRNA genes to the core transcriptional regulatory circuitry of embryonic stem cells. *Cell*. 134:521–533.

Mathew, O.P., K. Ranganna, and F.M. Yatsu. 2010. Butyrate, an HDAC inhibitor, stimulates interplay between different posttranslational modifications of histone H3 and differently alters G1-specific cell cycle proteins in vascular smooth muscle cells. *Biomed. Pharmacother.* 64:733–740.

McClellan, K.A., J.L. Vanderluit, L.M. Julian, M.G. Andrusiak, D. Dugal-Tessier, D.S. Park, and R.S. Slack. 2009. The p107/E2F pathway regulates fibroblast growth factor 2 responsiveness in neural precursor cells. *Mol. Cell. Biol.* 29:4701–4713.

McClellan, K.A., V.A. Ruzhynsky, D.N. Douda, J.L. Vanderluit, K.L. Ferguson, D. Chen, R. Bremner, D.S. Park, G. Leone, and R.S. Slack. 2007. Unique requirement for Rb/E2F3 in neuronal migration: evidence for cell cycle-independent functions. *Mol. Cell. Biol.* 27:4825–4843.

Michaloglou, C., L.C.W. Vredeveld, M.S. Soengas, C. Denoyelle, T. Kuilman, C.M.A.M. van der Horst, D.M. Majoor, J.W. Shay, W.J. Mooi, and D.S. Peeper. 2005. BRAFE600-associated senescence-like cell cycle arrest of human naevi. *Nature*. 436:720–724.

Miki, J., Y.-I. Fujimura, H. Koseki, and T. Kamijo. 2007. Polycomb complexes regulate cellular senescence by repression of ARF in cooperation with E2F3. *Genes Cells*. 12:1371–1382.

Mikkelsen, T.S., M. Ku, D.B. Jaffe, B. Issac, E. Lieberman, G. Giannoukos, P. Alvarez, W. Brockman, T.-K. Kim, R.P. Koche, W. Lee, E. Mendenhall, A. O'Donovan, A. Presser, C. Russ, X. Xie, A. Meissner, M. Wernig, R. Jaenisch, C. Nusbaum, E.S. Lander, and B.E. Bernstein. 2007. Genome-wide maps of chromatin state in pluripotent and lineage-committed cells. *Nature*. 448:553–560.

Milde-Langosch, K., A.M. Bamberger, G. Rieck, B. Kelp, and T. Löning. 2001. Overexpression of the p16 cell cycle inhibitor in breast cancer is associated with a more malignant phenotype. *Breast Cancer Res. Treat.* 67:61–70.

Milton, A., K. Luoto, L. Ingram, S. Munro, N. Logan, A.L. Graham, T.R. Brummelkamp, E.M. Hijmans, R. Bernards, and N.B. La Thangue. 2006. A functionally distinct member of the DP family of E2F subunits. *Oncogene*. 25:3212–3218.

Mohn, F., M. Weber, M. Rebhan, T.C. Roloff, J. Richter, M.B. Stadler, M. Bibel, and D. Schübeler. 2008. Lineage-specific polycomb targets and de novo DNA methylation

define restriction and potential of neuronal progenitors. *Mol. Cell*. 30:755–766.

Molofsky, A.V., S. He, M. Bydon, S.J. Morrison, and R. Pardal. 2005. Bmi-1 promotes neural stem cell self-renewal and neural development but not mouse growth and survival by repressing the p16Ink4a and p19Arf senescence pathways. *Genes Dev.* 19:1432–1437.

Molofsky, A.V., S.G. Slutsky, N.M. Joseph, S. He, R. Pardal, J. Krishnamurthy, N.E. Sharpless, and S.J. Morrison. 2006. Increasing p16INK4a expression decreases forebrain progenitors and neurogenesis during ageing. *Nature*. 443:448–452.

Müller, J., C.M. Hart, N.J. Francis, M.L. Vargas, A. Sengupta, B. Wild, E.L. Miller, M.B. O'Connor, R.E. Kingston, and J.A. Simon. 2002. Histone methyltransferase activity of a Drosophila Polycomb group repressor complex. *Cell*. 111:197–208.

Nielsen, S.J., R. Schneider, U.M. Bauer, A.J. Bannister, A. Morrison, D. O'Carroll, R. Firestein, M. Cleary, T. Jenuwein, R.E. Herrera, and T. Kouzarides. 2001. Rb targets histone H3 methylation and HP1 to promoters. *Nature*. 412:561–565.

Nobori, T., K. Miura, D.J. Wu, A. Lois, K. Takabayashi, and D.A. Carson. 1994. Deletions of the cyclin-dependent kinase-4 inhibitor gene in multiple human cancers. *Nature*. 368:753–756.

Noro, R., A. Miyanaga, Y. Minegishi, T. Okano, M. Seike, C. Soeno, K. Kataoka, K. Matsuda, A. Yoshimura, and A. Gemma. 2010. Histone deacetylase inhibitor enhances sensitivity of non-small-cell lung cancer cells to 5-FU/S-1 via down-regulation of thymidylate synthase expression and up-regulation of p21(waf1/cip1) expression. *Cancer Sci.* 101:1424–1430.

Ogawa, H., K.-I. Ishiguro, S. Gaubatz, D.M. Livingston, and Y. Nakatani. 2002. A complex with chromatin modifiers that occupies E2F- and Myc-responsive genes in G0 cells. *Science*. 296:1132–1136.

Ormondroyd, E., S. de la Luna, and N.B. La Thangue. 1995. A new member of the DP family, DP-3, with distinct protein products suggests a regulatory role for alternative splicing in the cell cycle transcription factor DRTF1/E2F. *Oncogene*. 11:1437–1446.

Pan, G., S. Tian, J. Nie, C. Yang, V. Ruotti, H. Wei, G.A. Jonsdottir, R. Stewart, and J.A. Thomson. 2007. Whole-genome analysis of histone H3 lysine 4 and lysine 27 methylation in human embryonic stem cells. *Cell Stem Cell*. 1:299–312.

Papp, B., and J. Müller. 2006. Histone trimethylation and the maintenance of transcriptional ON and OFF states by trxG and PcG proteins. *Genes Dev.* 20:2041–2054.

Pasini, D., A.P. Bracken, J.B. Hansen, M. Capillo, and K. Helin. 2007. The polycomb group protein Suz12 is required for embryonic stem cell differentiation. *Mol. Cell. Biol.* 27:3769–3779.

Pasini, D., A.P. Bracken, M.R. Jensen, E. Lazzerini Denchi, and K. Helin. 2004. Suz12 is

essential for mouse development and for EZH2 histone methyltransferase activity. *EMBO J.* 23:4061–4071.

Pasini, D., M. Malatesta, H.R. Jung, J. Walfridsson, A. Willer, L. Olsson, J. Skotte, A. Wutz, B. Porse, O.N. Jensen, and K. Helin. 2010. Characterization of an antagonistic switch between histone H3 lysine 27 methylation and acetylation in the transcriptional regulation of Polycomb group target genes. *Nucleic Acids Res.* 38:4958–4969.

Pevny, L., and M. Placzek. 2005. SOX genes and neural progenitor identity. *Curr. Opin. Neurobiol.* 15:7–13.

Philpott, A., T. Krude, and R.A. Laskey. 2000. Nuclear chaperones. *Semin. Cell Dev. Biol.* 11:7–14.

Pietersen, A.M., H.M. Horlings, M. Hauptmann, A. Langerød, A. Ajouaou, P. Cornelissen-Steijger, L.F. Wessels, J. Jonkers, M.J. van de Vijver, and M. van Lohuizen. 2008. EZH2 and BMI1 inversely correlate with prognosis and TP53 mutation in breast cancer. *Breast Cancer Res.* 10:R109.

Potten, C.S., and M. Loeffler. 1990. Stem cells: attributes, cycles, spirals, pitfalls and uncertainties. Lessons for and from the crypt. *Development*. 110:1001–1020.

Qian, Y.W., Y.C. Wang, R.E. Hollingsworth, D. Jones, N. Ling, and E.Y. Lee. 1993. A retinoblastoma-binding protein related to a negative regulator of Ras in yeast. *Nature*. 364:648–652.

Rabinovich, A., V.X. Jin, R. Rabinovich, X. Xu, and P.J. Farnham. 2008. E2F in vivo binding specificity: comparison of consensus versus nonconsensus binding sites. *Genome Res.* 18:1763–1777.

Rao, Z.-Y., M.-Y. Cai, G.-F. Yang, L.-R. He, S.-J. Mai, W.-F. Hua, Y.-J. Liao, H.-X. Deng, Y.-C. Chen, X.-Y. Guan, Y.-X. Zeng, H.-F. Kung, and D. Xie. 2010. EZH2 supports ovarian carcinoma cell invasion and/or metastasis via regulation of TGF-beta1 and is a predictor of outcome in ovarian carcinoma patients. *Carcinogenesis*. 31:1576–1583.

Reynolds, B.A., and R.L. Rietze. 2005. Neural stem cells and neurospheres--re-evaluating the relationship. *Nat. Methods*. 2:333–336.

Reynolds, B.A., and S. Weiss. 1992. Generation of neurons and astrocytes from isolated cells of the adult mammalian central nervous system. *Science*. 255:1707–1710.

Romagosa, C., S. Simonetti, L. López-Vicente, A. Mazo, M.E. Lleonart, J. Castellvi, and S. Ramon y Cajal. 2011. p16(Ink4a) overexpression in cancer: a tumor suppressor gene associated with senescence and high-grade tumors. *Oncogene*. 30:2087–2097.

Román-Trufero, M., H.R. Méndez-Gómez, C. Pérez, A. Hijikata, Y.-I. Fujimura, T. Endo, H. Koseki, C. Vicario-Abejón, and M. Vidal. 2009. Maintenance of

undifferentiated state and self-renewal of embryonic neural stem cells by Polycomb protein Ring1B. *Stem Cells*. 27:1559–1570.

Santos-Rosa, H., R. Schneider, A.J. Bannister, J. Sherriff, B.E. Bernstein, N.C.T. Emre, S.L. Schreiber, J. Mellor, and T. Kouzarides. 2002. Active genes are tri-methylated at K4 of histone H3. *Nature*. 419:407–411.

Schmitges, F.W., A.B. Prusty, M. Faty, A. Stützer, G.M. Lingaraju, J. Aiwazian, R. Sack, D. Hess, L. Li, S. Zhou, R.D. Bunker, U. Wirth, T. Bouwmeester, A. Bauer, N. Ly-Hartig, K. Zhao, H. Chan, J. Gu, H. Gut, W. Fischle, J. Müller, and N.H. Thomä. 2011. Histone methylation by PRC2 is inhibited by active chromatin marks. *Mol. Cell*. 42:330–341.

Schoeftner, S., A.K. Sengupta, S. Kubicek, K. Mechtler, L. Spahn, H. Koseki, T. Jenuwein, and A. Wutz. 2006. Recruitment of PRC1 function at the initiation of X inactivation independent of PRC2 and silencing. *EMBO J.* 25:3110–3122.

Seo, E., U. Basu-Roy, J. Zavadil, C. Basilico, and A. Mansukhani. 2011. Distinct functions of Sox2 control self-renewal and differentiation in the osteoblast lineage. *Mol. Cell. Biol.* 31:4593–4608.

Serrano, M. 1997. The tumor suppressor protein p16INK4a. *Exp. Cell Res.* 237:7–13.

Shao, Z., F. Raible, R. Mollaaghababa, J.R. Guyon, C.T. Wu, W. Bender, and R.E. Kingston. 1999. Stabilization of chromatin structure by PRC1, a Polycomb complex. *Cell*. 98:37–46.

Sher, F., E. Boddeke, M. Olah, and S. Copray. 2012. Dynamic Changes in Ezh2 Gene Occupancy Underlie Its Involvement in Neural Stem Cell Self-Renewal and Differentiation towards Oligodendrocytes. *PLoS ONE*. 7:e40399.

Sher, F., R. Rössler, N. Brouwer, V. Balasubramaniyan, E. Boddeke, and S. Copray. 2008. Differentiation of neural stem cells into oligodendrocytes: involvement of the polycomb group protein Ezh2. *Stem Cells*. 26:2875–2883.

Simon, J., A. Chiang, W. Bender, M.J. Shimell, and M. O'Connor. 1993. Elements of the Drosophila bithorax complex that mediate repression by Polycomb group products. *Dev. Biol.* 158:131–144.

Sing, A., D. Pannell, A. Karaiskakis, K. Sturgeon, M. Djabali, J. Ellis, H.D. Lipshitz, and S.P. Cordes. 2009. A vertebrate Polycomb response element governs segmentation of the posterior hindbrain. *Cell*. 138:885–897.

Song, J.-J., J.D. Garlick, and R.E. Kingston. 2008. Structural basis of histone H4 recognition by p55. *Genes Dev.* 22:1313–1318.

Squazzo, S.L., H. O'Geen, V.M. Komashko, S.R. Krig, V.X. Jin, S.-W. Jang, R. Margueron, D. Reinberg, R. Green, and P.J. Farnham. 2006. Suz12 binds to silenced

regions of the genome in a cell-type-specific manner. *Genome Res.* 16:890–900.

Stanbrough, M., G.J. Bubley, K. Ross, T.R. Golub, M.A. Rubin, T.M. Penning, P.G. Febbo, and S.P. Balk. 2006. Increased expression of genes converting adrenal androgens to testosterone in androgen-independent prostate cancer. *Cancer Res.* 66:2815–2825.

Steigen, S.E., B. Bjerkehagen, H.K. Haugland, I.S. Nordrum, E.M. Løberg, V. Isaksen, T.J. Eide, and T.O. Nielsen. 2008. Diagnostic and prognostic markers for gastrointestinal stromal tumors in Norway. *Mod. Pathol.* 21:46–53.

Suvà, M.-L., N. Riggi, M. Janiszewska, I. Radovanovic, P. Provero, J.-C. Stehle, K. Baumer, M.-A. Le Bitoux, D. Marino, L. Cironi, V.E. Marquez, V. Clément, and I. Stamenkovic. 2009. EZH2 is essential for glioblastoma cancer stem cell maintenance. *Cancer Res.* 69:9211–9218.

Svendsen, C.N., M.A. Caldwell, and T. Ostenfeld. 1999. Human neural stem cells: isolation, expansion and transplantation. *Brain Pathol.* 9:499–513.

Szutorisz, H., C. Canzonetta, A. Georgiou, C.-M. Chow, L. Tora, and N. Dillon. 2005. Formation of an active tissue-specific chromatin domain initiated by epigenetic marking at the embryonic stem cell stage. *Mol. Cell. Biol.* 25:1804–1820.

Takahashi, K., and S. Yamanaka. 2006. Induction of pluripotent stem cells from mouse embryonic and adult fibroblast cultures by defined factors. *Cell*. 126:663–676.

Tanaka, Y., Z.-I. Katagiri, K. Kawahashi, D. Kioussis, and S. Kitajima. 2007. Trithorax-group protein ASH1 methylates histone H3 lysine 36. *Gene*. 397:161–168.

Taniguchi, H., F.V. Jacinto, A. Villanueva, A.F. Fernandez, H. Yamamoto, F.J. Carmona, S. Puertas, V.E. Marquez, Y. Shinomura, K. Imai, and M. Esteller. 2012. Silencing of Kruppel-like factor 2 by the histone methyltransferase EZH2 in human cancer. *Oncogene*. 31:1988–1994.

Tie, F., R. Banerjee, C.A. Stratton, J. Prasad-Sinha, V. Stepanik, A. Zlobin, M.O. Diaz, P.C. Scacheri, and P.J. Harte. 2009. CBP-mediated acetylation of histone H3 lysine 27 antagonizes Drosophila Polycomb silencing. *Development*. 136:3131–3141.

Tie, F., T. Furuyama, J. Prasad-Sinha, E. Jane, and P.J. Harte. 2001. The Drosophila Polycomb Group proteins ESC and E(Z) are present in a complex containing the histone-binding protein p55 and the histone deacetylase RPD3. *Development*. 128:275–286.

Trimarchi, J.M., B. Fairchild, J. Wen, and J.A. Lees. 2001. The E2F6 transcription factor is a component of the mammalian Bmi1-containing polycomb complex. *Proc. Natl. Acad. Sci. U.S.A.* 98:1519–1524.

Tsai, S.-Y., R. Opavsky, N. Sharma, L. Wu, S. Naidu, E. Nolan, E. Feria-Arias, C. Timmers, J. Opavska, A. de Bruin, J.-L. Chong, P. Trikha, S.A. Fernandez, P. Stromberg, T.J. Rosol, and G. Leone. 2008. Mouse development with a single E2F activator. *Nature*.

454:1137–1141.

van Ginkel, P.R., K.M. Hsiao, H. Schjerven, and P.J. Farnham. 1997. E2F-mediated growth regulation requires transcription factor cooperation. *J. Biol. Chem.* 272:18367–18374.

Varambally, S., S.M. Dhanasekaran, M. Zhou, T.R. Barrette, C. Kumar-Sinha, M.G. Sanda, D. Ghosh, K.J. Pienta, R.G.A.B. Sewalt, A.P. Otte, M.A. Rubin, and A.M. Chinnaiyan. 2002. The polycomb group protein EZH2 is involved in progression of prostate cancer. *Nature*. 419:624–629.

Villasante, A., D. Piazzolla, H. Li, G. Gomez-Lopez, M. Djabali, and M. Serrano. 2011. Epigenetic regulation of Nanog expression by Ezh2 in pluripotent stem cells. *Cell Cycle*. 10:1488–1498.

Walker, E., J.L. Manias, W.Y. Chang, and W.L. Stanford. 2011. PCL2 modulates gene regulatory networks controlling self-renewal and commitment in embryonic stem cells. *Cell Cycle*. 10:45–51.

Walker, E., W.Y. Chang, J. Hunkapiller, G. Cagney, K. Garcha, J. Torchia, N.J. Krogan, J.F. Reiter, and W.L. Stanford. 2010. Polycomb-like 2 associates with PRC2 and regulates transcriptional networks during mouse embryonic stem cell self-renewal and differentiation. *Cell Stem Cell*. 6:153–166.

Wang, H., L. Wang, H. Erdjument-Bromage, M. Vidal, P. Tempst, R.S. Jones, and Y. Zhang. 2004. Role of histone H2A ubiquitination in Polycomb silencing. *Nature*. 431:873–878.

Wenzel, P.L., J.-L. Chong, M.T. Sáenz-Robles, A. Ferrey, J.P. Hagan, Y.M. Gomez, R. Rajmohan, N. Sharma, H.-Z. Chen, J.M. Pipas, M.L. Robinson, and G. Leone. 2011. Cell proliferation in the absence of E2F1-3. *Dev. Biol.* 351:35–45.

Wiebe, M.S., P.J. Wilder, D. Kelly, and A. Rizzino. 2000. Isolation, characterization, and differential expression of the murine Sox-2 promoter. *Gene*. 246:383–393.

Wu, C.L., L.R. Zukerberg, C. Ngwu, E. Harlow, and J.A. Lees. 1995. In vivo association of E2F and DP family proteins. *Mol. Cell. Biol.* 15:2536–2546.

Wu, L., C. Timmers, B. Maiti, H.I. Saavedra, L. Sang, G.T. Chong, F. Nuckolls, P. Giangrande, F.A. Wright, S.J. Field, M.E. Greenberg, S. Orkin, J.R. Nevins, M.L. Robinson, and G. Leone. 2001. The E2F1-3 transcription factors are essential for cellular proliferation. *Nature*. 414:457–462.

Xu, C., C. Bian, W. Yang, M. Galka, H. Ouyang, C. Chen, W. Qiu, H. Liu, A.E. Jones, F. MacKenzie, P. Pan, S.S.-C. Li, H. Wang, and J. Min. 2010. Binding of different histone marks differentially regulates the activity and specificity of polycomb repressive complex 2 (PRC2). *Proc. Natl. Acad. Sci. U.S.A.* 107:19266–19271.

Xu, L., Z. Zhao, A. Dong, L. Soubigou-Taconnat, J.-P. Renou, A. Steinmetz, and W.-H. Shen. 2008. Di- and tri- but not monomethylation on histone H3 lysine 36 marks active transcription of genes involved in flowering time regulation and other processes in Arabidopsis thaliana. *Mol. Cell. Biol.* 28:1348–1360.

Yadirgi, G., V. Leinster, S. Acquati, H. Bhagat, O. Shakhova, and S. Marino. 2011. Conditional activation of Bmi1 expression regulates self-renewal, apoptosis, and differentiation of neural stem/progenitor cells in vitro and in vivo. *Stem Cells*. 29:700–712.

Yoshikawa, K. 2000. Cell cycle regulators in neural stem cells and postmitotic neurons. *Neurosci. Res.* 37:1–14.

Yuan, W., M. Xu, C. Huang, N. Liu, S. Chen, and B. Zhu. 2011. H3K36 methylation antagonizes PRC2-mediated H3K27 methylation. *J. Biol. Chem.* 286:7983–7989.

Zhang, Y., and S.P. Chellappan. 1995. Cloning and characterization of human DP2, a novel dimerization partner of E2F. *Oncogene*. 10:2085–2093.

Zhao, X.D., X. Han, J.L. Chew, J. Liu, K.P. Chiu, A. Choo, Y.L. Orlov, W.-K. Sung, A. Shahab, V.A. Kuznetsov, G. Bourque, S. Oh, Y. Ruan, H.-H. Ng, and C.-L. Wei. 2007. Whole-genome mapping of histone H3 Lys4 and 27 trimethylations reveals distinct genomic compartments in human embryonic stem cells. *Cell Stem Cell*. 1:286–298.

Zhou, W., P. Zhu, J. Wang, G. Pascual, K.A. Ohgi, J. Lozach, C.K. Glass, and M.G. Rosenfeld. 2008. Histone H2A monoubiquitination represses transcription by inhibiting RNA polymerase II transcriptional elongation. *Mol. Cell*. 29:69–80.

Zindy, F., D.E. Quelle, M.F. Roussel, and C.J. Sherr. 1997. Expression of the p16INK4a tumor suppressor versus other INK4 family members during mouse development and aging. *Oncogene*. 15:203–211.

❖Appendix I – *Curriculum vitae*

Catherine Pakenham

EDUCATION

Sept 2011 – Present **M.Sc. Physiotherapy**
McMaster University, Hamilton, ON

Sept 2009 – Present **M.Sc. Neuroscience**
University of Ottawa, Ottawa, ON

Sept 2004 – May 2009 **B.Sc. Honours Biopharmaceutical Sciences–Genomics option**
University of Ottawa, Ottawa, ON

WORK EXPERIENCE

Sept 2009 – Present **M.Sc. Candidate** - *Dr. Ruth Slack's Lab, University of Ottawa, ON*
Maintenance of neural stem cell self-renewal by E2f3

Our lab has recently found that *E2f3*, an essential cell cycle regulator, regulates the self-renewal capacity of neural precursor cells (NPCs) in the developing mouse brain. Chromatin immunoprecipitation (ChIP) and immunoblotting techniques revealed several E2F3 target genes, including the polycomb group (PcG) protein, *Ezh2*. Further ChIP and immunoblotting techniques identified the neural stem cell self-renewal regulators *p16^{INK4a}* and *Sox2* as shared gene targets of E2F3 and PcG proteins, indicating that E2F3 and PcG proteins may co-regulate these target genes. *E2f3*-/- NPCs demonstrated dysregulated expression of EZH2, p16^{INK4a}, and SOX2 and decreased enrichment of PcG proteins at target genes. Restoring EZH2 expression to *E2f3*+/+ levels restores p16^{INK4a} and SOX2 expression levels to near *E2f3*+/+ levels, and also partially rescues NPC self-renewal capacity toward *E2f3*+/+ levels. Taken together, these results suggest that *E2f3* controls NPC self-renewal by modulating expression of p16^{INK4a} and SOX2 via regulation of PcG expression, and potentially PcG recruitment.

May 2008 – Aug 2009 **Honour's Student** - *Dr. Ruth Slack's Lab, University of Ottawa, ON*
The role of E2f3 in neural stem cell self-renewal

The E2f family of transcription factors are well known essential regulators of cell cycle progression. Recently, we have found that E2f3 performs unique, cell cycle independent functions in the brain, including the regulation of neural stem cell self-renewal. The role of E2f3 in stem cell self-renewal was examined by neurosphere assays which revealed that in the absence of the E2f3a isoform there is an initial increase in the number of neural stem cells and that these cells have a greater self-renewal capacity compared to their wild-type counterparts. However, with age, the self-renewal capacity of E2f3a-/- neural precursors is prematurely depleted. We report that, based on Western blot analysis, the cyclin-dependent kinase inhibitor p16^{INK4a} was specifically over-expressed in the absence of both E2f3 isoforms and to a lesser extent in the E2f3a-/-. Furthermore, chromatin immunoprecipitation experiments suggested that E2f3 regulates the expression of both p16^{INK4a} as well as several polycomb group proteins.

Jan 2007 – Dec 2007 **Research Assistant -** *Health Canada, Ottawa, ON*
The effect of plant sterol- and plant stanol-enriched diets on cholesterol absorption and expression of genes in the renin-angiotensin system

A mutation in the ATP binding cassette transporter abcg5 has been found to result in phytosterolemia, which leads to an earlier onset of stroke and decreased survival time in hypertensive rats. We investigated a possible mechanism for how the hyperabsorption of plant sterols and stanols leads to the onset of stroke and decreased survival time. We first examined the effects of high levels of dietary plant sterols and stanols on tissue incorporation of plant sterols, plant stanols, and cholesterol in the kidneys of hypertensive and normotensive rats by gas chromotography. As expected, rats fed a plant sterol- or plant stanol-enriched diet had the greatest deposition of plant sterols or plant stanols, respectively. It was demonstrated that the concentration of cholesterol in the kidney was not affected by either of the enriched diets, but was however affected by whether or not the rat was hypertensive. We then inspected the blood pressure as well as the expression of RAS genes in the kidney by qRT-PCR. Diastolic blood pressure was highest in hypertensive rats, although expression of angiotensin II type 1 receptors was highest in the kidney of normotensive rats, suggesting a downregulatory effect of angiotensin II on the expression of AT_1 receptors.

ACTIVITIES

Let's Talk Science	(2010-2011)
CMM/NSC Students' Council	(2009-2011)

AWARDS & SCHOLARSHIPS

Ontario Graduate Scholarship (Sep 2010-Aug 2011)
(Sep 2012-Aug 2013)

University of Ottawa Excellence Scholarship (Sep 2009-Aug 2011)

Ontario Graduate Scholarship in Science and Technology (Sep 2009-Aug 2010)

International Society for Developmental Neuroscience Student Travel Bursary
18th Biennial Meeting of the International Society for Developmental Neuroscience (Estoril, Portugal) (June 2010)

Dean's Honour List (Sep 2008-May 2009)

PUBLICATIONS

Julian LM, Vandenbosch R, **Pakenham CA**, Andrusiak MG, Nguyen AP, McClellan KA, Svoboda DS, Lagace DC, Park DS, Leone GE, Blais A, RS Slack R. 2013. Opposing regulation of *Sox2* by cell cycle effectors E2f3a&b in neural stem cells. *Cell Stem Cell*, in press.

Chen Q, Gruber H, Swist E, Coville K, **Pakenham C**, Ratnayake WM, Scoggan KA (Feb 2010) Dietary phytosterols and phytostanols decrease cholesterol levels but increase blood pressure in WKY inbred rats in the absence of salt-loading. *Nutrition & Metabolism* 7(11):1-9.

Chen Q, Gruber H, **Pakenham C**, Ratnayake WM, Scoggan KA (Oct 2009) Dietary phytosterols and phytostanols alter the expression of sterol-regulatory genes in SHRSP and WKY inbred rats. *Annals of Nutrition & Metabolism* 55(4):341-50.

Chen Q, Gruber H, Swist E, **Pakenham C**, Ratnayake WMN, Scoggan KA (Nov 2008) Influence of dietary phytosterols and phytostanols on diastolic blood pressure and the expression of blood pressure regulatory genes in SHRSP and WKY inbred rats. *British Journal of Nutrition* 24:1-9.

PUBLISHED ABSTRACTS

Pakenham C, Julian L, Park D, Leone G, Slack R (June 2010) Maintenance of neural stem cell self-renewal by E2f3. *18th Biennial Meeting of the International Society for Developmental Neuroscience (Estoril, Portugal)*

Julian L, **Pakenham C**, Vandenbosch R, Ruzhynsky V, Liu Y, Park D, Leone G, Blais A, Slack R (June 2010) Differential regulation of neural stem cell self-renewal and progenitor proliferation by distinct E2f3 isoforms: a genome-wide analysis. *18th Biennial Meeting of the International Society for Developmental Neuroscience (Estoril, Portugal)*

Scoggan KA, Chen Q, Swist E, Gruber, H, **Pakenham C**, Ratnayake WMN (Oct 2008) Increased diastolic blood pressure in phytosterol or phytostanol supplemented SHRSP rats is associated with increased Ace 1, Nos1, Nos3, Cox2, and Spon1 mRNA expression. *2nd Congress of the International Society of Nutrigenetics/Nutrigenomics (Geneva, Switzerland)*

ABSTRACTS

Pakenham C, Julian L, Park D, Leone G, Slack R (May 2011) E2f3 regulates neural stem cell populations by modulating polycomb group proteins. *5th Annual Canadian Neuroscience Meeting (Québec City, Canada)*

Pakenham C, Julian L, Park D, Leone G, Slack R (May 2011) E2f3 regulates neural stem cell populations by modulating polycomb group proteins. *Epigenetics Eh; Canadian Conference on Epigenetics (London, Canada)*

Pakenham C, Julian L, Park D, Leone G, Slack R (June 2010) Maintenance of neural stem cell self-renewal by E2f3.*2nd Annual Brain Health Research Day (Ottawa, Canada)*

Pakenham C, Julian L, Park D, Leone G, Slack R (Nov 2009) Maintenance of neural stem cell self-renewal by E2f3. *First International Rb Tumor Suppressor Meeting (Toronto, Canada)*

Julian L, **Pakenham C**, Vandenbosch R, Ruzhynsky V, Liu Y, Park D, Leone G, Blais A, Slack R (Nov 2009) Differential regulation of neural stem cell self-renewal and progenitor proliferation by distinct E2f3 isoforms. *First International Rb Tumor Suppressor Meeting (Toronto, Canada)*

Julian L, McClellan K, **Pakenham C**, Park D, Leone G, Slack R (Sept 2009) Individual E2f3 isoforms uniquely regulate neural precursor proliferation and self renewal. *Cold Spring Harbor-Wellcome Trust; Mouse genetics and genomics – Development and Disease (Cambridge, England)*

Julian L, McClellan K, **Pakenham C**, Park D, Leone G, Slack R (June 2009) Individual E2f3 isoforms uniquely regulate neural precursor proliferation and self renewal. *Keystone series; Deregulation of transcription in cancer: Controlling cell fate decisions (Killarney, Ireland)*

Chen Q, Gruber H, **Pakenham C**, Ratnayake WMN, Scoggan KA (Nov 2007) Influence of dietary plant sterols and stanols on diastolic blood pressure and the expression of genes involved in cholesterol metabolism in SHRSP and WKY inbred rats. *2007 Health Canada Science Forum (Ottawa, Canada)*

❖Appendix II – *Submitted manuscript*

Opposing Regulation of *Sox2* by Cell Cycle Effectors E2f3a&b in Neural Stem Cells

Lisa M Julian[1], Renaud Vandenbosch[1], Catherine A Pakenham[1], Matthew G Andrusiak[1], Angela P Nguyen[1], Kelly A McClellan[1], Devon S Svoboda[1], Diane C Lagace[1], David S Park[1], Gustavo E Leone[2], Alexandre Blais[3], and Ruth S Slack[1]

[1]Department of Cellular and Molecular Medicine, University of Ottawa

[2]Human Cancer Genetics Program, Department of Molecular Virology, Immunology and Medical Genetics, Ohio State University

[3]Ottawa Institute of Systems Biology, Department of Biochemistry, Microbiology and Immunology, University of Ottawa

SUMMARY

The mechanisms through which cell cycle control and cell fate decisions are coordinated in proliferating stem cell populations are largely unknown. Here, we show that E2f3 isoforms, which control cell cycle progression in cooperation with the retinoblastoma protein (pRb), have critical effects during developmental and adult neurogenesis. Loss of either E2f3 isoform disrupts *Sox2* gene regulation and the balance between precursor maintenance and differentiation in the developing cortex. Both isoforms target the *Sox2* locus to maintain baseline levels of Sox2 expression, but antagonistically regulate Sox2 levels to instruct fate choices. E2f3 mediated regulation of *Sox2* and precursor cell fate extends to the adult brain, where E2f3a loss results in defects in hippocampal neurogenesis and memory formation. Our results demonstrate a novel mechanism by which E2f3a and E2f3b differentially regulate Sox2 dosage in neural precursors, a finding that may have broad implications for the regulation of diverse stem cell populations.

INTRODUCTION

Stem cell fate decisions, such as self-renewal, precursor cell maintenance and commitment to differentiation, have critical outcomes for embryonic development, tissue maintenance, tumour suppression and regeneration. Cortical development depends on a precisely regulated balance of self-renewal within stem cell-like apical precursors (APs), production of rapidly proliferating basal progenitors (BPs) and differentiation of post-mitotic neurons (Englund et al.,2005; Farkas & Huttner, 2008; Hutton & Pevny, 2011) (Fig. 1A). Identifying mechanisms that control this balance can inform our understanding of developmental neurogenesis and, more broadly, reveal stem cell biological principles extending to embryonic stem cell (ESC) differentiation, tumour formation, and tissue regeneration.

The pluripotency factor Sox2 is an established regulator of neural precursor proliferation, self-renewal and differentiation during development, and is also required for maintenance of adult stem cell populations in many different tissues (reviewed in Sarkar & Hochedlinger, 2013). Over-expression of Sox2 in both mouse and chick embryonic NPCs results in maintenance of the Sox2+ population and defective neurogenesis (Bani-Yaghoub et al., 2006; Graham et al., 2003). Conversely, loss of function of Sox2 in neural precursors leads to precursor loss and reduced or aberrant differentiation, depending on the tissue type and degree of Sox2 loss (Cavallaro et al., 2008; Favaro et al., 2009; Ferri et al., 2004; Graham et al., 2003; Miyagi et al., 2008; Taranova, 2006). Taken together, these studies reveal that the function of Sox2 is strongly influenced by dosage, thus fine tuning of transcription from the *Sox2* locus is crucial for the generation of the correct proportion of precursors versus differentiated cell types. Interestingly, a recent study finds that the Cyclin-dependent kinase inhibitor 1A (p21) binds a *Sox2* enhancer region to regulate

Sox2 expression and adult neurogenesis, linking cell cycle regulation with Sox2-mediated control of neural stem cell (NSC) expansion (Marqués-Torrejón et al., 2013).

Previous evidence suggests that the cell cycle machinery plays a key role in regulating the proliferative expansion and self-renewal capacity of neural precursor cells (NPCs) (Nishino et al., 2008; Ruzhynsky et al., 2007; Vanderluit et al., 2004). However, how specific cell cycle regulatory proteins function in this context remains poorly defined. The Retinoblastoma pocket protein (pRb) family controls cell cycle progression by binding and inhibiting the E2f family of transcription factors. E2fs are classified into the 'activator' subclass, which drive proliferation and transcription, and the 'repressor' subclass, which are thought to repress gene transcription by modifying chromatin structure through association with pocket proteins (Asp et al., 2009). Earlier work has reported that E2f3 is the most highly expressed E2f family member in wild type and pRb deficient neural precursors (Callaghan et al., 1999); suggesting that it may be an important regulator of NPC functions. Understanding how the *E2f3* gene functions to regulate the cell cycle is not entirely straightforward, as the two isoforms (*E2f3a* and *E2f3b*) expressed from its locus have identical domains important for DNA binding, transactivation and pocket protein binding, and only have unique N-termini. Mice lacking both isoforms die perinatally due to cardiac defects (King et al., 2008), while those deficient in either isoform are fully viable (Danielian et al., 2008; Tsai et al., 2008), suggesting functional overlap. Tissue and cell type specific analysis of pRb and E2f knockout mice suggest that E2f3a is generally a potent activator of transcription and proliferation, while E2f3b weakly induces proliferation and promotes differentiation (Asp et al., 2009; Chong et al., 2009; Danielian et al., 2008) but whether individual E2f3 isoforms make a distinct contribution to developmental and adult neurogenesis is currently unknown.

Here, we use mouse models deficient for either E2f3 isoform to reveal that E2f3a and E2f3b antagonistically regulate Sox2 expression in NSCs. In E2f3b null animals, where E2f3a is the dominant isoform, we find that E2f3a represses *Sox2* in co-operation with the pRb family member p107, reduces precursor self-renewal and promotes differentiation. Conversely, in E2f3a null animals, where E2f3b is the dominant isoform, we find that E2f3b activates *Sox2* expression by recruiting RNA Polymerase II to its promoter, which leads to increased self-renewal and precursor expansion at the expense of differentiation. Knock-down of Sox2 in E2f3a deficient NPCs restored basal levels of self-renewal. Importantly, we find that adult E2f3a null mice have impaired neurogenesis and a reduced capacity for hippocampal-dependent contextual learning, underscoring how the antagonism between E2f3 isoforms is conserved to regulate adult neurogenesis and affect memory formation.

RESULTS

E2f3 Isoforms are Expressed in Neural Precursor Cells

E2f3 is a potent cell cycle regulator and a highly expressed E2f family member in NPCs (Callaghan et al., 1999; Mcclellan et al., 2007), suggesting a potential role for E2f3 in this cell type. Interestingly, we observed that expression of both E2f3 isoforms is enriched in NPCs but reaches negligible levels by day 5 of differentiation *in vitro* (Fig. 1B, S1A-B), pointing to a regulatory role for both isoforms within the proliferating precursor pool. We asked if E2f3 isoforms play an important role in regulating neural stem and progenitor cell fate decisions by examining mouse lines deficient for *E2f3a* and *E2f3b* (Chen et al., 2007; Tsai et al., 2008).

E2f3a and E2f3b Deficiency Impacts NPC Fate Decisions in an Opposing Manner

We first asked if loss of E2f3 isoforms impacts NPC fate decisions by performing a neuronal commitment assay. Mice were given a single BrdU injection and were sacrificed 24 hours later to visualize BrdU+ cells that had exited the cell cycle and initiated differentiation. There were visibly fewer BrdU+ cells migrating into the subventricular zone (SVZ) and intermediate zone (IZ) of E2f3a-/- mice, but more BrdU+ cells in these regions in E2f3b knock-outs (Fig. 1C-D), suggesting a differential commitment to neurogenesis. Newly committed cells that have undergone terminal mitosis can be identified by double labeling with BrdU and differentiation markers, including βIII-tubulin (TuJ1) and Doublecortin (DCX). These BrdU positive cells are also negative for the proliferation marker Ki67. E2f3a-/- mice exhibited a significant reduction in newly committed cells that co-labeled for BrdU/Tuj1 (Fig. 1E) or BrdU/DCX (Fig. S1C), and cells that were negative for Ki67 (BrdU+/Ki67-) (Fig. S1D). In contrast, these same experiments revealed that E2f3b deficient brains contain significantly more committed cells (Fig. 1F, S1E-F). These results were further supported *in vitro* by quantification of newly committed cells in

neurosphere cultures induced to differentiate. Here again, E2f3a deficient NPCs exhibited a reduction in differentiation, while E2f3b deficient precursors had an increase in differentiating cells (Fig. 1G-H). Deficiency of either E2f3 isoform does not lead to compensatory expression changes of other pRb/E2f family members (Fig. S1G-J), demonstrating specificity of E2f3 isoform dependent phenotypes. Thus, deficiency of E2f3 isoforms impacts neural precursor fate decisions in distinct ways, where E2f3a loss reduces, but E2f3b deficiency increases, commitment to a neuronal fate.

To determine if E2f3 isoforms are similarly required to regulate the size of the neural precursor pool in an opposing manner, we quantified the number of proliferating NPCs during forebrain development by performing a 2 hr BrdU incorporation (S phase) and phospho-histone H3 (PH-H3) (M phase) immuno-staining. E2f3a loss resulted in an expanded neural precursor pool (Fig. S2A&C), specifically affecting the Sox2+ stem-like APs in the VZ (Fig. 2A, 2C, S2E), culminating in a 38% in the size of this population by E17.5 (Fig. 2A). Alternatively, loss of E2f3b resulted in an average 25% decrease in precursor numbers throughout development (Fig. S2B&D), again specifically affecting Sox2 expressing stem-like APs (Fig. 2B&D, S2F). Concomitant with the expanded precursor population in E2f3a-/- brains, the neuronal output at birth was significantly reduced (e.g., a 24% decrease in later born neurons, layers I-III) (Fig. S3A). In contrast, neuronal output was increased in E2f3b knock-outs (Fig. S3B). Thus, E2f3a and E2f3b are differentially required to regulate both the expansion of the AP population and their commitment to a neuronal fate.

E2f3 is Expressed in Stem-like Sox2+ Apical Precursors

The impact of E2f3 isoforms on cell fate decisions within the AP population suggests that E2f3 is expressed in Sox2+ precursors. Using an N-terminal E2f3a specific antibody, we detected E2f3a protein within NPCs in the ganglionic eminence (GE), a ventrally located tissue that gives rise to inhibitory interneurons (Wonders & Anderson, 2006), as well as the VZ/SVZ surrounding the lateral ventricle (Fig. S4A-B). Importantly, E2f3a co-localizes with a subset of Sox2 expressing cells in the GE (Fig. S4C) and the dorsal cortex (Fig. 2E, G-H) (also marked by Pax6 (Fig. S4D)). Conversely, little E2f3a co-localization was found in committed basal progenitors, which express Tbr2 (Fig. 2F-H), or in Tuj1+ neurons (Fig. 2H). Quantification of cells co-labeled with E2f3a and cell cycle phase markers revealed that E2f3a is highly enriched in S phase, where 83% of E2f3a+ cells co-expressed BrdU following a 2hr pulse (Fig. S4E-G). E2f3a expression in S phase precursors supports a role in NPC fate decisions, as a recent study suggests that fate decisions in the developing brain are controlled by gene expression patterns during S phase (Arai et al., 2011). Thus, E2f3a is expressed predominantly in Sox2+ self-renewing precursors.

E2f3a is Required for Regulation of NSC Self-renewal

We asked next if E2f3 isoforms modulate the self-renewal capacity of the stem cell-like AP population. Loss of E2f3a increased the number of primary and secondary neurospheres generated by both cortical and GE-derived NPC populations by 1.4 to 2 fold at E14.5 (Fig. 2I) and E17.5 (Fig. S4H). Loss of E2f3b, however, showed no effect (Fig. 2J, S4I). To ask if E2f3a deficiency may affect the mode of AP cell division, we measured the orientation of mitotic spindle poles in control and E2f3a deficient brains. APs undergo mitosis at the apical surface of the lateral ventricle and the orientation of the mitotic spindle pole and cleavage furrow during cytokinesis has been linked with the resulting fate of daughter cells (Das & Storey, 2012; Farkas

& Huttner, 2008; Godin et al., 2010) (see Supplemental data for detailed methods). In E2f3a knock-outs, we observed 1.5-fold more APs with a cleavage angle within the vertical 75-90° range, associated with symmetric (self-renewing) cell divisions (Fig. S4J-K). In contrast, there was a corresponding 2.7-fold decrease in the number of divisions within the 0-15° range, suggesting a reduction in asymmetric, differentiative cell divisions. These results suggest that E2f3a deficient brains exhibit an increased proportion of AP cells undergoing symmetric cell divisions, consistent with our *in vitro* studies showing enhanced neural precursor self-renewal.

Opposing Regulation of the *Sox2* Gene by E2f3 Isoforms

To identify target genes through which E2f3 isoforms regulate NPC properties, we performed a genomic ChIP-on-chip screen to identify E2f3 binding sites and associated target genes in NPCs (Julian et al., in preparation). From three independent samples of wild-type, E2f3a-/- and E2f3b-/- E14.5 GE neurospheres, we identified the gene encoding the pluripotency factor *Sox2* as a potential target of E2f3 (Fig. 3A). Enrichment levels for E2f3 at the *Sox2* promoter were comparable in wild-type, as well as E2f3a and E2f3b deficient cells, indicating that both isoforms bind this locus. Previous studies have shown that changes in Sox2 expression can have dramatic effects on the maintenance and differentiation capacity of neural precursor populations, where elevated Sox2 leads to expansion of the precursor pool and impaired neurogenesis, and decreased Sox2 results in loss of NPCs and dose-dependent defects on neurogenesis (Bani-Yaghoub et al., 2006; Graham et al., 2003; Pevny & Nicolis, 2010; Taranova et al., 2006). As precursor numbers and neurogenesis are disrupted in E2f3a and E2f3b deficient brains, *Sox2* was a strong candidate to account for these biological effects. We first validated by conventional ChIP that E2f3 binds to the *Sox2* promoter, at an enrichment level comparable to that of previously established E2f3 target genes (Fig. 3B). An E2f consensus motif (CTTCCCGC) was identified within the center of

the E2f3 binding peak, 371bp upstream of the transcriptional start site (TSS) (Fig. 3A), and is conserved in the murine and human genomes. This E2f3 bound region is transcriptionally responsive to E2f3 activity, as indicated by a 2-fold increase in luciferase activity from a *Sox2* promoter fragment (800bp upstream to 285bp downstream of the *Sox2* TSS) following co-transfection of a full length E2f3 construct (Fig. 3C-D). Furthermore, point mutations within the E2f consensus motif reduced Luciferase activity by 50% (Fig. 3C-D), demonstrating a functional E2f consensus site at 371bp upstream of the *Sox2* TSS.

To determine if E2f3 isoforms regulate Sox2 levels *in vivo* and *in vitro*, we measured Sox2 protein levels in GE-derived tissue and cultured neurospheres, as NPCs from this region are predominantly Sox2+ (Fig. S5A-B). We show that E2f3a and E2f3b regulate Sox2 expression in a reciprocal manner. Specifically, E2f3a-/- neurospheres and GE tissue exhibited a 2.3 and 6-fold increase, respectively, in Sox2 levels (Fig. 3E-F). In contrast, E2f3b-/- neurospheres and GE tissue express Sox2 at 40% and 30% of wild-type levels (Fig. 3G-H). These results suggest an opposing role for E2f3 isoforms in the regulation of the *Sox2* gene.

E2f3a Represses NSC Self-renewal through *Sox2* Regulation

To directly determine if E2f3a represses self-renewal by regulating *Sox2*, we asked if Sox2 knockdown could rescue the enhanced self-renewal phenotype observed in E2f3a deficient cultures. E2f3a+/+ or E2f3a-/- neurospheres were infected with a bicistronic lentivirus expressing GFP and one of two shSox2 or scrambled control sequences. Importantly, each shSox2 construct reduced Sox2 expression in E2f3a-/- cells to a level comparable to GFP infected wild-type cells (Fig. 4A-B). shSox2 mediated knockdown of

Sox2 in E2f3a-/- cultures restored neurosphere numbers (Fig. 4C-D) and self-renewal capacity (Fig. 4E) back to basal levels. To ask whether elevated Sox2 can account for the increased self-renewal in E2f3a-/- precursors, we over-expressed Sox2 in wild-type cultures (Fig. 4F). Sox2 over-expression in E2f3a+/+ precursors increased self-renewal (Fig. 4G) and correspondingly decreased neurogenesis (Fig. 4H) to levels observed in E2f3a deficient cells. Furthermore, over-expression of Sox2 in E2f3a-/- precursors, which already express elevated Sox2, did not further increase neurosphere numbers. Thus, E2f3a functions to maintain Sox2 levels below a specific threshold, beyond which precursor self-renewal and cell fate decisions are markedly disrupted.

E2f3 Isoforms Recruit Distinct Transcriptional Co-factors to the *Sox2* Promoter

To determine the mechanism by which E2f3a and E2f3b antagonistically regulate Sox2 expression we identified the regulatory factors recruited to the *Sox2* locus by each isoform. First, we confirmed that both isoforms bind the *Sox2* promoter, within a 200bp region surrounding the conserved E2f motif ('US', upstream binding site) and at the transcriptional start site (TSS), as E2f3 enrichment is similar in wild-type, E2f3a-/- and E2f3b-/- neural precursors (Fig. 5A). Consistent with E2f3b as an activator of *Sox2* expression, in E2f3a-/- cells, where only the E2f3b isoform is present, we observed enrichment of RNA Polymerase II (Pol. II) at and beyond the TSS (Fig. 5B) and the trimethyl-H3K4 (H3K4Me3) chromatin modification (Fig. 5C), as well as a decrease in trimethyl-H3K27Me3 (Fig. 5C). Each of these changes are associated with transcriptional activation, demonstrating that in the absence of E2f3a, Sox2 expression is elevated due to an increased ratio of bound E2f3b/Pol. II complexes. Conversely, binding of the repressive pocket protein p107 was significantly enriched in the absence of E2f3b, where only E2f3a is present, and was decreased in E2f3a-/- cells (Fig. 5D). These findings show that E2f3a functions

as a repressor at the *Sox2* promoter by recruiting p107. Supporting this conclusion, GE tissue from p107 deficient animals exhibited a 2.2-fold increase in Sox2 levels compared to wild-type controls (Fig. 5E).

The percentage of precursor cells in each cell cycle phase was not altered by E2f3a or E2f3b deficiency (Fig. S6A&B), thus the changes in binding enrichments we observed in E2f3 isoform deficient cells could not be explained by disrupted cell cycle dynamics, but truly to altered enrichment of these factors. We show that *Sox2* expression is regulated by E2f3 isoforms in an opposing manner, whereby E2f3a recruits the transcriptional repressor p107, and E2f3b recruits activator complexes to the promoter. This reveals a novel mechanism for regulation of the pluripotency factor *Sox2*, through the cell cycle effectors E2f3a and E2F3b.

A Common Mechanism of E2f3a-mediated *Sox2* Regulation in Embryonic and Adult NSCs

The requirement for controlled Sox2 expression in NSCs extends from development to adulthood (Cavallaro et al., 2008; Favaro et al., 2009; Ferri et al., 2004; Pevny & Nicolis, 2010), thus we hypothesized that E2f3-dependent *Sox2* regulation is also important in adult NSCs. To evaluate the role of E2f3a in the adult we generated animals containing two modified E2f3 alleles: one *floxed* allele and a second E2f3a deficient allele (E2f3-*flox*/3a-). To induce acute removal of E2f3a, cultured SVZ precursors from adult E2f3-*flox*/3a- animals were infected with a Cre expressing lentivirus, which removes *E2f3a* but leaves *E2f3b* intact (Fig. 6A). As with embryonic E2f3a-/- precursors, Cre infected cells exhibited increased neurosphere self-renewal (Fig. 6B), and were impaired in their ability

to generate neurons (Fig. 6C). Importantly, these self-renewal and neurogenic changes were accompanied by increased Sox2 expression (Fig. 6D). Furthermore, absence of E2f3a reduced enrichment of E2f3 (Fig. 6E) and p107 (Fig. 6F), and significantly increased recruitment of RNA Polymerase II (Fig. 6G), at the *Sox2* promoter. Thus, NSCs maintain a common mechanism of E2f3a dependent *Sox2* regulation from development to adulthood.

Loss of E2f3a Disrupts Neurogenesis and Cognitive Function in the Adult Brain

Given that E2f3a regulates *Sox2* in both embryonic and adult NSCs, we asked if absence of E2F3a had a functional consequence in the adult brain. We first evaluated the levels of neurogenesis in E2f3a+/+ and E2f3a-/- adult brains in two distinct neurogenic regions, the SVZ and the dentate gyrus (DG) of the hippocampus, where neurogenesis is required, respectively, for olfactory function and hippocampal memory formation. As determined by NeuroD1 and DCX staining, the number of committed neurons was significantly decreased by 35% in the SVZ (Fig. 6H) and 31% in the DG (Fig. 6I-J), revealing an impairment in adult neurogenesis that has further progressed since late stages of development. We also found that E2f3a-/- mice are significantly impaired in their ability to learn and remember the association between an aversive experience and environment in the classical fear conditioning paradigm (Wehner & Radcliffe, 2004). In this test, animals are trained to acquire a learned response to an aversive stimulus (foot shock) that is associated with a specific environment (context) and a tone (cue). Following training, animals are tested for their ability to have learned that the context or cue is associated with the aversive stimulus by measuring their freezing behaviour during exposure to each

condition. E2f3a-/- mice exhibited a significant 45% decrease in freezing behavior associated with amygdala and hippocampal-dependent contextual learning (Marin-Burgin & Schinder, 2012), while freezing associated with amygdala-dependent cue learning (Wehner & Radcliffe, 2004) was decreased more subtly by 21% (Fig. 6K). The reduced freezing in E2f3a-/- versus control mice was not due to differences in the unconditioned freezing behavior, as assessed during training and before tone presentation in the cue trial (Fig S7A&B), nor to differences in foot shock threshold (Fig. S7C). These results suggest that E2f3a influences the formation of associative memories, and its loss reveals defects in at least two telencephalic structures, with the most severely affected function (contextual learning) being that which is influenced by adult neurogenesis (Marin-Burgin & Schinder, 2012). Thus, E2f3a is required to regulate neural precursor maintenance and neurogenesis in both the embryonic and adult brain, and this role significantly impacts cognitive function.

DISCUSSION

This study presents two key discoveries. First, we show that E2f3 isoforms play opposing roles in regulating the balance between neural precursor self-renewal and differentiation during developmental neurogenesis. Loss of E2f3a leads to neurogenic defects in adulthood, underscoring the importance of E2f3 in mediating fate choices in both embryonic and adult NSCs. Second, we report a transcriptional mechanism by which E2f3 isoforms antagonistically regulate levels of *Sox2* expression. Alteration of *Sox2* expression by loss of either E2f3 isoform shifts the equilibrium between precursor expansion and differentiation, thereby affecting downstream generation of cortical neurons and ultimately cognitive function.

Based on our findings and previous reports of E2f3 isoform expression patterns (Adams et al., 2000), we predict that E2f3a is predominant during S phase, while E2f3b is expressed throughout the cell cycle. Thus, at different phases of the cell cycle, E2f3a and b isoforms dynamically fine-tune Sox2 expression levels. We present a model of E2f3-dependent *Sox2* regulation in which both E2f3 isoforms, in a see-saw like fashion, regulate levels of Sox2 in proliferating NSCs to ensure the proper balance of precursor expansion and differentiation (Fig. 7A). When E2f3b is lost, E2f3a/p107 mediated repression is not balanced by E2f3b mediated activation, leading to lower Sox2 levels and increased neurogenesis at the expense of precursor expansion (Fig. 7B). Conversely, E2f3a deficiency leads to activation by E2f3b that is not balanced by E2f3a mediated repression, resulting in elevated Sox2 levels and, consequently, increased precursor self-renewal at the expense of neurogenesis (Fig. 7C). This functional model illustrates the requirement for a balance between E2f3a and E2f3b transcriptional activities to maintain the correct dosage of Sox2 in stem and progenitor cells.

Although E2f3a/b and p107 are highly expressed in neural precursor cells, these proteins become rapidly down-regulated as cells undergo differentiation. Uncovering other mechanisms by which long-term repression of *Sox2* is maintained as cells differentiate will therefore be important. Notably, a recent study has shown that the Cyclin-dependent kinase inhibitor (CKI) p27 is required for repression of *Sox2* during differentiation of pluripotent stem cells (Li et al., 2012). p27 is recruited to the *Sox2* SRR2 enhancer and functions in a complex together with p130 and E2f4 to silence *Sox2* expression during differentiation. As the pocket protein p130 is highly expressed in differentiated cells and plays a key role in long-term silencing of cell cycle genes, it may well play a crucial role in silencing *Sox2* in post-mitotic neurons. Another recent study demonstrated that the CKI p21 represses *Sox2* expression in adult NSCs (Marqués-Torrejón et al., 2013). In adult NSCs it has been shown that p21 represses *Sox2* through the SRR2 enhancer, and its loss results in excessive *Sox2* expression and precursor exhaustion. This exhaustion, however, is preceded by an initial expansion of the precursor pool (Kippin et al., 2005; Marqués-Torrejón et al., 2013). In E2f3a deficient embryonic and adult NSCs, we found that elevated levels of Sox2 over-expression lead to increased self-renewal; however, it is also possible that E2f3a deficient NSCs may exhaust with time, following extended passaging *in vitro* or with advanced animal age. It is also conceivable that E2f3 may participate in the recruitment of p21 to its SRR2 enhancer binding site. However, given that the E2f3 and p21 binding sites have been identified in distinct regulatory domains of the *Sox2* gene, and E2f-independent mechanisms of p21 recruitment to *Sox2* have been suggested (Marqués-Torrejón et al., 2013), it is likely that they regulate *Sox2* expression by distinct mechanisms. Examining these questions will be an important focus for future studies, and will contribute to our understanding of molecular events underlying *Sox2* gene silencing in differentiating cells.

Through our identification of *Sox2* as a functional target gene of the pRb/E2f pathway in neural precursors, we have linked the cell cycle machinery with pluripotent gene regulation in a biologically relevant context. E2f dependent regulation of *Sox2* has clear functional consequences in the developing brain, however we suggest that this may be a common feature of stem cell regulation and the pluripotent state, as both Sox2 and pRb/E2f proteins are expressed in diverse tissue specific, pluripotent, and cancer stem cell populations (Arnold et al., 2011; Galderisi et al., 2006; Pevny & Nicolis, 2010). In addition, the pRb binding proteins RBBP4 and RBBP9 have recently been implicated in regulation of the pluripotent state in human stem cells, and E2f motifs were identified in the promoters of key pluripotency factors, including *NANOG*, *POU5F1*, *FOXD3* and *SOX2* (O'Connor et al., 2011). ChIP based experiments have further demonstrated that E2fs are found at the promoters of a large number of pluripotency related genes (Chen et al., 2008; O'Connor et al., 2011), although direct functional consequences for these interactions have not previously been described. In conclusion, these studies point to the possibility that E2fs may regulate other pluripotency factors in addition to *Sox2*, and support the idea that E2f3 dependent *Sox2* regulation is a fundamental mechanism in tissue specific, tumourigenic and pluripotent stem cell populations.

EXPERIMENTAL PROCEDURES

Mouse models

Germline *E2f3a* and *E2f3b* null mice were originally generated by G. Leone and were maintained on an FVBN background (Chen et al., 2007; Tsai et al., 2008). Animal experiments were approved by the University of Ottawa's Animal Care Ethics Committee, which abides by the guidelines of the Canadian Council on Animal Care. E2f3-*flox*/E2f3a- mice were generated by crossing E2f3a-/- mice with E2f3-*flox/flox* animals maintained on an SV129 background. p107 deficient mice were generated as previously described (LeCouter et al., 1998). All Adult mice analyzed were 2 months of age or older.

Neural precursor cultures

Neural precursors were obtained by dissection of the ventral (GE) or dorsal (cortex) telencephalic tissue of developing embryos; neurosphere and *in vitro* differentiation assays were performed as previously described (Vanderluit et al., 2004), with exception for the lentivirus experiments. Here, neural precursors were plated at a density of 5 cells/ul 7 days post infection, and the number of regenerated neurospheres were counted after 6 days in culture. All neurosphere assays were performed on 4-7 independent samples, from at least 2 separate experiments.

Western blotting, Immunohistochemistry, Cell Counts, Primers and Antibodies

Details are described in Supplemental Experimental Procedures.

Statistical Analysis

All statistical comparisons in this study were performed using an unpaired two-tailed t test, with differences considered significant with a p value of <0.05 (*), ** $p<0.01$, *** $p<0.001$.

Lentiviral infections

shRNA Lentiviral expression constructs were obtained from Open Biosystems and include a scrambled control (Cat. #RHS4346), shSox2-1 (clone ID 153337) and shSox2-2 (153339) plasmids. Neurosphere cultures were infected with lentiviral particles at a multiplicity of infection (MOI) of 30. For Sox2 over-expression, the *Sox2* coding sequence was sub-cloned into the MCS of an IRES-GFP backbone, viruses were produced and neurospheres were infected at an MOI of 5. For Cre expression experiments, GFP or Cre coding sequences were sub-cloned into the NCS of a pWPXLD plasmid, and cells were infected at an MOI of 10.

Luciferase Reporter Assays

Reporter assays were performed in HEK-293T cells as previously described (Andrusiak et al., 2011). E2f consensus site mutagenesis was performed using the QuikChange Site-Directed Mutagenesis Kit and primer design software from Stratagene.

Chromatin Immunoprecipitation

ChIP analysis was performed as previously described (Andrusiak et al., 2011) in proliferating neurospheres, except that immuno-complexes were captured using protein A Dynabeads. RT-PCR was used to quantify ChIP enrichment values. Each experiment was performed on at least

three independent samples. ChIP-on-chip experiments were performed as previously described (Liu et al., 2010).

Fear Conditioning Analysis

Details are described in Supplemental Experimental Procedure

ACKNOWLEDGEMENTS

We thank Drs Valerie Wallace, Rod Bremner, Marc Germain and Mireille Khacho for critical review of the manuscript, as well as Jason MacLaurin, Linda Jui, Mirela Hasu, Alysen Clark and Delphie Dugal-Tessier for excellent technical assistance. We also thank Yubing Liu for help with ChIP-on-chip experiments and Drs Juliette Godin and Sandrine Humbert for assistance with the spindle pole analysis. This work was funded by CIHR grants to RSS; also by CIHR Canada Graduate Scholarships to LMJ and KAM, OGS and OGSST studentships to CAP and LMJ, OGS and HSFC scholarship to MGA, and fellowships from the Alzheimer Society of Canada, HSFC, University of Ottawa Vision 2010, and a travel award from Fonds Leon Fredericq (University of Liege, Belgium) to RV.

REFERENCES

Adams, M. R., Sears, R., Nuckolls, F., Leone, G., & Nevins, J. R. (2000). Complex transcriptional regulatory mechanisms control expression of the E2F3 locus. *Molecular and Cellular Biology*, *20*(10), 3633–3639.

Andrusiak, M. G., McClellan, K. A., Dugal-Tessier, D., Julian, L. M., Rodrigues, S. P., Park, D. S., Kennedy, T. E., et al. (2011). Rb/E2F regulates expression of neogenin during neuronal migration. *Molecular and Cellular Biology*, *31*(2), 238–247.

Arai, Y., Pulvers, J. N., Haffner, C., Schilling, B., Nüsslein, I., Calegari, F., & Huttner, W. B. (2011). Neural stem and progenitor cells shorten S-phase on commitment to neuron production. *Nature Communications*, *2*(1), 154.

Arnold, K., Sarkar, A., Yram, M. A., Polo, J. M., Bronson, R., Sengupta, S., Seandel, M., et al. (2011). Sox2+ Adult Stem and Progenitor Cells Are Important for Tissue Regeneration and Survival of Mice. *Cell Stem Cell*, *9*(4), 317–329.

Asp, P., Acosta-Alvear, D., Tsikitis, M., van Oevelen, C., & Dynlacht, B. D. (2009). E2f3b plays an essential role in myogenic differentiation through isoform-specific gene regulation. *Genes & Development*, *23*(1), 37–53.

Bani-Yaghoub, M., Tremblay, R. G., Lei, J. X., Zhang, D., Zurakowski, B., Sandhu, J. K., Smith, B., et al. (2006). Role of Sox2 in the development of the mouse neocortex. *Developmental biology*, *295*(1), 52–66.

Callaghan, D. A., Dong, L., Callaghan, S. M., Hou, Y. X., Dagnino, L., & Slack, R. S. (1999). Neural precursor cells differentiating in the absence of Rb exhibit delayed terminal mitosis and deregulated E2F 1 and 3 activity. *Developmental biology*, *207*(2), 257–270.

Cavallaro, M., Mariani, J., Lancini, C., Latorre, E., Caccia, R., Gullo, F., Valotta, M., et al. (2008). Impaired generation of mature neurons by neural stem cells from hypomorphic Sox2 mutants. *Development (Cambridge, England)*, *135*(3), 541–557.

Chen, D., Opavsky, R., Pacal, M., Tanimoto, N., Wenzel, P., Seeliger, M. W., Leone, G., et al. (2007). Rb-mediated neuronal differentiation through cell-cycle-independent regulation of E2f3a. *PLoS biology*, *5*(7), e179.

Chen, X., Xu, H., Yuan, P., Fang, F., Huss, M., Vega, V. B., Wong, E., et al. (2008). Integration of External Signaling Pathways with the Core Transcriptional Network in Embryonic Stem Cells. *Cell*, *133*(6), 1106–1117.

Chong, J.-L., Wenzel, P. L., Sáenz-Robles, M. T., Nair, V., Ferrey, A., Hagan, J. P., Gomez, Y. M., et al. (2009). E2f1-3 switch from activators in progenitor cells to repressors in differentiating cells. *Nature*, *462*(7275), 930–934.

Danielian, P. S., Friesenhahn, L. B., Faust, A. M., West, J. C., Caron, A. M., Bronson, R. T., & Lees, J. A. (2008). E2f3a and E2f3b make overlapping but different contributions to total E2f3 activity. *Oncogene*, *27*(51), 6561–6570.

Das, R. M., & Storey, K. G. (2012). Mitotic spindle orientation can direct cell fate and bias Notch

activity in chick neural tube. *EMBO reports*, *13*(5), 448–454.

Englund, C., Fink, A., Lau, C., Pham, D., Daza, R. A. M., Bulfone, A., Kowalczyk, T., et al. (2005). Pax6, Tbr2, and Tbr1 are expressed sequentially by radial glia, intermediate progenitor cells, and postmitotic neurons in developing neocortex. *The Journal of neuroscience : the official journal of the Society for Neuroscience*, *25*(1), 247–251.

Farkas, L. M., & Huttner, W. B. (2008). The cell biology of neural stem and progenitor cells and its significance for their proliferation versus differentiation during mammalian brain development. *Current Opinion in Cell Biology*, *20*(6), 707–715.

Favaro, R., Valotta, M., Ferri, A. L. M., Latorre, E., Mariani, J., Giachino, C., Lancini, C., et al. (2009). Hippocampal development and neural stem cell maintenance require Sox2-dependent regulation of Shh. *Nature Neuroscience*, *12*(10), 1248–1256.

Ferri, A. L. M., Cavallaro, M., Braida, D., Di Cristofano, A., Canta, A., Vezzani, A., Ottolenghi, S., et al. (2004). Sox2 deficiency causes neurodegeneration and impaired neurogenesis in the adult mouse brain. *Development (Cambridge, England)*, *131*(15), 3805–3819.

Galderisi, U., Cipollaro, M., & Giordano, A. (2006). The retinoblastoma gene is involved in multiple aspects of stem cell biology. *Oncogene*, *25*(38), 5250–5256.

Godin, J. D., Colombo, K., Molina-Calavita, M., Keryer, G., Zala, D., Charrin, B. C., Dietrich, P., et al. (2010). Huntingtin Is Required for Mitotic Spindle Orientation and Mammalian Neurogenesis. *Neuron*, *67*(3), 392–406.

Graham, V., Khudyakov, J., Ellis, P., & Pevny, L. (2003). SOX2 functions to maintain neural progenitor identity. *Neuron*, *39*(5), 749–765.

Hutton, S. R., & Pevny, L. H. (2011). SOX2 expression levels distinguish between neural progenitor populations of the developing dorsal telencephalon. *Developmental biology*, *352*(1), 40–47.

King, J. C., Moskowitz, I. P. G., Burgon, P. G., Ahmad, F., Stone, J. R., Seidman, J. G., & Lees, J. A. (2008). E2F3 plays an essential role in cardiac development and function. *Cell cycle (Georgetown, Tex)*, *7*(23), 3775–3780.

Kippin, T. E. (2005). p21 loss compromises the relative quiescence of forebrain stem cell proliferation leading to exhaustion of their proliferation capacity. *Genes & Development*, *19*(6), 756–767.

LeCouter, J. E., Kablar, B., Hardy, W. R., Ying, C., Megeney, L. A., May, L. L., & Rudnicki, M. A. (1998). Strain-dependent myeloid hyperplasia, growth deficiency, and accelerated cell cycle in mice lacking the Rb-related p107 gene. *Molecular and Cellular Biology*, *18*(12), 7455–7465.

Li, H., Collado, M., Villasante, A., Matheu, A., Lynch, C. J., Cañamero, M., Rizzoti, K., et al. (2012). p27Kip1 Directly Represses Sox2 during Embryonic Stem Cell Differentiation. *Cell Stem Cell*, *11*(6), 845–852.

Liu, Y., Chu, A., Chakroun, I., Islam, U., & Blais, A. (2010). Cooperation between myogenic regulatory factors and SIX family transcription factors is important for myoblast differentiation. *Nucleic Acids Research, 38*(20), 6857-6871.

Marqués-Torrejón, M. Á., Porlan, E., Banito, A., Gómez-Ibarlucea, E., Lopez-Contreras, A. J., Fernández-Capetillo, Ó., Vidal, A., et al. (2013). Cyclin-Dependent Kinase Inhibitor p21 Controls Adult Neural Stem Cell Expansion by Regulating Sox2 Gene Expression. *Cell Stem Cell*, *12*(1), 88–100.

Mcclellan, K. A., Ruzhynsky, V. A., Douda, D. N., Vanderluit, J. L., Ferguson, K. L., Chen, D., Bremner, R., et al. (2007). Unique Requirement for Rb/E2F3 in Neuronal Migration: Evidence for Cell Cycle-Independent Functions. *Molecular and Cellular Biology*, *27*(13), 4825–4843.

Miyagi, S., Masui, S., Niwa, H., Saito, T., Shimazaki, T., Okano, H., Nishimoto, M., et al. (2008). Consequence of the loss of Sox2 in the developing brain of the mouse. *FEBS Letters*, *582*(18), 2811–2815.

Marin-Burgin, A. M., & Schinder, A. F. (2012). Requirement of adult-born neurons for hippocampus-dependent learning. *Behavioural Brain Research*, *227*(2), 391–399.

Nishino, J., Kim, I., Chada, K., & Morrison, S. J. (2008). Hmga2 Promotes Neural Stem Cell Self-Renewal in Young but Not Old Mice by Reducing p16Ink4a and p19Arf Expression. *Cell*, *135*(2), 227–239.

O'Connor, M. D., Wederell, E., Robertson, G., Delaney, A., Morozova, O., Poon, S. S. S., Yap, D., et al. (2011). Retinoblastoma-binding proteins 4 and 9 are important for human pluripotent stem cell maintenance. *Experimental Hematology*, *39*(8), 866–879.

Pevny, L. H., & Nicolis, S. K. (2010). Sox2 roles in neural stem cells. *The international journal of biochemistry & cell biology*, *42*(3), 421–424.

Ruzhynsky, V. A., McClellan, K. A., Vanderluit, J. L., Jeong, Y., Furimsky, M., Park, D. S., Epstein, D. J., et al. (2007). Cell cycle regulator E2F4 is essential for the development of the ventral telencephalon. *The Journal of neuroscience : the official journal of the Society for Neuroscience*, *27*(22), 5926–5935.

Sarkar, A., & Hochedlinger, K. (2013). The Sox Family of Transcription Factors: Versatile Regulators of Stem and Progenitor Cell Fate. *Cell Stem Cell*, *12*(1), 15–30.

Taranova, O. V. (2006). SOX2 is a dose-dependent regulator of retinal neural progenitor competence. *Genes & Development*, *20*(9), 1187–1202.

Tsai, S.-Y., Opavsky, R., Sharma, N., Wu, L., Naidu, S., Nolan, E., Feria-Arias, E., et al. (2008). Mouse development with a single E2F activator. *Nature*, *454*(7208), 1137–1141.

Vanderluit, J. L. (2004). p107 regulates neural precursor cells in the mammalian brain. *The Journal of cell biology*, *166*(6), 853–863.

Wehner, J.M., & Radcliffe, R.A. (2004). Cued and Contextual Fear Conditioning in mice. *Current Protocols in Neuroscience*, 8.5C.1-14.

Wonders, C. P., & Anderson, S. A. (2006). The origin and specification of cortical interneurons. *Nature Reviews Neuroscience*, *7*(9), 687–696.

FIGURE LEGENDS

Figure 1. E2f3 Isoforms are Differentially Required for Neuronal Commitment

(A) Cortical development depends on a finely controlled balance of apical precursor (AP) cell proliferation, self-renewal and differentiation. APs can divide symmetrically to expand their population, or asymmetrically to generate one AP and a neuron, glial cell or basal progenitor (BP). BPs generate neurons through asymmetric divisions. VZ = ventricular zone; SVZ = sub-ventricular zone; CP = cortical plate.

(B) Immunoblot for E2f3 in cultured neurospheres induced to differentiate over 5 days. Both E2f3a and E2f3b are expressed in proliferating neurospheres (Day 0), but expression is decreased as differentiation progresses (days 1, 3, and 5). GAPDH was included to ensure equal protein loading.

(C-D) BrdU staining in E14.5 coronal sections following a 24 hour BrdU pulse, to identify cells that have exited the cell cycle. Fewer BrdU+ cells are observed in the E2f3a-/- SVZ/IZ, while more BrdU+ cells are apparent in E2f3b-/-. IZ = intermediate zone; CP = cortical plate.

(E&F) Sections described in panels C-D were immuno-stained for BrdU and Tuj1. The number of BrdU+/Tuj1+ cells was quantified within a defined area through the SVZ/IZ (arrows identify examples of quantified cells). Results are expressed as a percentage of E2f3a+/+ average values +/- SEM (n=4).

(G&H) Neurospheres were expanded *in vitro* and upon first passage were cultured in differentiation media on poly-L-ornithine coated dishes for 3 days, PFA fixed and immuno-stained for Tuj1 and DAPI. E2f3a-/- possesses fewer Tuj1+ cells; E2f3b-/- has more Tuj1+ cells. Results are presented as the percentage of DAPI+ cells expressing Tuj1 +/- SEM (n=4).

For panels E-H, (*$p<0.05$, **$p<0.01$). Scale bars = 50um. See also Figure S1.

Figure 2. E2f3 Isoforms are Differentially Required for Regulation of NPC numbers and Self-renewal

(A&B) PH-H3 staining in E17.5 coronal sections, to label mitotic cells. PH-H3+ cells were quantified along the dorsal surface of the lateral ventricle in either the VZ or SVZ, and numbers were normalized to a defined ventricular length (500um). Quantification demonstrates an expansion in E2f3a-/- and a decrease in E2f3b-/- specifically in the VZ (n=4).

(C&D) Quantification of Sox2+ and Tbr2+ cells within the dorsal cortex at E17.5 demonstrates an increased number of Sox2+ cells in E2f3a-/-, and fewer Sox2+ cells in E2f3b-/- (n=4).

(E) Co-localization of E2f3a (green) with Sox2 (red) in the dorsal cortex (E14.5).

(F) Lack of co-localization between E2f3a (red) and the basal progenitor marker Tbr2 (green) in the dorsal cortex (E14.5).

(G) Quantification of the percentage of all E2f3a+ cells/ section in the dorsal cortex (E14.5) co-expressing Sox2, Pax6, Tbr2 or Tuj1 (n=3).

(H) Quantification of the percentage of Pax6, Sox2, or Tbr2 expressing cells/ section in the dorsal cortex (E14.5) that also express E2f3a (n=3).

(I&J) Increased number of primary and secondary neurospheres in E2f3a-/- precursors derived from both GE and dorsal cortex (CTX) (I); E2f3b knock-outs generate the same number of neurospheres as wild-types (J). Included in the right side of each figure are phase contrast images of neurospheres from the indicated genotypes (n=5-7).

For all panels, results are presented as mean +/- SEM (*$p<0.05$, **$p<0.01$, ***$p<0.001$). Scale bar = 100um. See also Figures S2-4.

Figure 3. E2f3 Isoforms Regulate *Sox2* Expression in an Opposing Manner

(A) Binding peak profiles for E2f3 from E2f3a+/+, E2f3a-/- and E2f3b-/- ChIP-on-chip experiments, generated with UCSC Genome Browser (http://genome.ucsc.edu/). E2f3 binding peaks extend throughout the proximal promoter region and the TSS. An E2f consensus motif was identified at 371bp upstream of the TSS.

(B) RT-PCR analysis of E2f3 ChIP experiments shows E2f3 binding at the *Sox2* promoter with a similar enrichment value as for other known E2f targets. Plotted is the mean from at least three independent experiments +/- SEM (n=4).

(C) Model for Luciferase experiments. E2f3 dependent activity was tested from a Sox2 promoter fragment covering -800bp to +285bp relative to the TSS. For E2f consensus site mutation, 5 core nucleotides were replaced with Adenine.

(D) E2f3a drives Sox2-Luciferase activity. Mutation of the E2f consensus motif reduced E2f3 mediated transcription by 50% (n=4-6).

(E&G) Immunoblot for Sox2 from cultured E2f3a (E) or E2f3b (G) neural precursors or GE tissue. GAPDH and mtHsp70 were included as protein loading controls.

(F&H) Quantification by densitometry of immunoblots shows that E2f3a knock-outs express significantly more Sox2 (F), while E2f3b knockouts have lower Sox2 levels (H).

For all quantifications, data are plotted as mean +/- SEM (*$p<0.05$, **$p<0.01$, ***$p<0.001$). See also Figure S5.

Figure 4. Regulation of NSC Self-renewal by E2f3a is Sox2-dependent

(A-B) Immunoblot analysis (A) and densitometry quantification (B) of Sox2 expression in cultured GE neurospheres (E14.5) 5 days post infection (p.i.) with scrambled (Scr) control or sh-Sox2 lentiviruses (n=3). mtHsp70 was included as a measure of protein loading.

(C) Representative images of GFP positive neurospheres 7 days p.i. Scale bar = 200um.

(D&E) Infected cultures were plated immediately for primary neurosphere assays (D) and one week later were used in secondary neurosphere assays (E). Neurosphere numbers are restored in E2f3a knock-outs following Sox2 knock-down (n=4).

(F) Immunoblot demonstrating increased Sox2 expression in neurospheres infected with a Sox2 expressing lentivirus compared to GFP infected cells, 4 days p.i.

(G) Cells were plated 7 days p.i. for secondary neurosphere assays. Sox2 over-expression in wild-type cells increases self-renewal (n=3).

(H) E2f3a+/+ and E2f3a-/- neurospheres were cultured in differentiation media on poly-L-ornithine plates 7 days p.i. and were fixed and stained for Tuj1/ DAPI after 6 days. The percentage of DAPI+ cells that express Tuj1 were quantified. Sox2 over-expression inhibits neuronal differentiation *in vitro*. Scale bar = 50um (n=3).

Significance was determined for all samples compared to E2f3a-/- (panels B, D&E) or E2f3a+/+ (panels G&H) cells infected with control virus. All data are presented as the mean +/- SEM (*$p<0.05$, **$p<0.01$).

Figure 5. E2f3 isoforms recruit distinct transcriptional co-factors to the *Sox2* promoter

(A-D) ChIP was performed in E2f3a-/-, E2f3b-/- and wild-type (both E2f3a+/+ and E2f3b+/+) GE derived neurospheres using antibodies against E2f3 (A), RNA Polymerase II (B), H3K4Me3 and H3K27Me3 (C), and p107 (D). Chromatin enrichment was quantified by RT-PCR using primers designed to amplify 200bp regions centered on either the upstream conserved E2f motif or the TSS of the *Sox2* promoter. For all panels we have plotted values for the specific antibody IP with IgG values subtracted (n=3-5).

(E) Immunoblot analysis and densitometry quantification of p107+/+ and p107-/- GE tissue shows a significant increase in Sox2 levels in the absence of p107 (n=3). See also Figure S6.

Data for all panels are plotted as the mean +/- SEM (*$p<0.05$, **$p<0.01$).

Figure 6. E2f3a Regulates *Sox2*, Neurogenesis and Cognitive Function in the Adult Brain

(A) Immunoblot showing loss of E2f3a, but not E2f3b, in E2f3-*flox*/E2f3a- adult SVZ precursors 4 days after Cre infection. Results were quantified by densitometry, using mtHsp70 as a loading control (n=4).

(B) Infected cells were plated for neurosphere assays 7 days p.i. and regenerated neurospheres were counted 6 days later. Cre infected cells generate more neurospheres than controls. Image to the right shows GFP expressing neurospheres infected with either control (GFP) or GFP-CRE virus 7 days p.i. (n=7).

(C) Neurospheres were plated in differentiation media on poly-L-ornithine coated dishes 7 days p.i. and were fixed and stained for Tuj1/DAPI after 6 days. The percentage of DAPI+ cells

expressing Tuj1 was quantified. Cre infected cells have a reduced capacity to generate neurons (n=5).

(D) Elevated Sox2 in Cre versus GFP infected E2f3-*flox*/E2f3a- adult precursors (5 days p.i.), quantified by densitometry, using mtHsp70 as a loading control (n=3).

(E-G) RT-PCR analysis of ChIP assays for E2f3 (E), p107 (F) and RNA Polymerase II (G) in GFP or Cre infected E2f3-*flox*/E2f3a-/- precursors (n=4).

(H-L) Neurogenesis was measured in the adult brain by quantifying the total area of DCX staining along the SVZ (n=4) (H), and the number of NeuroD1+ or DCX+ cells in the DG of the hippocampus (n=3) (I-J).

(K) E2f3a-/- mice spent 45% and 21% less time freezing in the context ($p=0.015$) and after the auditory cue ($p=0.047$), respectively, following fear conditioning training (n=18 for E2f3a+/+, n=13 for E2f3a-/-).

For all panels, data are presented as mean +/- SEM. Scale bar = 100um for panels B, H & J and 25um for panel C (*$p<0.05$, **$p<0.01$, ***$p<0.001$). See also Figure S7.

Figure 7. Model of E2f3 Function: E2f3 Isoforms Regulate *Sox2* Transcription in an Opposing manner to Direct NSC Fate Choice

(A) In wild-type conditions, E2f3b activates and E2f3a represses *sox2* transcription, allowing for dynamic fine-tuning of Sox2 levels. This fine-tuning maintains the proper balance between neurogenesis and expansion of the NPC pool.

(B) In the absence of E2f3b, E2f3a/p107 mediated repression dominates and reduces Sox2 levels, thereby increasing neurogenesis at the expense of precursor expansion.

(C) In the absence of E2f3a, E2f3b mediated activation is unbalanced by E2f3a repression, thus increasing Sox2 levels and promoting NPC expansion at the expense of neurogenesis.

FIGURE 1

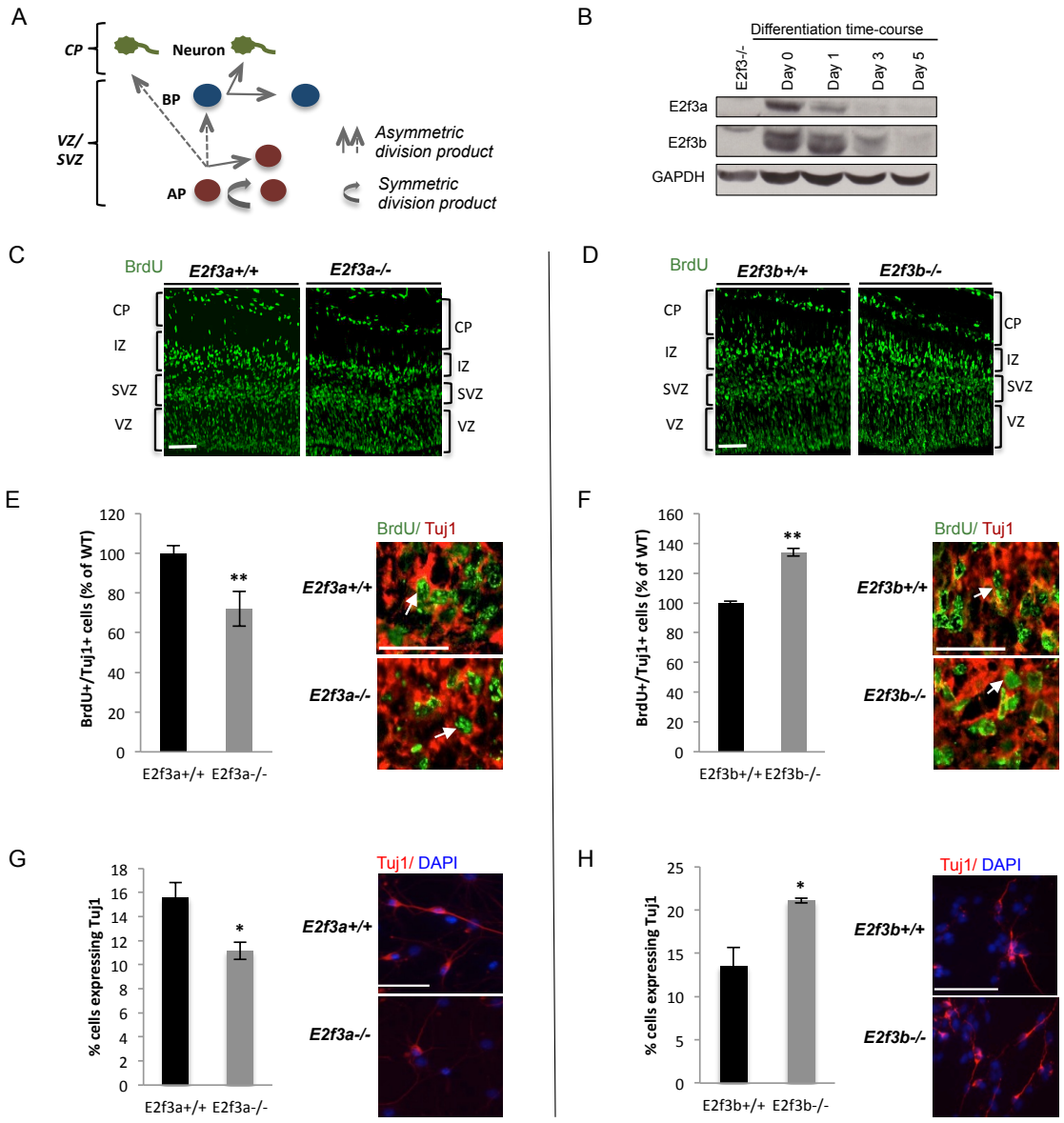
A
CP
Neuron
BP
VZ/
SVZ
AP
Asymmetric
division product
Symmetric
division product
B
Differentiation time-course
E2f3-/-
Day 0
Day 1
Day 3
Day 5
E2f3a
E2f3b
GAPDH
C
BrdU
E2f3a+/+
E2f3a-/-
CP
IZ
SVZ
VZ
D
BrdU
E2f3b+/+
E2f3b-/-
E
BrdU+/Tuj1+ cells (% of WT)
E2f3a+/+ E2f3a-/-
BrdU/ Tuj1
F
BrdU+/Tuj1+ cells (% of WT)
E2f3b+/+ E2f3b-/-
BrdU/ Tuj1
G
% cells expressing Tuj1
E2f3a+/+ E2f3a-/-
Tuj1/ DAPI
H
% cells expressing Tuj1
E2f3b+/+ E2f3b-/-
Tuj1/ DAPI

FIGURE 2

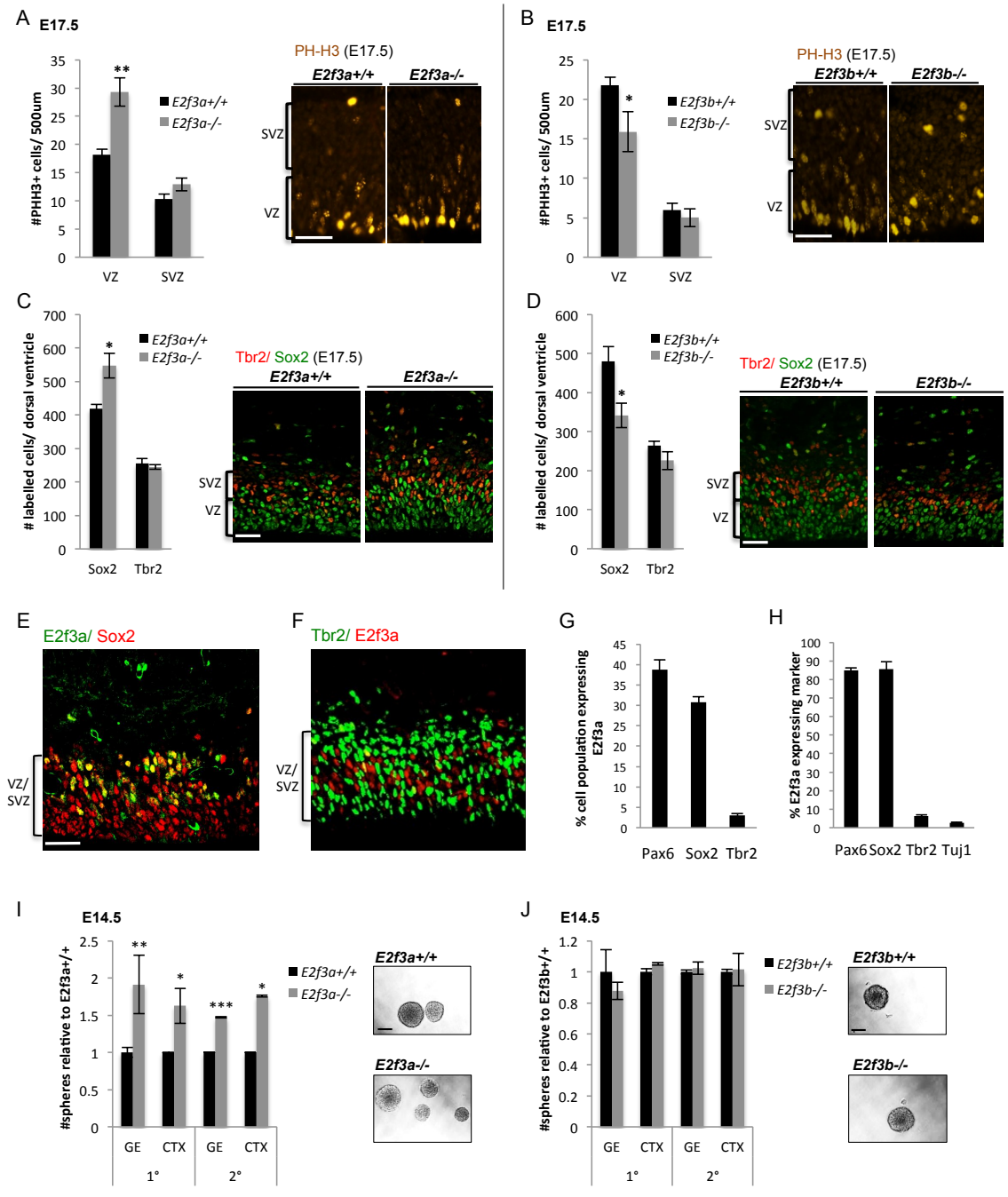
A
E17.5
#PHH3+ cells/ 500um
E2f3a+/+
E2f3a-/-
VZ
SVZ
PH-H3 (E17.5)
E2f3a+/+
E2f3a-/-
SVZ
VZ
B
E17.5
#PHH3+ cells/ 500um
E2f3b+/+
E2f3b-/-
VZ
SVZ
PH-H3 (E17.5)
E2f3b+/+
E2f3b-/-
SVZ
VZ
C
labelled cells/ dorsal ventricle
E2f3a+/+
E2f3a-/-
Sox2
Tbr2
Tbr2/ Sox2 (E17.5)
E2f3a+/+
E2f3a-/-
SVZ
VZ
D
labelled cells/ dorsal ventricle
E2f3b+/+
E2f3b-/-
Sox2
Tbr2
Tbr2/ Sox2 (E17.5)
E2f3b+/+
E2f3b-/-
SVZ
VZ
E
E2f3a/ Sox2
VZ/
SVZ
F
Tbr2/ E2f3a
VZ/
SVZ
G
% cell population expressing E2f3a
Pax6
Sox2
Tbr2
H
% E2f3a expressing marker
Pax6
Sox2
Tbr2
Tuj1
I
E14.5
#spheres relative to E2f3a+/+
E2f3a+/+
E2f3a-/-
GE
CTX
GE
CTX
1°
2°
E2f3a+/+
E2f3a-/-
J
E14.5
#spheres relative to E2f3b+/+
E2f3b+/+
E2f3b-/-
GE
CTX
GE
CTX
1°
2°
E2f3b+/+
E2f3b-/-

FIGURE 3

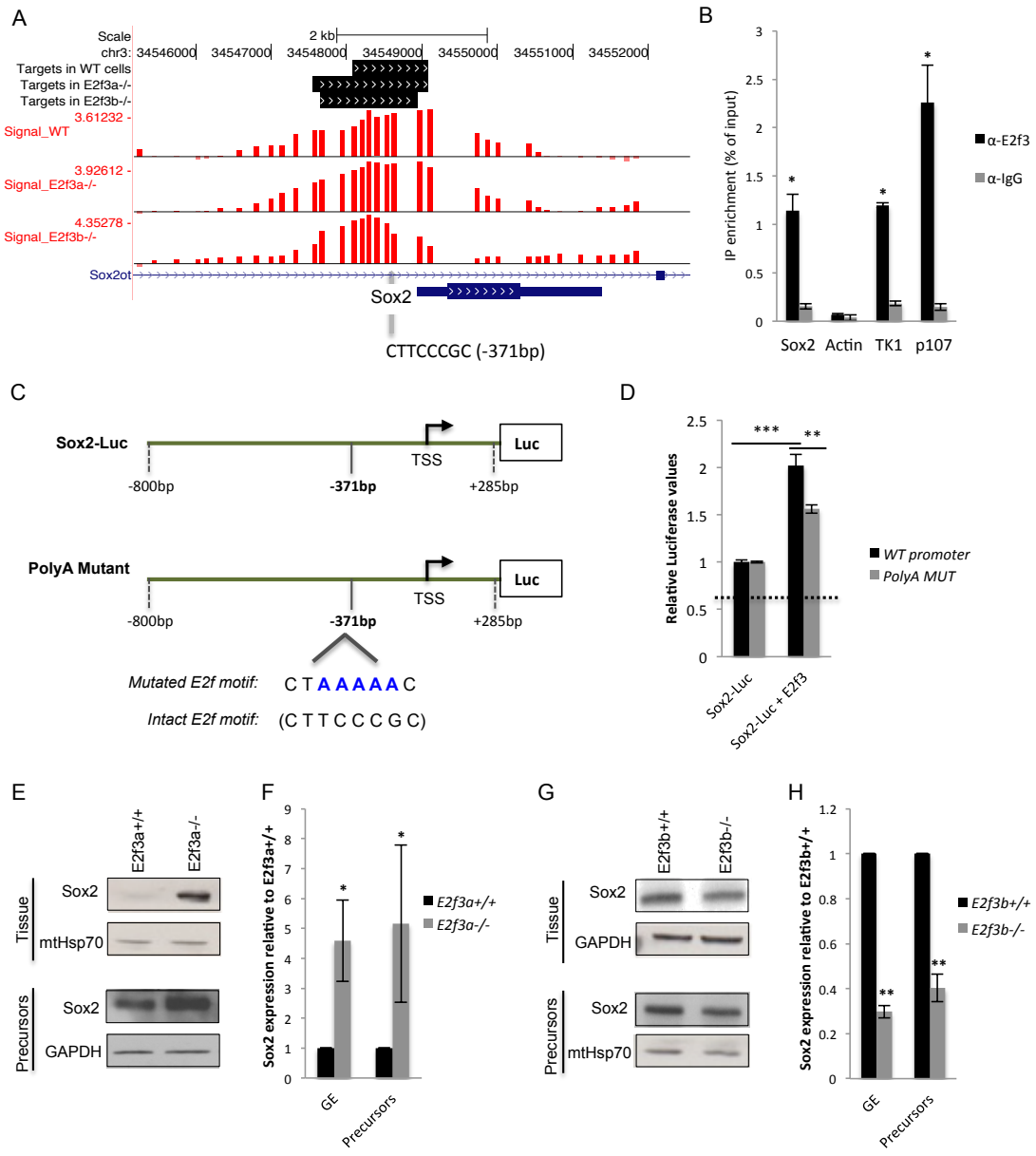
A
Scale
2 kb
chr3: 34546000 34547000 34548000 34549000 34550000 34551000 34552000
Targets in WT cells
Targets in E2f3a-/-
Targets in E2f3b-/-
3.61232
Signal_WT
3.92612
Signal_E2f3a-/-
4.35278
Signal_E2f3b-/-
Sox2ot
Sox2
CTTCCCGC (-371bp)
B
IP enrichment (% of input)
α-E2f3
α-IgG
Sox2 Actin TK1 p107
C
Sox2-Luc
Luc
TSS
-800bp
-371bp
+285bp
PolyA Mutant
Mutated E2f motif: C T A A A A A C
Intact E2f motif: (C T T C C C G C)
D
Relative Luciferase values
WT promoter
PolyA MUT
Sox2-Luc
Sox2-Luc + E2f3
E
E2f3a+/+
E2f3a-/-
Tissue
Sox2
mtHsp70
Precursors
Sox2
GAPDH
F
Sox2 expression relative to E2f3a+/+
E2f3a+/+
E2f3a-/-
GE
Precursors
G
E2f3b+/+
E2f3b-/-
Tissue
Sox2
GAPDH
Precursors
Sox2
mtHsp70
H
Sox2 expression relative to E2f3b+/+
E2f3b+/+
E2f3b-/-
GE
Precursors

FIGURE 4

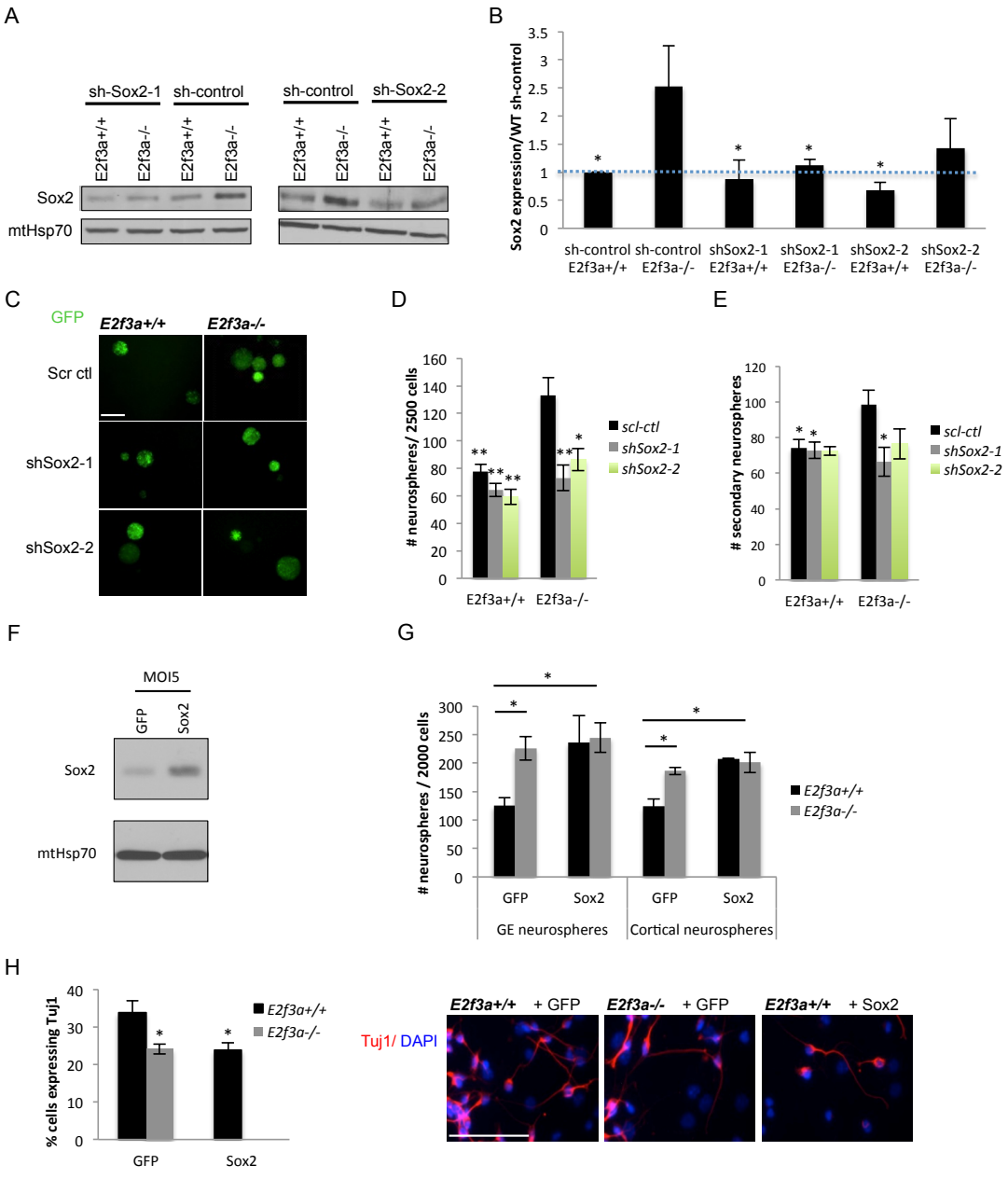
A
sh-Sox2-1
sh-control
sh-control
sh-Sox2-2
E2f3a+/+
E2f3a-/-
E2f3a+/+
E2f3a-/-
E2f3a+/+
E2f3a-/-
E2f3a+/+
E2f3a-/-
Sox2
mtHsp70
B
Sox2 expression/WT sh-control
3.5
3
2.5
2
1.5
1
0.5
0
sh-control E2f3a+/+
sh-control E2f3a-/-
shSox2-1 E2f3a+/+
shSox2-1 E2f3a-/-
shSox2-2 E2f3a+/+
shSox2-2 E2f3a-/-
C
GFP
E2f3a+/+
E2f3a-/-
Scr ctl
shSox2-1
shSox2-2
D
neurospheres/ 2500 cells
160
140
120
100
80
60
40
20
0
scl-ctl
shSox2-1
shSox2-2
E2f3a+/+
E2f3a-/-
E
secondary neurospheres
120
100
80
60
40
20
0
scl-ctl
shSox2-1
shSox2-2
E2f3a+/+
E2f3a-/-
F
MOI5
GFP
Sox2
Sox2
mtHsp70
G
neurospheres / 2000 cells
300
250
200
150
100
50
0
E2f3a+/+
E2f3a-/-
GFP
Sox2
GFP
Sox2
GE neurospheres
Cortical neurospheres
H
% cells expressing Tuj1
40
30
20
10
0
E2f3a+/+
E2f3a-/-
GFP
Sox2
E2f3a+/+ + GFP
E2f3a-/- + GFP
E2f3a+/+ + Sox2
Tuj1/ DAPI

FIGURE 5

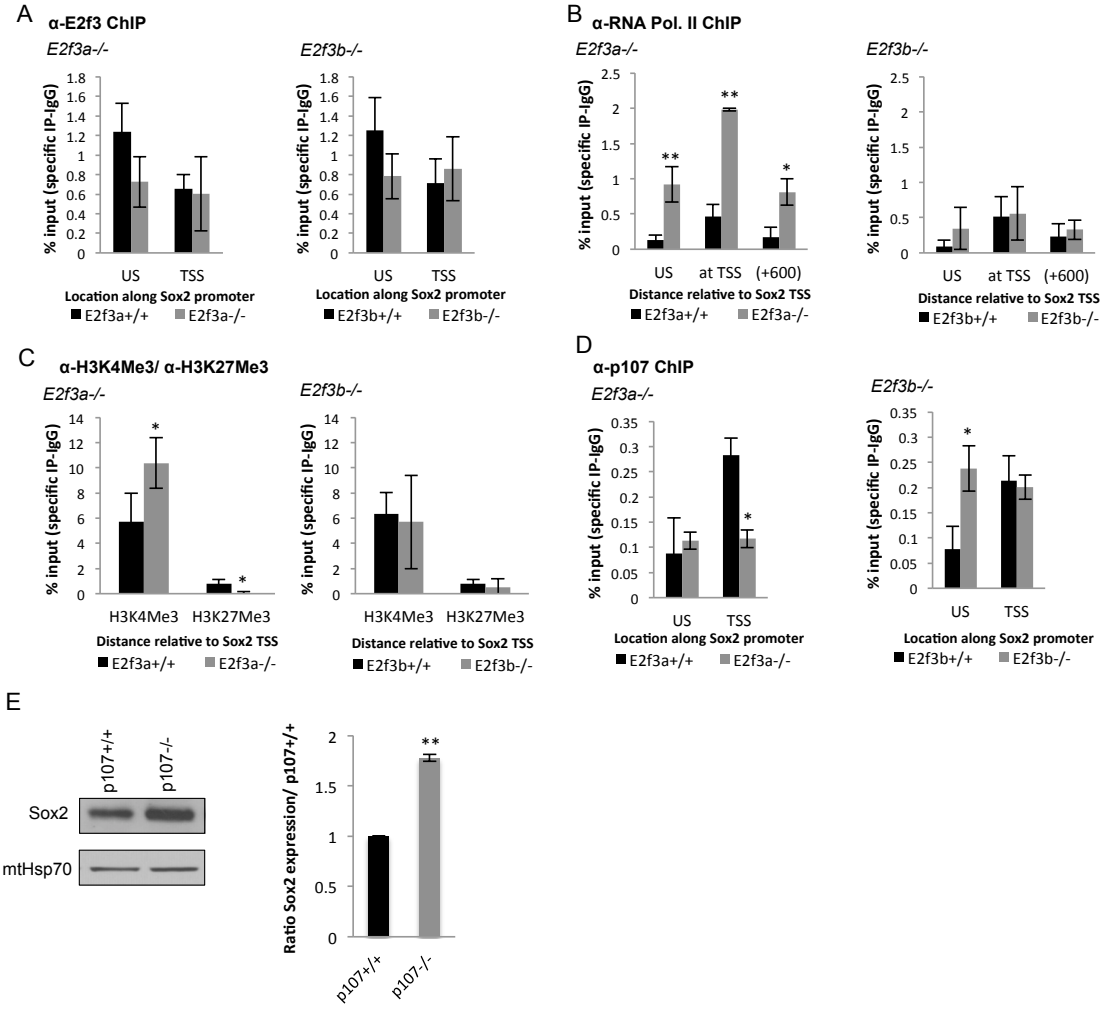
A
α-E2f3 ChIP
E2f3a-/-
E2f3b-/-
% input (specific IP-IgG)
US
TSS
Location along Sox2 promoter
E2f3a+/+
E2f3a-/-
E2f3b+/+
E2f3b-/-
B
α-RNA Pol. II ChIP
at TSS
(+600)
Distance relative to Sox2 TSS
C
α-H3K4Me3/ α-H3K27Me3
H3K4Me3
H3K27Me3
D
α-p107 ChIP

E
p107+/+
p107-/-
Sox2
mtHsp70
Ratio Sox2 expression/ p107+/+

FIGURE 6

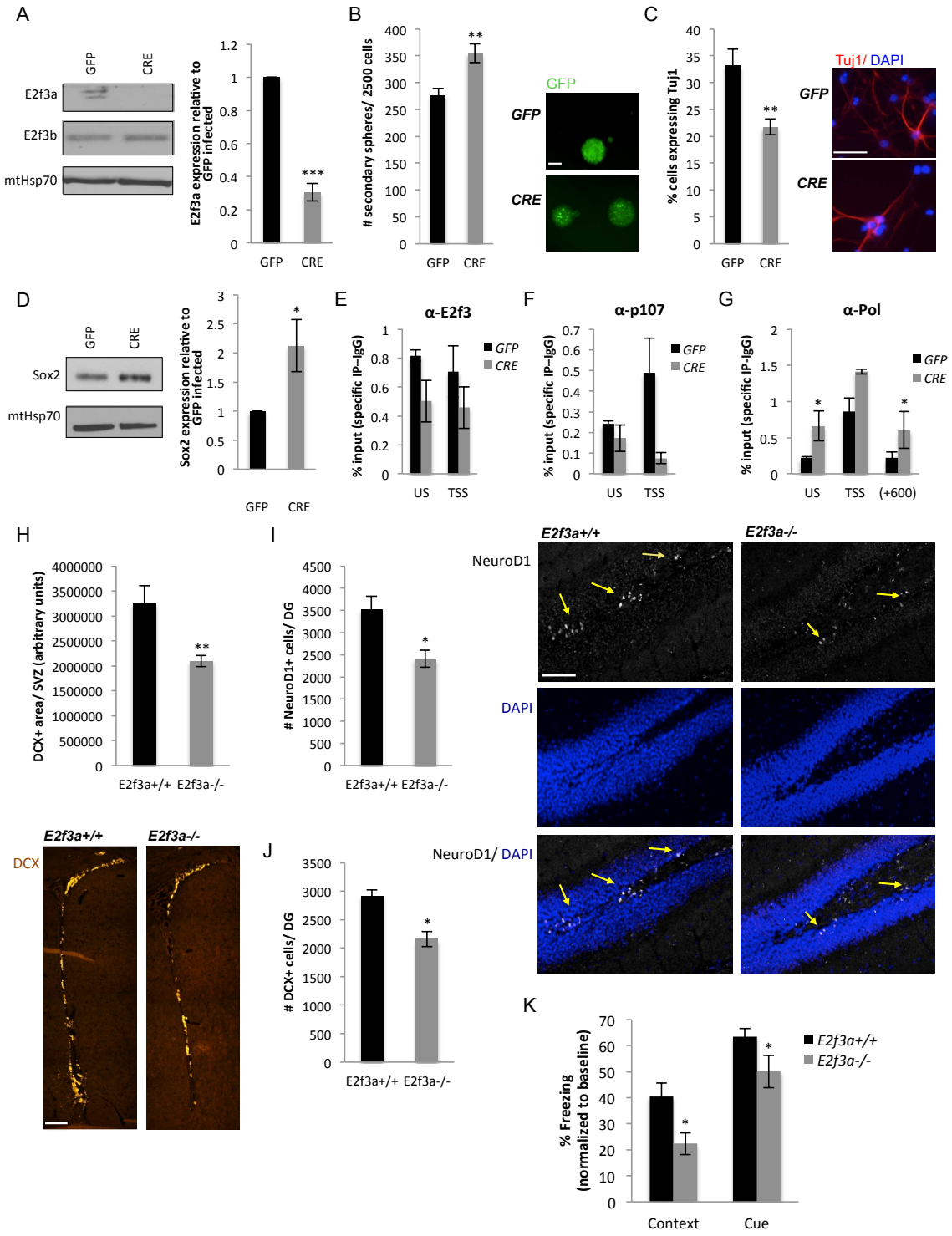
A
GFP
CRE
E2f3a
E2f3b
mtHsp70
E2f3a expression relative to GFP infected
GFP
CRE
B
secondary spheres/ 2500 cells
GFP
CRE
C
% cells expressing Tuj1
Tuj1/ DAPI
GFP
CRE
D
Sox2
mtHsp70
Sox2 expression relative to GFP infected
E
α-E2f3
% input (specific IP–IgG)
US
TSS
F
α-p107
G
α-Pol
(+600)
H
DCX+ area/ SVZ (arbitrary units)
E2f3a+/+
E2f3a-/-
I
NeuroD1+ cells/ DG
NeuroD1
DAPI
NeuroD1/ DAPI
DCX
J
DCX+ cells/ DG
K
% Freezing (normalized to baseline)
Context
Cue

FIGURE 7

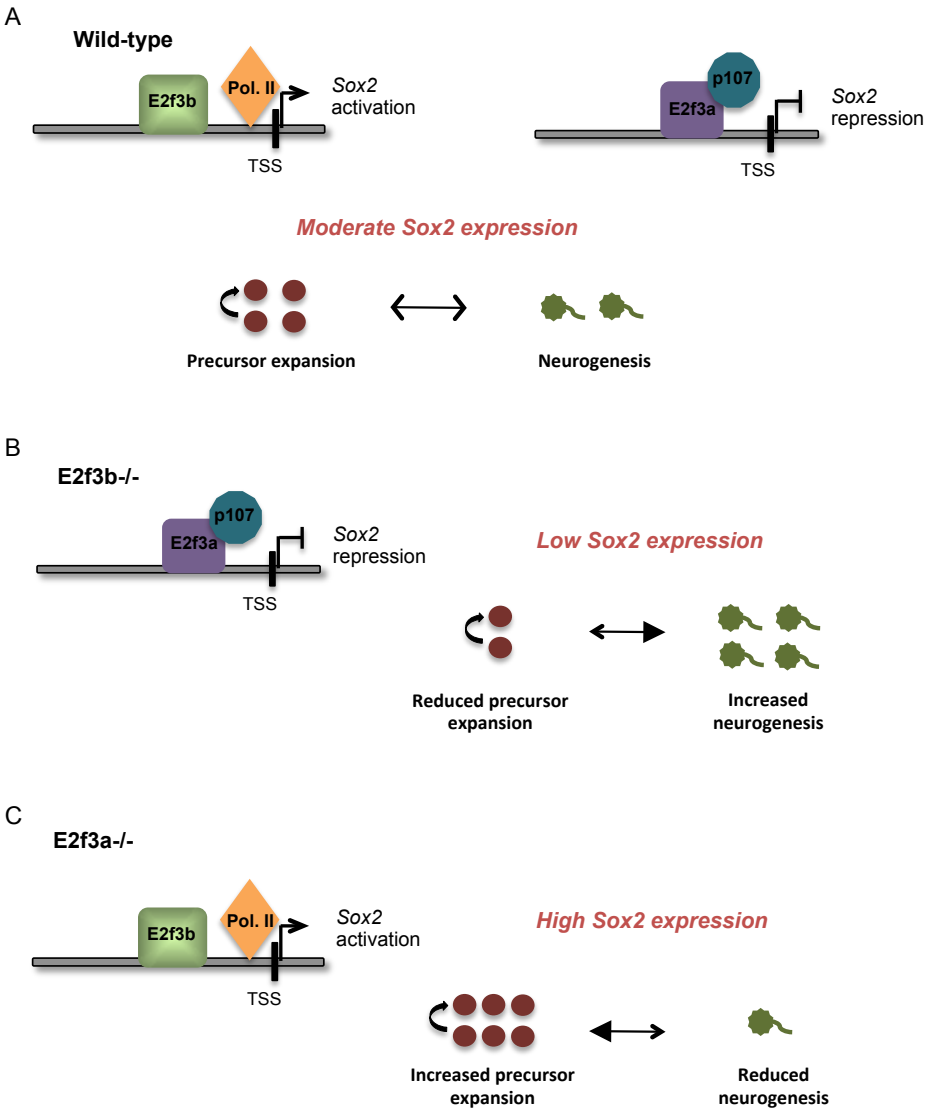
A
Wild-type
E2f3b
Pol. II
Sox2
activation
TSS
p107
E2f3a
Sox2
repression
TSS
Moderate Sox2 expression
Precursor expansion
Neurogenesis
B
E2f3b-/-
p107
E2f3a
Sox2
repression
TSS
Low Sox2 expression
Reduced precursor
expansion
Increased
neurogenesis
C
E2f3a-/-
E2f3b
Pol. II
Sox2
activation
TSS
High Sox2 expression
Increased precursor
expansion
Reduced
neurogenesis

Supplemental Information

Opposing Regulation of *Sox2* by Cell Cycle Effectors E2f3a&b in Neural Stem Cells

Lisa M Julian, Renaud Vandenbosch, Catherine A Pakenham, Matthew G Andrusiak, Angela P Nguyen, Kelly A McClellan, Devon S Svoboda, Diane C Lagace, David S Park, Gustavo E Leone, Alexandre Blais, and Ruth S Slack

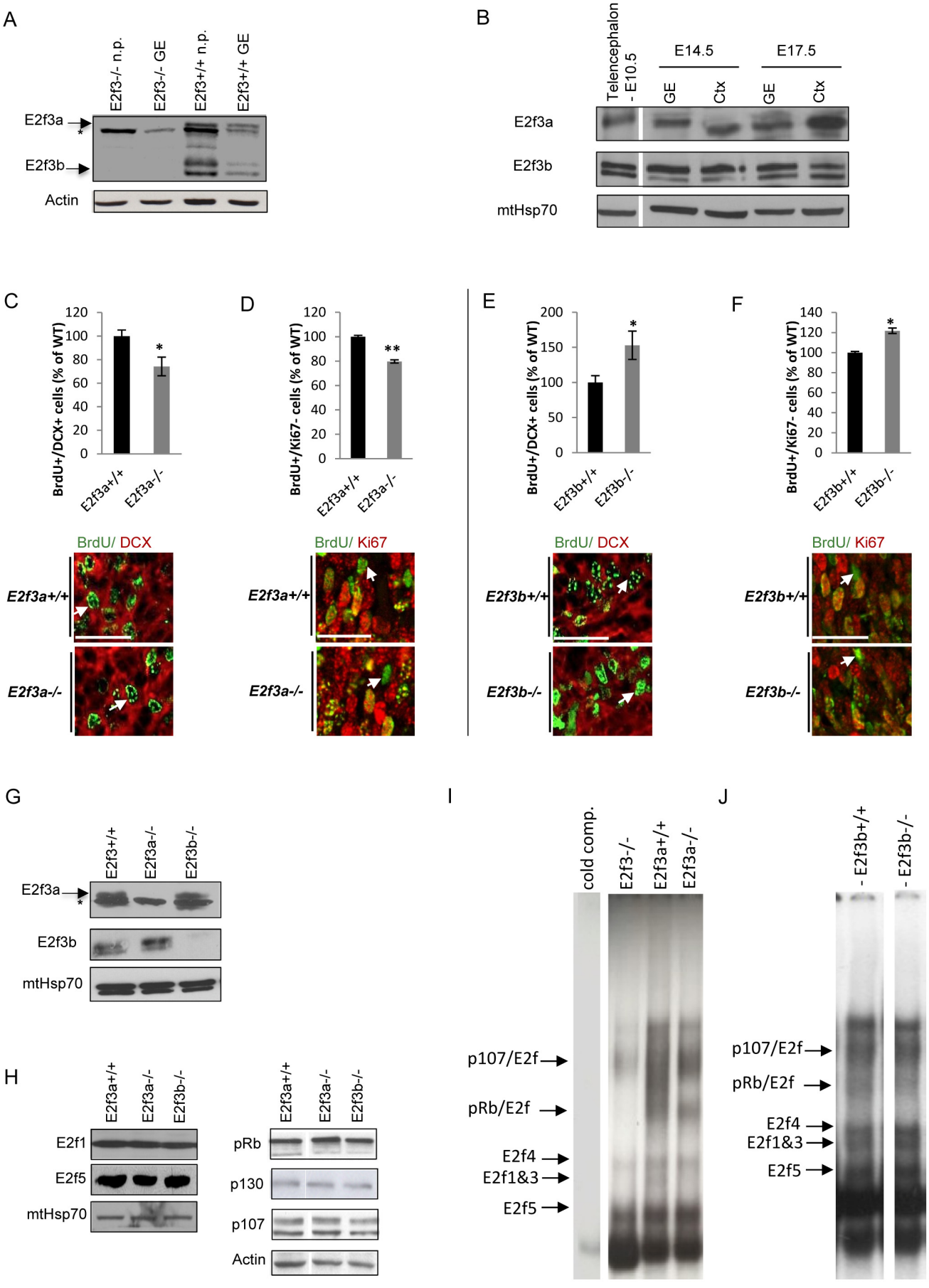
A
E2f3-/- n.p.
E2f3-/- GE
E2f3+/+ n.p.
E2f3+/+ GE
E2f3a
E2f3b
Actin
B
Telencephalon - E10.5
E14.5
E17.5
GE
Ctx
GE
Ctx
E2f3a
E2f3b
mtHsp70
C
BrdU+/DCX+ cells (% of WT)
E2f3a+/+
E2f3a-/-
BrdU/ DCX
E2f3a+/+
E2f3a-/-
D
BrdU+/Ki67- cells (% of WT)
E2f3a+/+
E2f3a-/-
BrdU/ Ki67
E2f3a+/+
E2f3a-/-
E
BrdU+/DCX+ cells (% of WT)
E2f3b+/+
E2f3b-/-
BrdU/ DCX
E2f3b+/+
E2f3b-/-
F
BrdU+/Ki67- cells (% of WT)
E2f3b+/+
E2f3b-/-
BrdU/ Ki67
E2f3b+/+
E2f3b-/-
G
E2f3+/+
E2f3a-/-
E2f3b-/-
E2f3a
E2f3b
mtHsp70
H
E2f3a+/+
E2f3a-/-
E2f3b-/-
E2f1
E2f5
mtHsp70
pRb
p130
p107
Actin
I
cold comp.
E2f3-/-
E2f3a+/+
E2f3a-/-
p107/E2f
pRb/E2f
E2f4
E2f1&3
E2f5
J
- E2f3b+/+
- E2f3b-/-
p107/E2f
pRb/E2f
E2f4
E2f1&3
E2f5

Figure S1. Expression pattern of pRb/E2f family members in wild-type and E2f3a/b deficient neural precursors. Quantification of newly committed DCX+ and Ki67- cells *in vivo*. Related to Figure 1.

(A) Immunoblot for E2f3 in cultured neural precursors (neurospheres) (n.p.) and GE tissue at E14.5. Actin was used as a protein loading control. Arrows indicate the bands for E2f3a and E2f3b, * denotes a non-specific band.

(B) Immunoblot for E2f3 in GE and dorsal cortex tissue (Ctx) at E14.5 and E17.5, and whole telencephalon at E10.5, demonstrating that both isoforms are expressed at different developmental stages and in telencephalic proliferative zones. mtHsp70 was included as a loading control.

(C-F) Pregnant mothers received an IP injection of BrdU at gestation day E13.5, embryos were sacrificed 24 hours later and their brains were sectioned coronally and processed for immuno-staining. The number of newly committed neurons in the dorsal cortex were identified as those cells expressing both BrdU and doublecortin (DCX), an immature neuronal marker. BrdU+/DCX+ cells were quantified within a defined area through the SVZ/IZ of wild-type and knock-out E2f3a (C) and E2f3b (E) mice. Additionally, the number of newly committed cells that were no longer cycling were identified as BrdU+/Ki67- cells (D&F) (n=4). Results are presented as a percentage of the wild-type average +/- SEM (*$p<0.05$, **$p<0.01$).

(G) Immunoblot for E2f3 from E14.5 cultured neurospheres, demonstrating that expression of the other E2f3 isoform is not changed when the other isoform is absent. * non-specific band. mtHsp70 was included as a loading control.

(H) Immunoblot in neural precursor cultures from the indicated genotypes for pRb and E2f family members demonstrates a lack of compensatory expression changes in the absence of E2f3a or E2f3b. mtHsp70 and Actin were included as loading controls.

(I&J) Electrophoretic mobility shift assays demonstrate that DNA binding by other E2fs is not highly deregulated in the absence of E2f3a (I) or E2f3b (J).

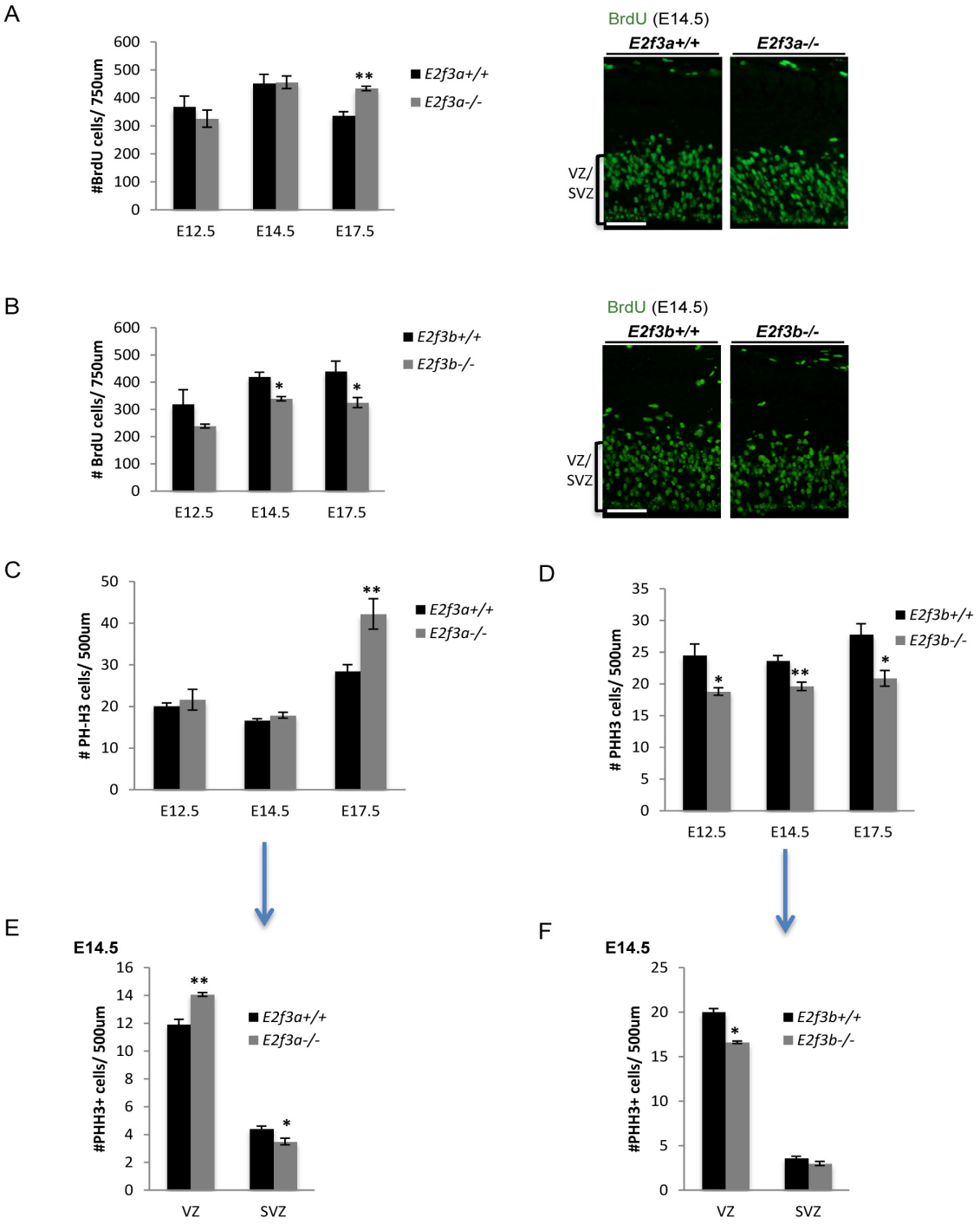
A
#BrdU cells/ 750um
600
500
400
300
200
100
0
E12.5
E14.5
E17.5
**
E2f3a+/+
E2f3a-/-
BrdU (E14.5)
E2f3a+/+
E2f3a-/-
VZ/
SVZ
B
BrdU cells/ 750um
600
500
400
300
200
100
0
E12.5
E14.5
E17.5
*
*
E2f3b+/+
E2f3b-/-
BrdU (E14.5)
E2f3b+/+
E2f3b-/-
VZ/
SVZ
C
PH-H3 cells/ 500um
50
40
30
20
10
0
E12.5
E14.5
E17.5
**
E2f3a+/+
E2f3a-/-
D
PHH3 cells/ 500um
35
30
25
20
15
10
5
0
E12.5
E14.5
E17.5
*
**
*
E2f3b+/+
E2f3b-/-
E
E14.5
#PHH3+ cells/ 500um
16
14
12
10
8
6
4
2
0
VZ
SVZ
**
*
E2f3a+/+
E2f3a-/-
F
E14.5
#PHH3+ cells/ 500um
25
20
15
10
5
0
VZ
SVZ
*
E2f3b+/+
E2f3b-/-

Figure S2. PH-H3 immuno-staining and 2 hour BrdU pulse in E2f3a and E2f3b knock-outs at additional time-points. Related to Figure 2.

(A-D) Quantification of BrdU+ (A&C) or PH-H3+ (B&D) cells in the dorsal cortex following a 2hr BrdU pulse in E12.5, E14.5 and E17.5 sections from E2f3a (A&C) and E2f3b (B&D) wild-type and knock-out mice. BrdU and PH-H3 expressing cells were quantified throughout both the VZ and SVZ.

(E&F) Quantification of the number of PH-H3+ cells in the VZ and SVZ separately demonstrates that at E14.5 precursors in the VZ of E2f3a-/- mice are already expanded compared to E2f3a+/+ (E), and that VZ precursors are the only population affected in E2f3b-/- mice (F).

Results are presented as the mean number of cells per ventricular length of 500um (PH-H3) or 750um (BrdU) +/- SEM (*$p<0.05$, **$p<0.01$) (n=4). Scale bars = 100um.

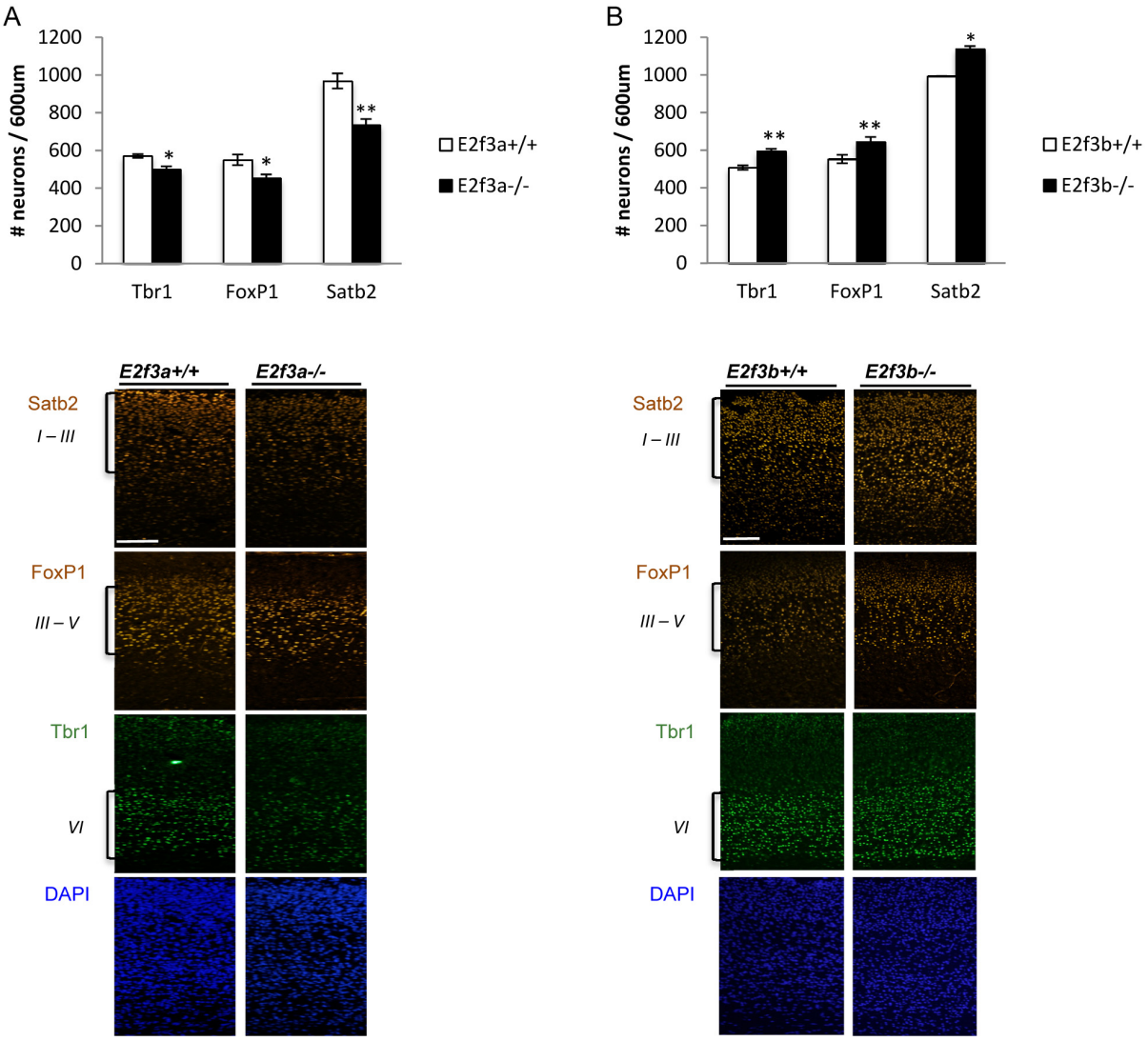
A
neurons / 600um
1200
1000
800
600
400
200
0
Tbr1
FoxP1
Satb2
E2f3a+/+
E2f3a-/-
B
neurons / 600um
1200
1000
800
600
400
200
0
Tbr1
FoxP1
Satb2
E2f3b+/+
E2f3b-/-
E2f3a+/+
E2f3a-/-
Satb2
I – III
FoxP1
III – V
Tbr1
VI
DAPI
E2f3b+/+
E2f3b-/-
Satb2
I – III
FoxP1
III – V
Tbr1
VI
DAPI

Figure S3. Neuronal Output in E2f3a-/- and E2f3b-/- new-born cortex. Related to Figure 2.

Brain sections at post-natal day 1 were stained for layer VI Tbr1+ neurons (early born), layer III-V FoxP1+ neurons, and layer I-III Satb2+ neurons (late born) to identify neuronal output in the new-born brain.

(A) In E2f3a-/- brains, the number of Tbr1+ neurons was decreased by 13%, FoxP1 by 18%, and Satb2 by 24, demonstrating that later born neurons are more reduced than early born neurons when E2f3a is absent (n=3).

(B) In E2f3b-/- brains, Tbr1+ neurons were increased by 15%, and FoxP1 and Satb2 were each increased by 13% (n=3).

Results are presented as the average number of positive neurons from 3 sections per animal over a 600um ventricular length +/- SEM. Scale bars = 50um.

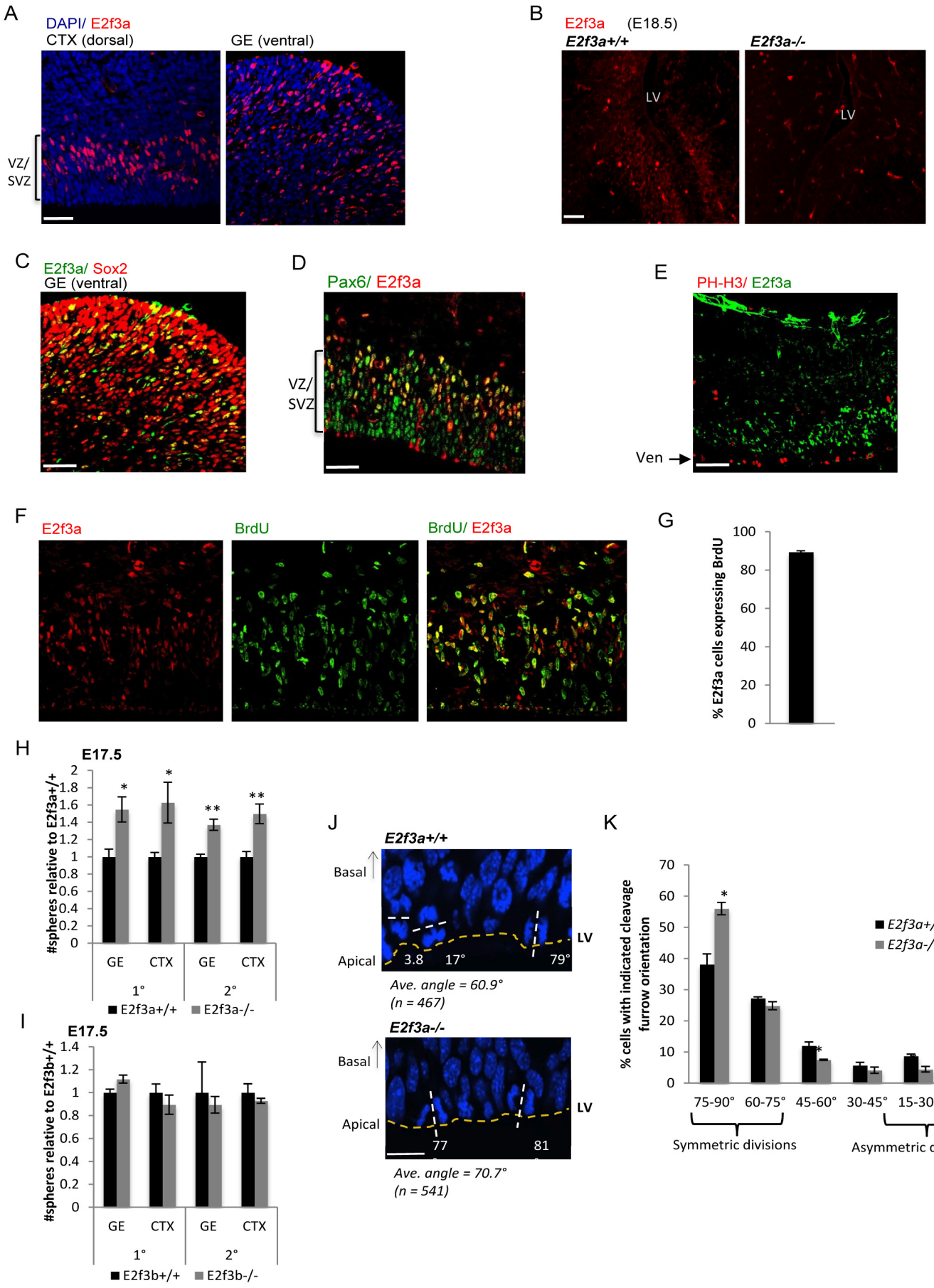
A
DAPI/ E2f3a
CTX (dorsal)
GE (ventral)
VZ/
SVZ
B
E2f3a (E18.5)
E2f3a+/+
E2f3a-/-
LV
LV
C
E2f3a/ Sox2
GE (ventral)
D
Pax6/ E2f3a
VZ/
SVZ
E
PH-H3/ E2f3a
Ven
F
E2f3a
BrdU
BrdU/ E2f3a
G
% E2f3a cells expressing BrdU
100
80
60
40
20
0
H
E17.5
#spheres relative to E2f3a+/+
2
1.8
1.6
1.4
1.2
1
0.8
0.6
0.4
0.2
0
*
*
**
**
GE
CTX
GE
CTX
1°
2°
E2f3a+/+
E2f3a-/-
I
E17.5
#spheres relative to E2f3b+/+
1.4
1.2
1
0.8
0.6
0.4
0.2
0
GE
CTX
GE
CTX
1°
2°
E2f3b+/+
E2f3b-/-
J
E2f3a+/+
Basal
Apical
LV
3.8
17°
79°
Ave. angle = 60.9°
(n = 467)
E2f3a-/-
Basal
Apical
LV
77
81
Ave. angle = 70.7°
(n = 541)
K
% cells with indicated cleavage furrow orientation
70
60
50
40
30
20
10
0
*
*
E2f3a+/+
E2f3a-/-
75-90°
60-75°
45-60°
30-45°
15-30°
0-15°
Symmetric divisions
Asymmetric divisions

Figure S4. E2f3a is expressed in S phase apical precursors *in vivo*. Analysis of self-renewal defects by neurosphere assay at E17.5, and mitotic spindle pole analysis. Related to Figure 2.

(A) Immunohistochemistry (IHC) using an N-terminal E2f3 (red) antibody at E14.5 demonstrates expression of E2f3a in a subset of cells in the VZ/SVZ within the dorsal cortex, and the GE.

(B) IHC for E2f3a at E18.5 in wild-type and E2f3a deficient brain sections demonstrates specificity of E2f3a detection around the lateral ventricle (LV) by our antibody.

(C) IHC for E2f3a (green) and Sox2 (red) in the GE at E14.5 shows that E2f3a is also expressed in ventral telencephalic Sox2+ precursors.

(D) Pax6 was used as an independent marker of apical precursor cells. IHC demonstrates co-labeling between E2f3a and Pax6 in the dorsal cortex.

(E) IHC for E2f3a and PH-H3 in the E14.5 dorsal cortex, indicates no expression of E2f3a in mitotic cells (Ven = ventricle).

(F) Brain sections that received a 2hr BrdU pulse were stained for BrdU and E2f3a, and were imaged along the dorsal cortex.

(G) Quantification of E2f3a+/BrdU+ cells. The number of E2f3a expressing cells per section that also express BrdU was quantified. The majority (89%) of E2f3a+ cells co-express BrdU and are therefore in S phase. Results are presented as averages +/- SEM (n=3). Scale bars for panels A-F is 100um.

(H&I) Primary and secondary neurosphere assays were performed at E17.5 from wild-type and knock-out E2f3a (H) and E2f3b (I) neurosphere cultures derived from both the GE and dorsal cortex (Ctx). Again, as with E14.5 neurosphere assays, E2f3a deficiency leads to increased neurosphere numbers and self-renewal, while E2f3b loss has no effect. The data is presented as mean +/- SEM (n=4).

(J) Orientation of the mitotic spindle pole has been linked to asymmetric versus symmetric divisions due to the segregation pattern of cell fate determinants. Vertical cleavage planes (60-90°) are associated with symmetric divisions, and horizontal (0-30°) and intermediate (30-60°) cleavage planes correlate with asymmetric divisions. Chromatin was visualized by DAPI, and lines were drawn to trace the apical surface of the lateral ventricle (LV) (yellow line) or through sister chromatids to mark the cleavage furrow (white line). The smallest angle between them was calculated. Scale bar = 10um.

(E) Spindle pole angle measurements were collected for over 460 cells per genotype from 3 separate animals. The percentage of all cells measured that fell within specific angle ranges was calculated. E2f3a loss results in a greater percentage of vertical cleavage planes (associated with symmetric divisions), and a lower percentage of horizontal cleavage planes (correlated with asymmetric divisions). Mean values +/ SEM is shown.

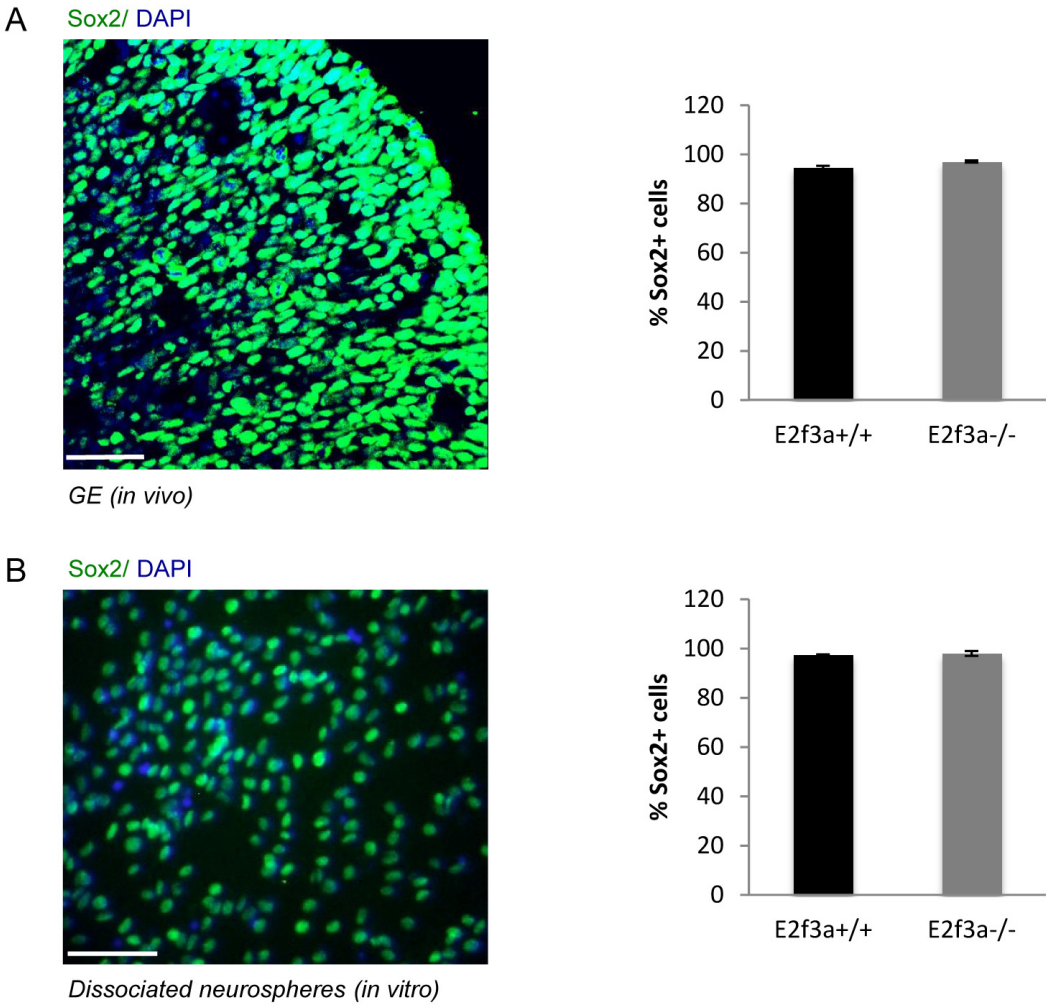

Figure S5. GE precursors *in vivo* and *in vitro* virtually all express Sox2. Related to Figure 3.

(A) E14.5 brain sections were stained for DAPI and Sox2 and the ganglionic eminence (GE) was imaged. The structure shown in the image is representative of the GE tissue that is obtained in our dissections and that was used in our Immunoblot analysis. Quantification of the percentage of DAPI+ cells that are also Sox2+ shows that 95% of E2f3a+/+ and 97% of E2f3a-/- GE cells *in vivo* express Sox2, and there is no significant difference between genotypes. Results are presented as the mean +/- SEM for n=4. Scale bar is 100um.

(B) In neurosphere cultures derived from E14.5 GE dissections, 97% and 98% of cells from E2f3a+/+ and E2f3a-/- cultures, respectively, express Sox2.

Results are presented as the mean, and error bars representing the range of values, for n=2. Scale bar is 100um.

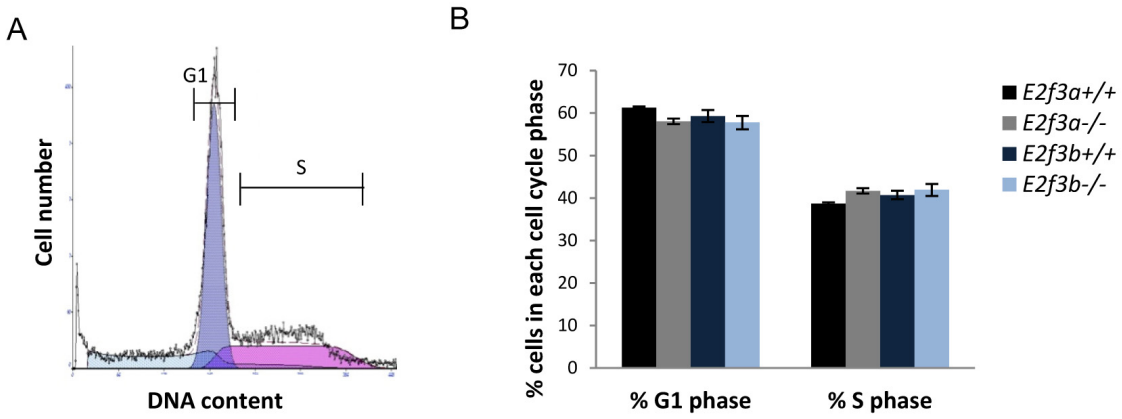

Figure S6. Loss of E2f3 isoforms does not alter cell cycle dynamics. Related to Figure 5.

(A) Actively proliferating neurosphere cultures were fixed, stained with DAPI and prepared for flow cytometry. The number of cells in G1 and S phases of the cell cycle was determined based on 2N and 4N DNA, respectively, as determined by DAPI fluorescence.

(B) The percentage of cells in G1 or S phases was similar in E2f3a and E2f3b control and knockout neural precursors. Data shown is the mean +/- SEM (n=4).

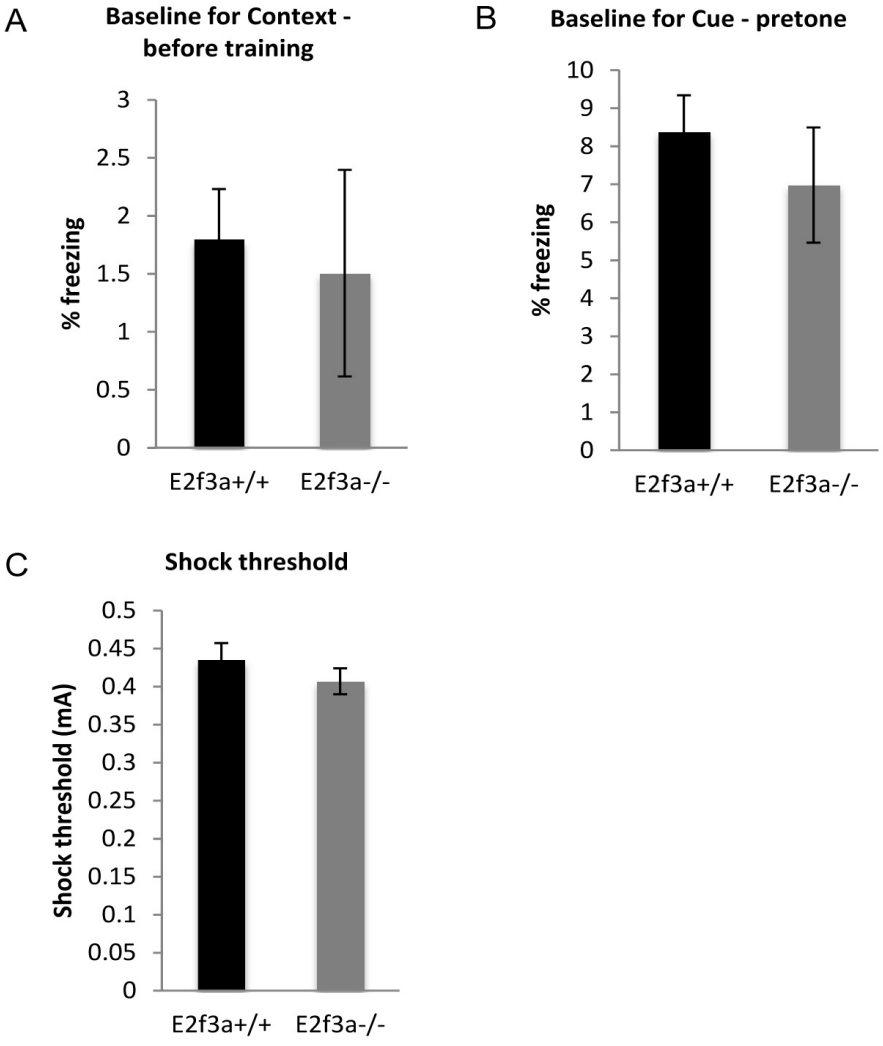
A
Baseline for Context - before training
% freezing
3
2.5
2
1.5
1
0.5
0
E2f3a+/+
E2f3a-/-
B
Baseline for Cue - pretone
% freezing
10
9
8
7
6
5
4
3
2
1
0
E2f3a+/+
E2f3a-/-
C
Shock threshold
Shock threshold (mA)
0.5
0.45
0.4
0.35
0.3
0.25
0.2
0.15
0.1
0.05
0
E2f3a+/+
E2f3a-/-

Figure S7. Baseline freezing for context and cue experiments and shock threshold are unchanged between genotypes. Related to Figure 6.

(A) Mice were placed in the fear conditioning apparatus for two minutes before the first foot shock was administered, and the percent of time spent freezing was measured and reported as baseline freezing relevant to the context. E2f3a+/+ and E2f3a-/- mice exhibit similar baseline freezing levels, and baseline levels were significantly lower than post-training contextual freezing levels (data not shown) (E2f3a+/+: $p=4.06x10^{-9}$; 24-fold decrease).

(B) Following fear conditioning training and prior to cue testing, mice are placed in a second novel environment and the percent of time spent freezing during a 3 minute duration was recorded. This represents the pre-tone or baseline for the cue testing; E2f3a+/+ and E2f3a-/- mice exhibit similar freezing levels, and baseline levels were significantly lower than post-tone cue testing freezing levels (data not shown) (E2f3a+/+: $p=1.39x10^{-18}$;8.4-fold decrease). Data for panels A&B is presented as mean +/- SEM (n=18 for E2f3a+/+, n=13 for E2f3a-/-).

(C) E2f3a+/+ and E2f3a-/- mice were exposed to gradually increasing levels of foot shock intensity to determine their relative shock thresholds. Shock threshold was identified when the mouse exhibited vocalization concurrent with movement two consecutive times at the same shock level. There is no difference in shock threshold between genotypes. Data is presented as mean +/- SEM (n=10 for E2f3a+/+, n=7 for E2f3a-/-).

SUPPLEMENTAL EXPERIMENTAL PROCEDURES

Immunohistochemistry and Western blotting

For immunohistochemistry, tissue was treated and sectioned as previously described (Mcclellan et al., 2007). Before antibody incubation, antigen retrieval was performed by heating sections at 95°C for 30 minutes in DAKO retrieval solution, followed by 25 minutes at room temperature. For BrdU incorporation, pregnant mice were given a single IP injection of 50mg/kg BrdU and were harvested 2 hours later to visualize cells in S phase, or 24 hours later for commitment assays. Prior to immunostaining, antigen retrieval was performed followed by incubation in 2N HCl at 37°C for 30 minutes and neutralization in 0.1M Na borate, pH8.5, for 15 minutes at room temperature. Protein isolation and Western blots were performed as previously described (Andrusiak et al., 2011). Additionally, lysed samples were sonicated for 3 x 10 seconds at 25% intensity, and debris was spun down. Quantification was performed using ImageJ software and at least 3 independent sets of control and knockout material were included for these experiments.

Cell counts, measurements

For PH-H3 and short-term BrdU counts, brightly labeled cells in the VZ/SVZ were quantified along a ventricular length of 500 or 750um. The number of E2f3a+ cells co-stained with Sox2, Pax6, Tbr2 or BrdU were quantified in the dorsal cortex along a ventricular length of 500um. Sox2 and Tbr2 were quantified along the entire dorsal cortex, and cortical layer markers were counted over a ventricular length of 600um. For commitment assays, co-labeled cells (or BrdU+/Ki67-) were quantified along a ventricular length of 375um, throughout the width of the SVZ/IZ. NeuroD1 and DCX were quantified in every 12^{th} (40um) section throughout the rostral caudal length of the DG and the number of positive cells from all sections was multiplied by 12 to obtain the estimated cell number per DG. For SVZ counts, every 6th coronal section (14 um) from the most rostral crossing of the corpus callosum to the third ventricle (crossing of the anterior commissure) was stained for DCX. The DCX+ area was measured using ImageJ, and the area from all sections combined was multiplied by 6 to obtain the estimated DCX+ area per SVZ.

Antibodies

Antibodies against the following proteins were used in this study: PH-H3 (Millipore, 06-570), BrdU (Accurate Chemicals, OBT0030), DCX (Santa Cruz, sc-8066), βIII-tubulin (Tuj1) (J L Vanderluit et al., 2007), E2f3a (NeoMarkers, MS-1063-P1), Sox2 (sc-17320), Tbr2(Abcam, AB-23345), Pax6 (Covance, PRB278P) and Ki67 (Cell Marque, SP6), E2f3 (pan-E2f3) (sc-878), p107 (sc-318), H3K4Me3 (Millipore, CS200580), H3K27Me3 (ABE44), RNA Polymerase II (Covance, MMS-126R), mtHsp70 (Thermo Scientific, MA3-028), E2f1(sc-193), E2f5 (sc-1083x), pRb (BD, 554136), p130 (sc-317), and NeuroD (sc-1086).

Primers

Primers used for ChIP analysis on the *Sox2* promoter:

Upstream Forward primer: 5'-CAGAAACAATGGCACACCAC-3'

Upstream Reverse primer: 5'-CAAGACGACAGCTCCTTTCC-3'

TSS Forward primer: 5'-CCCATTTATTCCCTGACAGC-3'

TSS Reverse primer: 5'-CTCTTCTTTCTCCCAGCCCTA-3'

Primers for amplification of the *Sox2* promoter fragment (-800bp to +285bp):

Forward primer: 5'-GCCTTTGCACCCTTTGGATGG-3'

Reverse primer: 5'-CGCGGAGATCTGGCGGAGAA-3'

Primers for Poly-A mutagenesis of E2f consensus motif in *Sox2* promoter fragment:

Forward primer: 5'-TTGCCCCACCCTGGCCCCAGCTAAAAACGCCCCATCCACC-3'

Reverse primer: 5'-GGTGGATGGGGCGTTTTTAGCTGGGGCCAGGGTGGGGCAA-3'

Mitotic Spindle Pole Analysis

To quantify the orientation of the mitotic spindle pole, E14.5 cortical sections were stained with DAPI to visualize chromatin and cells undergoing anaphase were imaged along the apical surface of the lateral ventricle. Using ImageJ, one line was drawn to trace the surface of ventricle and a second line traced the cleavage furrow, bisecting the spindle poles. The smallest angle formed between the two intersecting lines was calculated. At least 460 anaphase cells were measured for each genotype, and the final data combines measurements from 5 distinct rostral-caudal levels in 3 different animals. Protocol adapted from (Godin et al., 2010).

Fear Conditioning Analysis

Fear conditioning experiments were performed according to (Villasana et al., 2009), with few modifications. Briefly, on training day (day 1) mice were placed in an Ethovision PhenoTyper clear box (Noldus Information Technology, North America) for 2 minutes, and were given a 30 second, 90 dB tone co-terminating in a 2 second, 0.45 mA foot-shock delivered twice with a 1 minute inter-stimulus interval. On day 2 (~24 hours after training), the contextually conditioned fear testing was performed by placing the mice back into the same fear conditioning apparatus (context) for a total duration of 6 minutes. On day 3 (~48 hours after training), cue conditioned fear testing was performed to measure the amount of freezing in a new context, as well as freezing occurring in the new context with a tone that was previously paired with a foot shock during training. The new context consisted of the same type of apparatus, however the mice were placed into a different box than the one they were trained in, and the conditions for testing were

modified by changing the interior shape of the apparatus, removing white noise from the testing room, adding the odor of vanilla, changing lighting conditions, changing floor and wall texture, and using a different handling technique to place mice into the box. For cue testing, the mice were allowed to freely explore for 3 minutes before re-exposure to the fear conditioning tone for a duration of 3 minutes. During training and context and cue testing, the duration and percent of time spent freezing (immobile) was recorded using Ethovision 8 XT video tracking system as previously described (Pham et al., 2009). To exclude potential effects of anxiety-like or locomotor behavior contributing to differences in freezing behavior, immobility was also analyzed during the first 2 minutes of fear conditioning training occurring on Day 1 prior to the tone/shock exposure, as well as during cue testing on Day 3 prior to tone exposure. Statistical analysis was performed using SPSS Version 19 and outliers were removed prior to analysis comparing E2f3a+/+ (n=18) and E2f3a-/- (n=13) animals using a two-tailed unpaired t-test (*$p<0.05$).

Foot Shock Sensitivity Analysis

Shock sensitivity/ threshold analysis was performed as previously described (Klemenhagen et al., 2005). Briefly, mice were placed into the fear conditioning apparatus for 2 minutes followed by a 1 second foot shock at 0.05mA which was gradually increased in intensity by 0.05mAs. Mice received 2 exposures to each shock level with a random inter-stimulus interval ranging from 30 to 60 seconds. The intensity required for each mouse to flinch, move, jump and vocalize was recorded by an observer (who was blind to genotype) and the test was stopped when shock threshold was achieved as indicated by the mouse moving accompanied by either jumping or vocalization in response to the same shock intensity for two consecutive exposures. Statistical analysis was performed using SPSS Version 19 and outliers were removed prior to analysis comparing E2f3a+/+ (n=10) and E2f3a-/- (n=7) animals using a two-tailed unpaired t-test (*$p<0.05$).

Electrophoretic Mobility Shift Assay

Electrophoretic mobility shift assays (EMSAs) were performed on total protein extracts from E2f3a-/-, E2f3b-/-, or wild type control cultured neural precursor cells, as previously described (Mcclellan et al., 2007).

Flow Cytometry

Proliferating neurosphere cultures were harvested, triturated, fixed in 1%PFA for 1hr at 4C, and in 70% EtOH at 4C overnight. Cell pellets were washed with 1XPBS and resuspended in 1ug/ml DAPI for 30 minutes at room temperature. Cells were analyzed for DNA content using a Dako MoFlo Legacy Flow Cytometer (Beckman Coulter) and Dako Summit Software v4.3. Cell cycle analysis was performed using MultiCycle analysis software.

SUPPLEMENTAL REFERENCES

Klemenhagen, K. C., Gordon, J. A., David, D. J., Hen, R., & Gross, C. T. (2005). Increased Fear Response to Contextual Cues in Mice Lacking the 5-HT1A Receptor. *Neuropsychopharmacology*. doi:10.1038/sj.npp.1300774

Pham, J., Cabrera, S. M., Sanchis-Segura, C., & Wood, M. A. (2009). Automated scoring of fear-related behavior using EthoVision software. *Journal of Neuroscience Methods*, *178*(2), 323–326. doi:10.1016/j.jneumeth.2008.12.021

Villasana, L., Rosenberg, J., & Raber, J. (2009). Sex-dependent effects of 56Fe irradiation on contextual fear conditioning in C57BL/6J mice. *Hippocampus*, NA–NA. doi:10.1002/hipo.20659